

REGULATION OF RECEPTOR TRAFFICKING IN  
MAMMALIAN CELLS BY ANDROGRAPHOLIDE

TAN YINGROU B.SC (HONS)

A THESIS SUBMITTED FOR THE FULFILLMENT OF THE  
DEGREE OF DOCTOR OF PHILOSOPHY

DEPARTMENT OF MICROBIOLOGY

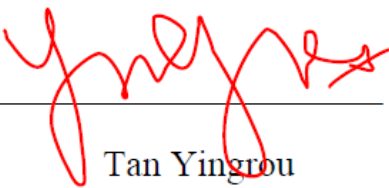
NATIONAL UNIVERSITY OF SINGAPORE

2012

## DECLARATION

I hereby declare that this thesis is my original work and it has been written by me in its entirety. I have duly acknowledged all the sources of information which have been used in the thesis.

This thesis has also not been submitted for any degree in any university previously.



---

Tan Yingrou

9 June 2012

## Acknowledgements

This thesis is the culmination of close to 6 years work, and it is not the result of hard work by only one person. I would like to express my utmost gratitude to the people below:

To my supervisor, Dr Wong Siew Heng: you have been a truly great mentor; you have taught me what it means to be a scientist with an open mind, to be flexible in facing up to the fact when the proposed model or the hypothesis is wrong and to think of the problem using a new angle. You've shown me the importance of being a scientist with integrity, and to accept the results and not to try to force our preconceptions onto the data. Thank you for your patience through the years, I very nearly didn't make it past Masters, but thanks to your training, I've finally completed this PhD thesis.

To my labmates, who have made the unendurable times in lab not only bearable, but fun, I miss you all so much: Kher Hsin, my bestest ever lab partner, I learnt many lab techniques from you, and we've spent so much time together that we saw each other for a greater number of hours than our own families. You have been a precious friend through all the ups and downs of lab life, thank you for all your encouragement, for your listening ear and providing cookies or chocolates whenever I was down. Da Chuan, thank you for teaching me techniques during the two years when our paths crossed. Dennis, Ray and Michael, one of the things from this lab I will definitely miss is the scientific discussions that we had, I really enjoyed being able to debate models and techniques with you guys. Thank you all also for the help, advice and friendship that was so freely offered. Tarika and Sunny, I learnt many techniques from you both, and it was through the both of you that I realised that theoretical knowledge of science was not sufficient, practical techniques are so utterly critical to the success of any scientist.. May Ling, the mommy of the lab, thank you for being such a joy to be around, I love your cheerfulness, it always perks me up whenever I have a tough day. Thank you also for all the help you've provided through getting reagents, you're a real-life Doraemon! Yu Lan, Esabelle, Wen Jie, and especially Minting (gal gal) and Rebecca, thank you also for the friendship through the years, you all really made lab life fun, and I loved being able to work together with you all!

To my reading room friends: Huiyu, my dear exercise partner, thanks for your listening ear whenever I needed to vent, Jun Ji, Jason, Hui Xian, Audrey-Ann and Joon Pu, thank you for the companionship through these years.

To the staff of Microbiology, especially Mrs Phoon, Mr Chan, Mrs Thong, Kelly, Siti, Madam Zainal, Uncle Bala, Auntie Annie, thank you all for the support that you have given us students through your work. You all are unsung heroes that keep the department running day to day

To my church friends, Uncle James, Pei Fen, Ailing, Fiana, Xinling, Jia Hui, Kai Xuan, my dear cousin Yi Hui, and the rest of the fellowship, thank you for always being concerned about my thesis, even though I really don't know how give a proper answer to the frequent question "So how's your thesis going?". Thank you all for the support and understanding, for giving me the time to finish this, and taking some part of the ministry load so I can focus more.

To my family, I love you all. Thank you for putting up with me, especially during the times when I have been a grouchy person because of all the stress. To my dad, thank you for always fetching me to and fro from school, even at some crazy hours like 6 am, just so that I can be in time to start my incubations. Thank you for all the times when you had to wait for me because my incubations took longer than I expected. To my mom, thank you for faithfully doing the housework without complaining. To my brother, thanks for listening to my griping whenever things were not going well.

Lastly, to God my Creator, Father, my Lord and Saviour: I am able to experience the love and blessings from all these people because You have placed them in my life. All praise belongs to you! Psalms 8:3-4 (ESV) aptly describes it: *“When I look at your heavens, the work of your fingers, the moon and the stars, which you have set in place, what is man that you are mindful of him, and the son of man that you care for him?”* It has been an exciting 6 years of exploration and discovering the great and wonderful systems which You have so lovingly put together to sustain life. I love microscopy because each time I look through the microscope, I am filled with wonder as I catch a glimpse of the intricacies of what you have made. May the depths of Your wisdom continue to be revealed as this journey of discovery continues on!

•

Soli deo Gloria

## Presentations and Papers

### Poster Presentations:

1. 1st Singaporean Immunology PhD student retreat, Singapore, 2 Dec 2008; Effect of andrographolide on cellular trafficking; Y. Tan & S.H. Wong.
2. 2nd International Singapore Symposium of Immunology, Singapore. 19-20th Jan 2009; Effect of andrographolide on cellular trafficking; Y. Tan & S.H. Wong.
3. The American Society for Cell Biology 49th Annual Meeting, San Diego, USA, 5<sup>th</sup> -9<sup>th</sup> December 2009; Andrographolide regulates epidermal growth factor receptor (EGFR) and transferrin receptor (TfR) trafficking in epidermoid carcinoma A-431; Y. Tan, K.H. Chiow, D. Huang & S.H. Wong.
4. 4<sup>th</sup> International Singapore Symposium of Immunology, Singapore. 17<sup>th</sup>-18<sup>th</sup> Jan 2011; Inhibition of phagocytosis: A possible function of andrographolide in the control of brain inflammation; Y.Tan, D. Huang & S.H. Wong.
5. Inaugural Yong Loo Lin School of Medicine Graduate Scientific Congress, Singapore. 25<sup>th</sup> Jan 2011; Inhibition of phagocytosis: A possible function of andrographolide in the control of brain inflammation; Y.Tan, D. Huang & S.H. Wong.
6. British Society of Allergy and Clinical Immunology Annual Meeting 2011, Nottingham, UK. 11<sup>th</sup> – 13<sup>th</sup> July 2011; Nitric oxide modulator, andrographolide regulates surface membrane protein trafficking in mammalian cells; Y. Tan & S.H. Wong.

### Papers published/ prepared from this work:

1. Tan, Y, Chiow, KH, Huang, D, Wong, SH (2010) Andrographolide regulates epidermal growth factor receptor and transferrin receptor trafficking in epidermoid carcinoma (A-431) cells. *Br J Pharmacol* **159**(7): 1497-1510.
2. Tan, Y, Wong, SH, Andrographolide increases surface EGFR downregulation through p38 MAPK. (Manuscript in preparation)
3. Tan, Y, Huang, WJ, Chiow, KH, Leong, ML, Wong, SH, Andrographolide regulates phagocytosis through downregulation of CD204 (Manuscript in preparation)
4. Tan, Y, Wong, SH Multi-faceted effects of andrographolide (Manuscript in preparation)

Other papers published:

1. Chiow, KH, Tan, Y, Chua, RY, Huang, D, Ng, ML, Torta, F, Wenk, MR, Wong, SH (2012) SNX3-dependent regulation of epidermal growth factor receptor (EGFR) trafficking and degradation by aspirin in epidermoid carcinoma (A-431) cells. *Cell Mol Life Sci.* **69**(9): 1505-21
2. Lau, PLR, Tan, Y, Chen C, Wong, WSF, Wong, SH Andrographolide regulates EGF-induced synthesis and secretion of mucin by lung epithelial cells (manuscript in preparation).

# Table of Contents

<b>Acknowledgements</b>	<b>iii – v</b>
<b>Presentations and Papers</b>	<b>vi – vii</b>
<b>Table of Contents</b>	<b>viii – x</b>
<b>Summary and Project Aims</b>	<b>xi – xii</b>
<b>Abbreviations</b>	<b>xiii</b>
<b>List of Tables and Figures</b>	<b>xiv – xvi</b>

## Contents

<b>1. LITERATURE REVIEW .....</b>	<b>2</b>
1.1. Natural products as alternative therapies .....	2
1.2. <i>Andrographis paniculata</i> .....	2
1.3. Andrographolide .....	4
1.4. Pharmacokinetics of andrographolide and andrographolide delivery systems .....	7
1.5. Side effects of andrographolide .....	9
1.6. Andrographolide and Immune Suppression.....	9
1.6.1.    ADO effect <i>in vitro</i> .....	10
1.6.2.    ADO effect in animal disease models .....	13
1.6.3.    ADO in clinical trials.....	17
1.7. Andrographolide and Immunostimulation.....	20
1.8. Anti-cancer effects of andrographolide .....	21
1.8.1.    Inhibition of cellular proliferation and induction of apoptosis .....	21
1.8.2.    Inhibition of tumour-promoting signalling .....	26
1.8.3.    Inhibition of migration .....	27
1.8.4.    Induction of cytotoxic immune response.....	29
<b>2. MATERIALS AND METHODS .....</b>	<b>32</b>
2.1. Maintenance of cell lines .....	32
2.1.1.    Media and growth conditions .....	32
2.1.2.    Cryopreservation of cell lines.....	32
2.2. Antibodies.....	33
2.3. Other Reagents.....	34
2.4. Cellular Analysis.....	34



2.4.1.	Cell Viability Assay .....	34
2.4.2.	Indirect Immunofluorescence .....	35
2.4.3.	Fluorescence-activated Cell Sorting (FACS) .....	36
2.4.4.	Western Blot Analysis.....	38
2.4.5.	Reverse-transcription polymerase chain reaction (RT-PCR) .....	39
2.4.6.	Recycling Assay .....	40
2.4.7.	Phagocytosis Assay .....	40
2.4.8.	p38 MAP Kinase assay.....	41
2.4.9.	CD204 secretion assay .....	41
<b>3. ANDROGRAPHOLIDE AFFECTS RECEPTOR TRAFFICKING IN A-431 CELLS.....</b>		<b>44</b>
3.1.	Abstract.....	44
3.2.	Introduction.....	44
3.2.1.	Epidermal Growth Factor Receptor (EGFR).....	45
3.2.2.	Transferrin Receptor.....	47
3.3.	Results.....	48
3.3.1.	Andrographolide inhibits growth and downregulates surface EGFR.....	48
3.3.2.	Andrographolide changed the rate of degradation of both EGFR and TfR.....	52
3.3.3.	Andrographolide induced the accumulation of EGFRs into an intracellular LAMP-1- and VAMP-8-positive but VAMP-3-negative membrane compartment.....	55
3.3.4.	Downregulation of surface EGFR upon andrographolide treatment was not due to the inhibition of receptor recycling but due to the enhanced internalisation of EGFR from the cell surface of A-431 cells.....	64
3.4.	Discussion.....	68
<b>4. ANDROGRAPHOLIDE INCREASES SURFACE EGFR DOWNREGULATION THROUGH ACTIVATION OF P38 MAPK.....</b>		<b>77</b>
4.1.	Abstract.....	77
4.2.	Introduction.....	77
4.2.1.	MAPK Pathways .....	78
4.2.2.	Crosstalk between MAPK signalling and receptor endocytosis.....	79
4.3.	Results.....	81
4.3.1.	Andrographolide upregulates the MAPK signalling pathways independently of EGF .....	81
4.3.2.	JNK and p38 MAPK activity regulate ADO induced EGFR internalisation .....	85

4.4. Discussion.....	90
<b>5. ANDROGRAPHOLIDE REGULATES PHAGOCYTOSIS IN MICROGLIA CELLS THROUGH DOWNREGULATION OF CD204 .....</b>	<b>99</b>
5.1. Abstract.....	99
5.2. Introduction.....	99
5.3. Results.....	104
5.3.1. Andrographolide regulates phagocytosis in microglial cells.....	104
5.3.2. Andrographolide decreases the surface expression of CD204 and CD36.....	107
5.3.3. CD204 is important for phagocytosis of <i>E. coli</i> in N9 microglia cells.....	109
5.3.4. CD204 accumulates within the cell upon ADO treatment .....	111
5.3.5. ADO does not inhibit endocytosis or degradation of CD204.....	114
5.4. Discussion.....	122
<b>6. CONCLUSIONS AND FUTURE DIRECTIONS .....</b>	<b>130</b>
6.1. Conclusions.....	130
6.2. Delving into additional drug mechanisms .....	130
6.3. Future Directions .....	132
<b>7. BIBLIOGRAPHY.....</b>	<b>134</b>
<b>8. APPENDICES.....</b>	<b>156</b>

## Summary and Project Aims

Andrographolide (ADO) is one of the many active components of the traditional herb *Andrographis paniculata*, which has been extensively used in various forms of Ayurvedic and Chinese Medicine. It is a highly versatile compound and has effects on different systems. The most well-known effect of ADO to date is its anti-inflammatory effect due to its ability to inhibit NF- $\kappa$ B activation, and it has been shown to alleviate the effects of many inflammatory diseases. However, the cellular mechanism of ADO has not yet been fully elucidated, and hence the purpose of this project is to elucidate the mechanism through which ADO exerts its various effects.

The first part of the project focuses on the effect ADO has on receptor trafficking, using the epidermal growth factor receptor (EGFR) and the transferrin receptor (TfR) in the A-431 epidermoid carcinoma cell model. As ADO has been shown to affect the expression of surface receptors such as MHC class II, CD40 and CD86 in dendritic cells, we hypothesised that ADO could affect endocytic trafficking of receptors. We hoped to identify the endocytic pathways that ADO perturbs using EGFR as a model receptor that is degraded after internalisation, and TfR as a model receptor that constitutively recycles. For the first part of the project, we established that ADO downregulates EGFR surface expression by enhancing the endocytosis of EGFRs, and endocytosed EGFRs accumulate at the VAMP-8 and LAMP-1 positive late endosomes.

The second part of the project seeks to elucidate the molecular mechanism of how ADO increases EGFR endocytosis and how ADO effect on EGFR trafficking may

affect its down-stream mitogen activated protein kinase (MAPK) signalling pathways and thus affect cell proliferation. We demonstrate that ADO is able to activate the p38 MAPK, which then phosphorylates EGFR at the serine 1046/1047 residue, inducing its internalisation from the cell surface.

The third part of the project seeks to apply the information we have gained from the A-431 epidermoid carcinoma model in an immune cell model to investigate if the anti-inflammatory effect from ADO could also be mediated through affecting surface expression of immune receptors. We chose to focus on scavenger receptors, which are known to be important for bacterial binding, and phagocytic uptake by microglia cells of the brain. Phagocytic uptake of bacteria in the brain may potentially induce immune activation and causes inflammation of the brain. In this study, we found that ADO inhibits phagocytosis through downregulating surface scavenger receptor CD204 in microglia. This presents a novel mechanism by which ADO could possibly exert its anti-inflammatory effect in the brain.

The results in this study demonstrate an approach to understand the effects of a pharmacophore with a known mechanism on other cellular mechanisms, with a particular focus on receptors, which are important for mediating the cellular response to external cues.

**Abbreviations**

ADO	Andrographolide
EEA-1	Early endosomal antigen-1
EGFR	Epidermal growth factor receptor
ERK	Extracellular signal regulated kinase
FACS	Fluorescence activated cell sorting
IL	Interleukin
iNOS	Inducible nitric oxide synthase
IFN- $\gamma$	Interferon gamma
JNK	c-Jun-N-terminal kinase
LAMP-1	Lysosomal associated membrane protein-1
LPS	Lipopolysaccharide
MAPK	Mitogen activated protein kinase
NO	Nitric oxide
p38 MAPK	p38 mitogen activated protein kinase
TNF- $\alpha$	Tumour necrosis factor alpha
TfR	Transferrin receptor
VAMP	Vesicle associated membrane protein
v/v	Volume to volume
w/v	Weight to volume

**List of Tables**

<b>Table Number</b>	<b>Title</b>	<b>Page</b>
<b>Table 2.1</b>	Catalogue of antibodies used	33
<b>Table 4.1</b>	Transcription factors phosphorylated by different MAPKs. (Adapted from (Turjanski <i>et al.</i> , 2007))	79
<b>Table 8.1</b>	Maximal plasma concentrations ( $C_{\max}$ ) levels of differing treatments of ADO	156
<b>Table 8.2</b>	Anti-inflammatory effects of ADO <i>in vitro</i> .	157
<b>Table 8.3</b>	Anti-inflammatory effects of ADO <i>in vivo</i> .	160
<b>Table 8.4</b>	Anti-inflammatory effects of ADO or <i>Andrographis paniculata</i> in humans	161
<b>Table 8.5</b>	Immunostimulatory effects of ADO or <i>Andrographis paniculata</i>	162
<b>Table 8.6</b>	Anti-cancer effects of ADO or <i>Andrographis paniculata</i>	163

## List of Figures

<b>Figure Number</b>	<b>Title</b>	<b>Page</b>
<b>Figure 1.1:</b>	Chemical structures of various active compounds extracted from <i>Andrographis paniculata</i> .	4
<b>Figure 1.2:</b>	Summary of the wide variety of effects of andrographolide on various human disease conditions.	6
<b>Figure 1.3:</b>	Extrinsic and intrinsic pathways of apoptosis and roles of pro-apoptotic and anti-apoptotic proteins (Ola <i>et al.</i> , 2011).	25
<b>Figure 3.1:</b>	Assessment of cell viability upon ADO treatment.	49
<b>Figure 3.2:</b>	Surface expression of EGFR after ADO treatment.	49
<b>Figure 3.3:</b>	Surface expression of EGFR after 48 h of ADO treatment.	49
<b>Figure 3.4:</b>	Western blot analysis of ADO effect on total EGFRs in A-431.	51
<b>Figure 3.5:</b>	Reverse-transcription polymerase chain reaction (RT-PCR) of EGFR mRNA transcripts.	51
<b>Figure 3.6:</b>	ADO changed the rate of degradation of EGFR.	53
<b>Figure 3.7:</b>	ADO changed the rate of degradation of TfR.	54
<b>Figure 3.8:</b>	ADO affected the intracellular distribution of EGFRs.	56
<b>Figure 3.9:</b>	Intracellular distribution of EGFRs in ADO treated cells..	58
<b>Figure 3.10</b>	X-Z/Y-Z projection of EGFR with VAMP-3 after ADO treatment	58
<b>Figure 3.11:</b>	ADO co-localises EGFR with VAMP-8.	60
<b>Figure 3.12:</b>	ADO affected intracellular distribution of TfRs.	61
<b>Figure 3.13:</b>	Epidermal growth factor receptor (EGFR) accumulated in an intracellular membrane compartment that co-localises with LAMP-1 upon treatment with ADO.	63
<b>Figure 3.14:</b>	ADO did not affect the recycling pathway, but increased the internalisation of EGFR.	66
<b>Figure 3.15:</b>	Proposed mechanism of ADO-induced inhibition of receptor degradation in late endosomes.	72
<b>Figure 4.1</b>	ADO upregulates the MAPK signalling pathways	83

---

	independently of EGF.	
<b>Figure 4.2</b>	ADO upregulates MAPK signalling pathways phosphorylation independently of EGF in A-431 (A) and Hela (B) cells.	84
<b>Figure 4.3</b>	ADO enhances endocytosis of EGFR via activation of the p38 MAPK.	87
<b>Figure 4.4</b>	Activated p38 MAPK phosphorylates EGFR in A-431 cells	89
<b>Figure 4.5</b>	Activated p38 MAPK phosphorylates EGFR, causing downregulation of surface EGFR in Hela cells.	90
<b>Figure 4.6</b>	L-cysteine inhibits MAPK induced signalling.	92
<b>Figure 4.7</b>	Production and removal of reactive oxygen species (ROS)	94
<b>Figure 4.8</b>	Proposed model of ADO effect on p38 MAPK signalling and EGFR endocytosis.	95
<b>Figure 4.9</b>	MAPKi can partially restore cell viability in A-431 cells.	97
<b>Figure 5.1</b>	ADO downregulates phagocytosis in microglia.	106
<b>Figure 5.2</b>	ADO induces a decrease in surface expression of CD204 and CD36.	108
<b>Figure 5.3</b>	CD204 is important for phagocytosis in N9 microglia cells.	110
<b>Figure 5.4</b>	ADO causes an accumulation of CD204 in intracellular endosomal compartments	113
<b>Figure 5.5</b>	ADO does not alter the rate of CD204 endocytosis or degradation.	117
<b>Figure 5.6</b>	ADO affects the secretion of CD204	120
<b>Figure 5.7</b>	Sites regulating internalisation and surface localization of SR-A.	124
<b>Figure 5.8</b>	ADO acts as a PI3 kinase inhibitor.	128



# **Chapter 1**

# **Literature Review**

## **1. Literature Review**

### **1.1. Natural products as alternative therapies**

Traditional medicine systems, which have existed for thousands of years, have amassed a huge amount of data in utilising natural products as therapies for various diseases. These age-old remedies offer a cheap and easily available alternative approach as a multi-target therapy for diseases such as cancer and inflammatory diseases which involve many different pathways as opposed to conventional therapies which focus on a single target (Gupta *et al.*, 2010). In recent times, a larger amount of research has focused on the effect of natural product derived compounds in combating cancer, metabolic disorders, neurodegenerative diseases, inflammation and cardiovascular diseases (Houston, 2010; Kannappan *et al.*, 2011). However, not much is known about the mechanisms through which these compounds affect cells. Hence we focus here on elucidating the effect and mechanism of andrographolide (ADO), an active component of the medicinal plant *Andrographis paniculata*, on receptor trafficking.

### **1.2. *Andrographis paniculata***

*Andrographis paniculata* (*A. paniculata*), commonly known as the “King of Bitters”, due to its extremely bitter taste, is a plant belonging to the family of Acanthaceae. In Mandarin, it is known as 穿心莲 (*Chuan Xin Lian*). The plant grows in shaded areas, and is found in several Asian countries such as Malaysia, Indonesia, India, Thailand and Singapore. It is commonly used in Indian and Chinese complementary medicine treatments as an anti-inflammatory agent, and is also one of the active components in

the Swedish drug, Kan Jang, sold by the Swedish Herbal Institute for the treatment of upper respiratory tract infections. Traditionally, it has been used for the treatment of snake bites. Various studies show that it can offer some protection against venom from cobra (*Naja sp.*) (Kumarappan *et al.*, 2011; Premendran *et al.*, 2011), rattlesnake (*Crotalus adamanteus*) (Samy *et al.*, 2008), as well as the deadly red scorpion (*Mesobuthus tumulus*) (Brahmane *et al.*, 2011). *A. paniculata* extracts also prevented scorpion venom (*Heterometrus laoticus*) induced lysis of fibroblasts (Uawonggul *et al.*, 2006). *A. paniculata* contains several active components of which a few have been more extensively studied – ADO, neoandrographolide, deoxyandrographolide, 14-deoxy-11,12-didehydroandrographide and isoandrographolide (Chao & Lin, 2010). Their chemical structures can be seen in figure 1.1.

There are various methods of extracting active compounds from *A. paniculata*. Extraction of active compounds can be done using methanol, ethanol, ethyl acetate, hexane and water, and an excellent review of the various methods of extractions has been covered by Chao *et al.* (Chao & Lin, 2010).

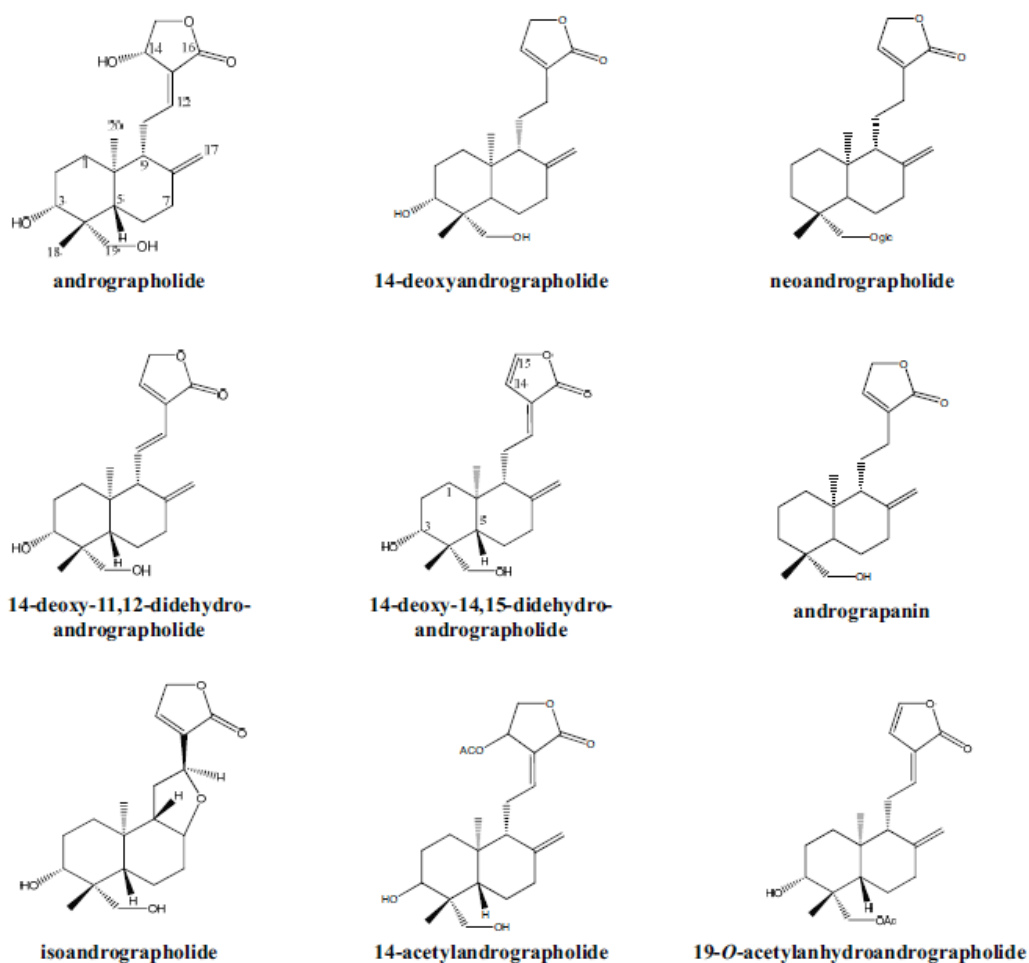


**Figure 1.1** Chemical structures of various active compounds extracted from *Andrographis paniculata*. (Chao & Lin, 2010)

### 1.3. Andrographolide

Of all the active compounds found in *A. paniculata*, andrographolide (ADO) has been the most extensively studied, and has been shown to be a highly versatile compound (Figure 1.2). ADO is the main component that contributes to the bitter taste of *A. paniculata* as it acts as an agonist for the bitter taste receptor hTAS2R50 (Behrens *et al.*, 2009). Much work has been carried out on the varying effects of ADO, and thus far, it is known that ADO has hepatoprotective effects against toxic substances like carbon tetrachloride, paracetamol, glucosamine and ethanol (Ghosh *et al.*, 2011). It

has also been found to be effective in the killing of cancer cells, and as an anti-oxidant (Chao & Lin, 2010). A summary of the various effects of ADO is shown in figure 1.2.

The majority of this literature review focuses on the compound ADO as it is the main active component of *Andrographis paniculata*, and it is much easier to investigate the effects induced by a purified compound as compared to plant extracts that consist of a mixture of various compounds. However, the effect of ADO may be limited in some contexts, hence various groups have synthesised different derivatives of ADO through varying the side chains in a bid to increase its efficacy (Jada *et al.*, 2006; Wang *et al.*, 2010b; Aromdee *et al.*, 2011; Aromdee, 2012). The literature review focuses on ADO effect on the immune system and on its anti-cancer effect, as those are the main areas of our investigation.

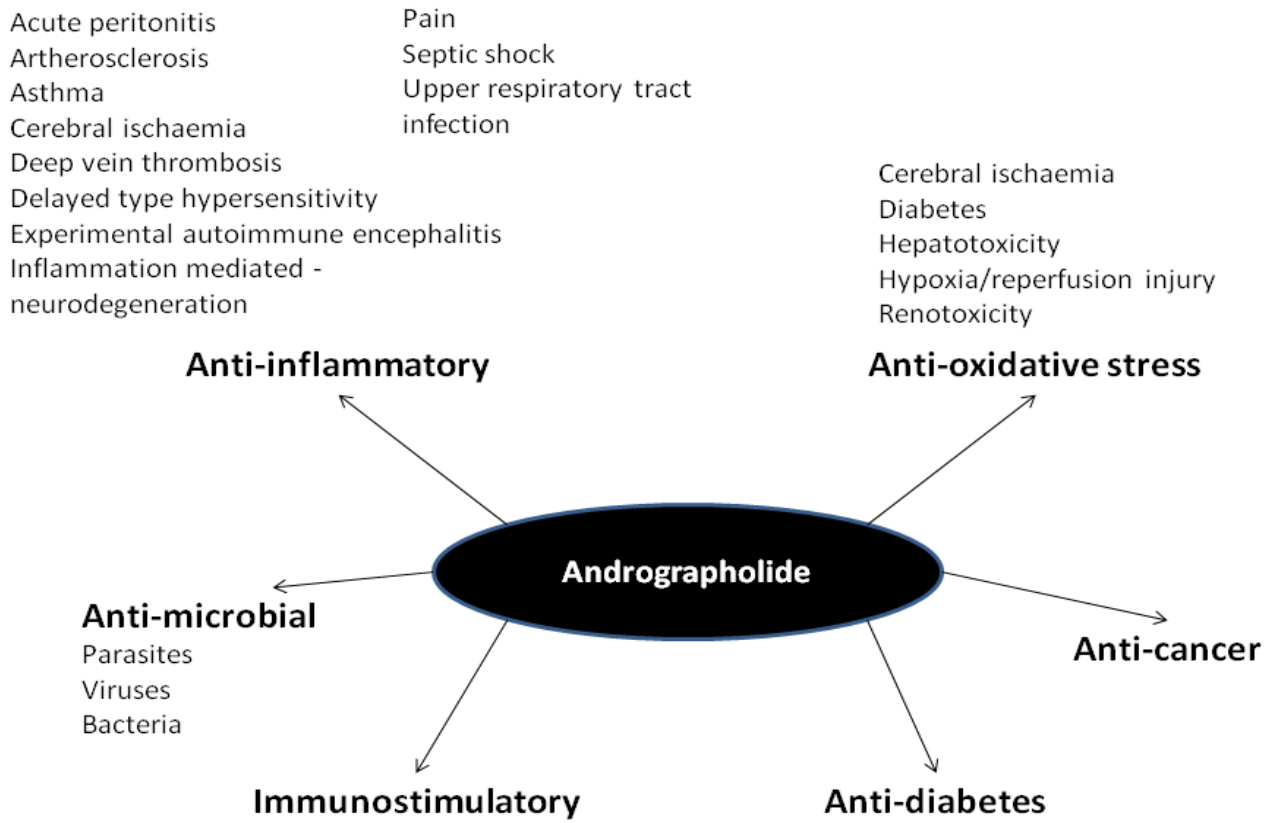


**Figure 1.2 Summary of the wide variety of effects of andrographolide on various human disease conditions.**

#### **1.4. Pharmacokinetics of andrographolide and andrographolide delivery systems**

The bioavailability of any drug is particularly important as it refers to the amount of drug that is made available to the system. The pharmacokinetics of ADO has been extensively studied in animal models and humans, and a variety of methods utilizing high performance liquid chromatography (HPLC) in combination with ultraviolet detection have been developed to quantitate the amount of available ADO in the plasma as summarised in table 8.1. These studies have found that the amount of free ADO within the plasma is rather low as a large proportion of ADO binds to plasma proteins, leading to reduced availability of free ADO in the blood (Panossian *et al.*, 2000). Another factor contributing to the low bioavailability of ADO is the metabolism of ADO as well as the efflux of ADO by P-glycoprotein, an important ATP efflux transporter in the intestine. Ye *et al.* found that incubating ADO with saline perfused through rat duodenum and jejunum led to the significant degradation of ADO, due to the rapid metabolism of ADO to form 14-deoxy-12-sulfo-ADO, which was detected in high amounts in the liver, kidney and blood 2 h after oral administration (Ye *et al.*, 2011), and also as a metabolite in the urine of rats (He *et al.*, 2003). Absorption of ADO across the ileum and colon sections was also poor due to efflux of the drug by P-glycoprotein, which was inhibited upon the addition of P-glycoprotein inhibitors.

Hence, various groups have attempted to increase the bioavailability of ADO through different methods. One group tried to increase the poor solubility of ADO by spray drying the lipophilic ADO together with the water-soluble complex polyvinylpyrrolidone (PVP K-30). In comparison to isolated ADO as well as physical

mixtures with PVP K-30, the solid dispersions (SD) of ADO-PVP K-30 only needed 20 minutes, as compared to more than 120 minutes (isolated ADO and physical mixtures with PVP K-30), to release 75% of the drug. The SD of ADO-PVP K-30 was also more efficacious therapeutically and it took only 30 minutes to reduce carrageenan induced paw oedema in rats by 50%, as compared to isolated ADO which took 3 h (Bothiraja *et al.*, 2009). Maiti *et al.* utilised the phospholipid 1,2-distearoyl-*sn*-glycero-3-phosphocholine to form a complex with ADO which they termed a herbasome (Maiti *et al.*, 2010). An equivalent dose of ADO in the herbasome was able to generate a higher maximum plasma concentration of 9.64  $\mu\text{g/ml}$  as compared to 6.79  $\mu\text{g/ml}$  generated by ADO. The herbasome also increased the elimination half-life of the drug by about 3 times, hence improving the bioavailability and hepatoprotective effect of ADO. Other groups attempted to package ADO in liposomes using phosphatidylethanolamine (PE), cholesterol, dicetyl phosphate (DCP) (Sinha *et al.*, 2000; Suo *et al.*, 2007); nanoparticles made of poly(DL-lactide-co-glycolic acid) (PLGA) (Roy *et al.*, 2010), or a pH sensitive patented material Eudragit® EPO as a matrix and Pluronic® F-68 as a surfactant (Chellampillai & Pawar, 2011) to facilitate drug release in the acidic environment of the gastrointestinal tract. Thus far, the method which maximises the amount of bioavailable ADO in pharmacokinetic studies after factoring in the difference in the dosage levels is the herbasome method which gives an area under the plasma concentration curve ( $\text{AUC}_{0-\infty}$ ) of 87.30  $\mu\text{g ml}^{-1}\text{h}$ .



### **1.5. Side effects of andrographolide**

A main concern of any drug being utilised is the side effects that are associated with it. *Andrographis paniculata* extract has no known acute toxicity at a dose of 17 g/kg, nor subchronic toxicity (Burgos *et al.*, 1997). A study conducted on a standardised extract of *Andrographis paniculata*, known as KalmCold™, which contains a variety of pharmacological compounds which include ADO, demonstrated that it has no genotoxic effects through three tests: the Ames test for dosages up to 5000 µg/ml, the *in vitro* chromosome aberration test and the *in vitro* micronucleus test for concentrations up to 80 µg/ml without metabolic activation and up to 345 µg/ml with metabolic activation. KalmCold™ also showed no acute oral toxicity in female rats at 5000 mg/kg after an observation period of 14 days (Chandrasekaran *et al.*, 2009). However, in a clinical trial consisting of HIV positive and healthy individuals utilising doses of ADO at 5mg/kg for 3 weeks followed by 10mg/kg for 3 weeks, adverse effects such as headache, fatigue, rash, itching of the skin were observed.. This led to the trial being stopped (Calabrese *et al.*, 2000). Severe adverse effects were not noted at other clinical trials involving human volunteers.

### **1.6. Andrographolide and Immune Suppression**

One of the most extensively characterised effects of ADO is its ability to suppress the immune system (Lim *et al.*, 2011). It accomplishes this via the following mechanisms: inhibition of the NF-κB pathway (Xia *et al.*, 2004; Bao *et al.*, 2009), and inhibiting nuclear translocation of NFAT, which is an important transcription factor for genes mediating the differentiation of T cells, and is critical in the production of cytokines such as IL-2, IL-4, IL-6, IL-10, IL-13, IL-17, IL-21, IL-22, IFN-γ in Th1, Th2 and Th17 T cells. ADO also inhibits monocyte adhesion and migration. The anti-

inflammatory mechanism of ADO is likely to contribute to its ability to reduce symptoms in diseases where inflammation plays a role in disease progression: autoimmune diseases; cardiovascular diseases where vascular inflammation is involved like atherosclerosis; cancer and insulin resistance in diabetes (Chao & Lin, 2010; Lim *et al.*, 2011). The anti-inflammatory effects of ADO *in vitro*, *in vivo* and in clinical trials have been summarised in tables 8.2 to 8.4 respectively.

### **1.6.1. ADO effect *in vitro***

*In vitro*, ADO is known to inhibit the upregulation of pro-inflammatory molecules. For instance, ADO inhibited the upregulation of inducible nitric oxide synthase (iNOS) in RAW 264.7 macrophages activated with lipopolysaccharide (LPS) (Chiou *et al.*, 1998) through inhibiting synthesis of iNOS, as well as increasing its degradation (Chiou *et al.*, 2000). Nitric oxide (NO), prostaglandin E<sub>2</sub> (PGE<sub>2</sub>), IL-1 $\beta$ , IL-6 production in LPS stimulated macrophages, as well as thromboxane B<sub>2</sub> (TXB<sub>2</sub>) production in differentiated HL-60 leukaemia cells were also dose dependently inhibited (Chandrasekaran *et al.*, 2011). TNF- $\alpha$  and IL-12 production was also reduced in ADO treated mouse peritoneal macrophages, and reduction of TNF- $\alpha$  levels is most likely due to suppression of the extracellular regulated kinase (ERK) pathway (Qin *et al.*, 2006). IL-8 and TNF- $\alpha$  secretion were significantly decreased at a non-cytotoxic dose of ADO in human keratinocytes induced with dead *Propionibacterium acne*, the bacteria that cause acne, an inflammatory condition of the skin (Fu *et al.*, 2011).

Monocyte recruitment and adhesion were also reduced by ADO due to the downregulation of adhesion molecules. N-formyl-methionyl-leucyl-phenylalanine (fMLP) induced human peripheral neutrophils demonstrated a reduced level of adhesion and transmigration due to downregulation of surface levels of macrophage antigen-1 (Mac-1) upon ADO treatment. Mac-1 surface expression is controlled by the levels of reactive oxygen species (ROS) in neutrophils, which was lowered with ADO (Shen *et al.*, 2002). Chemotactic migration of macrophages induced by complement 5a (C5a) was repressed by ADO treatment as it was capable of suppressing the downstream signalling cascades of mitogen associated protein extracellular kinase 1/2 (MEK1/2) and phosphoinositide 3 kinase (PI3K) activation. Migration induced by macrophage inflammatory protein 1- $\alpha$  was also inhibited upon ADO treatment (Tsai *et al.*, 2004). ADO could also reduce adhesion of HL-60 promyeloid leukaemia cells to EA.hy926 and human umbilical vein endothelial cells by inhibiting the upregulation of intercellular adhesion molecule 1 (ICAM-1) upon TNF- $\alpha$  stimulation (Yu *et al.*, 2010; Chen *et al.*, 2011).

In T lymphocytes, the translocation of the transcription factor, nuclear factor of activated T cells (NFAT1), into the nucleus upon stimulation by phorbol myristate acetate (PMA) and ionomycin was inhibited, hence reducing the production of cytokines such as IL-2 (Carretta *et al.*, 2009). This inhibition was linked to ADO's upregulation of c-Jun-N-terminal kinase (JNK) phosphorylation, which is known to phosphorylate NFAT1. JNK phosphorylation of the calcineurin targeting domain of NFATc1 (transcription factor) prevents calcineurin from dephosphorylating NFAT, and hence inhibits NFAT1 nucleus translocation. (Chow *et al.*, 2000).

One of the key findings, which reveals the anti-inflammatory effect of ADO, is the discovery that ADO inhibits NF- $\kappa$ B binding to DNA by modifying the cysteine residue 62 on the p50 subunit. This critical discovery of ADO inhibition of the NF- $\kappa$ B pathway was carried out by two groups at about the same time: Hidalgo *et al.* discovered that NF- $\kappa$ B binding to DNA in platelet-activating factor (PAF) and fMLP induced HL-60 derived neutrophils was inhibited (Hidalgo *et al.*, 2005), and Xia *et al.* demonstrated similarly that NF- $\kappa$ B binding was affected in TNF- $\alpha$  treated 293T cells. They went further to identify that the cysteine residue 62 is modified by ADO through mutation studies. As NF- $\kappa$ B is inhibited, E-selectin expression on activated endothelial cells was decreased hence leading to decreased leukocyte adhesion (Xia *et al.*, 2004).

NF- $\kappa$ B inhibition also led to the inhibition of dendritic cell (DC) maturation after induction by LPS. Thus, antigen presentation by DCs to T cells, as well as the surface expression of molecules important for T cell activation like MHC class II, CD40 and CD86 was also diminished upon ADO treatment, leading to the inhibition of T cell activation, as well as a reduction in antibody production against the antigen of interest. Interestingly, phagocytosis remained unaffected upon ADO treatment (Iruretagoyena *et al.*, 2005; Iruretagoyena *et al.*, 2006).

Cyclooxygenase-1 (COX-1), is constitutively active, while COX-2 is an inducible target gene for NF- $\kappa$ B, and is responsible for the production of pro-inflammatory prostaglandins and its product thromboxanes, as well as leukotrienes. ADO was

shown to inhibit both COX-1 and COX-2 activities in human platelet cell suspensions, and it also decreased the total level of pro-inflammatory cytokines in human whole blood such as TNF- $\alpha$ , IL-6, IL-1 $\beta$  and anti-inflammatory cytokine IL-10 due to downregulation of mRNA expression (Parichatikanond *et al.*, 2010)

ADO also inhibited LPS induced neurotoxicity and activation in dopaminergic neuronal cultures. Hence, LPS induced superoxide, TNF- $\alpha$ , nitric oxide and PGE<sub>2</sub> production and intracellular reactive oxygen species (ROS) levels were also reduced. LPS induced mRNA expression of COX-2 and TNF- $\alpha$  was similarly decreased upon ADO treatment, and protein stability of COX-2 dropped (Wang *et al.*, 2004). This finding was further substantiated in a rat model of permanent cerebral ischaemia, where rats were administered ADO after ischaemia was induced. A reduction in infarct volume and decrease in activated OX-42 microglia, as well as a drop in IL-1 $\beta$ , TNF- $\alpha$  and PGE<sub>2</sub> production in the ischaemic hemisphere in ADO treated rats was observed. The amount of NF- $\kappa$ B translocated into the nucleus from the cytosol was also decreased upon ADO treatment, accounting for the drop in pro-inflammatory cytokines (Chan *et al.*, 2010).

### **1.6.2. ADO effect in animal disease models**

*In vivo*, ADO has been proven to be efficacious in a variety of autoimmune mouse models, including asthma, peritonitis, septic shock, experimental autoimmune encephalomyelitis (EAE) and hemophilia.

ADO has been demonstrated to inhibit the effects of ovalbumin (OVA) induced asthma in sensitized mice. In ADO treated asthmatic mice, infiltrating leukocyte cell count dropped compared to control mice; levels of OVA- specific IgE and pro-inflammatory cytokines such as IL-4, IL-5, IL-13 were also decreased in bronchoalveolar lavage fluid. Interestingly, ADO was found to prevent activation of the NF- $\kappa$ B pathway further upstream by inhibiting phosphorylation of inhibitory  $\kappa$ B – kinase  $\beta$  (IKK $\beta$ ) upon induction with tumour necrosis factor- $\alpha$  (TNF- $\alpha$ ) (Bao *et al.*, 2009). LPS induced E-selectin and vascular cell adhesion molecule 1 (VCAM-1) upregulation on endothelial cells in the blood vessels from the lungs of asthmatic mice was also downregulated upon ADO treatment (Xia *et al.*, 2004).

In mouse models of peritonitis induced by TNF- $\alpha$ , IL-1 $\beta$  or LPS, the infiltrating neutrophils were decreased in number upon ADO treatment, whereas in the mouse model of septic shock induced by LPS, the rate of mouse survival was improved upon treatment (Xia *et al.*, 2004). The severity of EAE, the mouse model of the human disease multiple sclerosis, was also decreased upon ADO treatment, due to inhibition of DC maturation, leading to reduction of antimyelin T cell and antibody response in ADO treated mice. In addition, numbers of Fox3p regulatory T cells were increased in ADO treated mice (Iruretagoyena *et al.*, 2005; Iruretagoyena *et al.*, 2006). Not surprisingly, in a separate test for the humoral response upon vaccination, serum antibody titres of mice injected with the yeast derived human hepatitis B surface antigen (HBsAg) and treated with ADO were decreased in comparison to the control (Wang *et al.*, 2010a).

In the mouse models for nociception, the acetic acid induced writhing test and the hot-plate tests were used for mice pretreated with ADO, and ADO was shown to reduce the levels of pain induced through a non-opioid mechanism (Suebsasana *et al.*, 2009). Intraperitoneal injection of ADO was capable of reducing the swelling of the paw (Sheeja *et al.*, 2006; Suebsasana *et al.*, 2009; Sulaiman *et al.*, 2010) in the carageenan induced paw oedema mouse model, which is dependent on COX-2 induction of prostaglandin E<sub>2</sub> production (Guay *et al.*, 2004). ADO suppression of edema is not surprising as it is capable of inhibiting NF-κB and COX-2 activity. A separate study by Suebsasana *et al.* on mice for baker's yeast induced fever, the writhing test and hot plate tests showed no effect of ADO. However, this is likely to be due to the differences in the dosage of ADO used, as Suebsasana *et al.* used a much lower dose of 4 mg/kg as compared to Sulaiman *et al.*, who used dosages up to 50 mg/kg (Suebsasana *et al.*, 2009; Sulaiman *et al.*, 2010).

In a haemophilic mouse model, ADO led to the increased secretion of immunosuppressive cytokines IL-10 and TGF-β in an immature dendritic cell-T cell co-culture, as well as decrease in factor VIII (FVIII) inhibitors, which are responsible for sequestering the FVIII protein infused as therapy for Haemophilia A (Qadura *et al.*, 2008).

Not surprisingly, ADO was similarly effective in animal models of vascular inflammation, as NF-κB is the main signal integrator which responds to cytokines and vasoactive peptides, and its activation results in monocyte adhesion and chemotaxis into the vascular tissue, and finally monocyte activation. Monocytes then release

reactive oxygen species and activate metalloproteinases which cause the remodelling of the extracellular matrix (Brasier, 2010). In a mouse model of arterial injury, ADO treatment had the same effect on inhibiting neointima hyperplasia as NF- $\kappa$ B p50 knock-out mice. As NF- $\kappa$ B controls transcription of E-selectin, vascular cell adhesion molecule-1 (VCAM-1) and tissue factor (TF), it was not surprising that ADO treated mice had decreased E-selectin, VCAM-1 and TF protein and mRNA expression levels. The decreased E-selectin and VCAM-1 levels on endothelial cells led to reduced leukocyte deposition (Wang *et al.*, 2007). A separate study on vein graft in rats similarly demonstrated a reduction in intima hyperplasia for ADO treated rats. Similarly, E-selectin, p65 subunit of NF- $\kappa$ B and matrix metalloproteinase-9 (MMP-9) expression was also downregulated in ADO rats (Zhi-Tao *et al.*, 2011). In primary cultures of rat vascular smooth muscle cells (VSMCs) induced with both LPS and IFN- $\gamma$ , production of NO, an inflammatory mediator from VSMCs was decreased upon ADO treatment. Both iNOS protein and mRNA levels were also decreased upon addition of ADO; production of matrix metalloproteinase-9 (MMP-9), a hallmark of vascular inflammatory disease, also dropped after treatment. This was due to the reduction in NF- $\kappa$ B transcription activity, as ADO led to reduced nuclear translocation of NF- $\kappa$ B (Hsieh *et al.*, 2010).

Thrombosis is a condition where activation of coagulation factors leads to platelet activation and aggregation, finally forming a blood clot, leading to ischaemic conditions. TF plays a pivotal role in initiating thrombosis as it triggers the coagulation cascade, causing the formation of a fibrin clot which obstructs blood flow. In a mouse model of deep vein thrombosis, both p50 knockout mice and ADO treated



mice showed a reduction in the amount of TF produced, as well as a drop in the levels of fibrin deposited. Proliferation of venous endothelial cells, upregulation of E-selectin and VCAM-1 levels and leukocyte infiltration were also reduced in both types of mice (Li *et al.*, 2009). ADO treatment was able to inhibit platelet aggregation in both platelet aggregation factor (PAF) induced human blood platelets (Amroyan *et al.*, 1999; Thisoda *et al.*, 2006) and thrombin induced rat platelets (Thisoda *et al.*, 2006), which could prevent clot formation, through the inhibition of ERK2. Sodium induced microthrombus formation in mice was also delayed upon treatment with ADO, with a longer time period needed for vessel occlusion and lowered mortality rate. This is due to inhibition of platelet aggregation, which arose from inhibition of the phosphatidylinositol-3 kinase (PI3K)-Akt-p38 MAPK and phospholipase C  $\gamma$ -2 (PLC  $\gamma$ -2)-diacylglycerol (DAG)-protein kinase C (PKC) pathways and through activation of the endothelial nitric oxide synthase (eNOS)-nitric oxide (NO)-cyclic GMP pathway, which led to the decreased release of calcium ions, which are important for platelet activation (Lu *et al.*, 2011).

### **1.6.3. ADO in clinical trials**

In humans, ADO typically makes up one of the components in a herbal concoction. Thus far, the available commercial products which contain ADO are Immunoguard®, Kan Jang SHA-10 as well as Paractin® tablets, made up of 30% ADO. Various reviews conducting a meta-analysis of the clinical trials focusing on upper respiratory tract infection found that either *A. paniculata* extract or its combination with *Eleutherococcus senticosus* was able to significantly contribute to an improvement of symptoms. The drug is also generally safe as there were low incidences of adverse

reactions, and these adverse reactions were mild and infrequent (Coon & Ernst, 2004; Poolsup *et al.*, 2004; Kligler *et al.*, 2006).

Immunoguard®, a mixture of *Andrographis paniculata*, *Eleutherococcus senticosus*, *Schizandra chinensis*, *Glycyrrhiza glabra*, has been tested in patients with a genetic inflammatory disease – familial Mediterranean fever (FMF) in a double blind placebo controlled trial. Such patients typically experience attacks lasting two to four days in the form of fever, inflammation in the lungs, abdominal cavity, joints and peritoneal cavity. Immunoguard® was found to reduce the number, duration and severity of attacks (Amaryan *et al.*, 2003). Interestingly, it worked by increasing the amount of NO to normal levels, as well as by decreasing elevated levels of the pro-inflammatory cytokine IL-6 (Panossian *et al.*, 2003).

Kan Jang is a combination of *Andrographis paniculata* and *Eleutherococcus senticosus*, and administration of Kan Jang to patients with an upper respiratory tract infection and sinusitis in a double blind, placebo controlled study resulted in a reduction of sore throat, dryness in throat, nasal symptoms, headache and general malaise (Melchior *et al.*, 2000; Gabrielian *et al.*, 2002; Kulichenko *et al.*, 2003). When tested in children using Immunal (a concoction containing 80% *Echinacea purpurea* juice and 20% ethanol) as the control, patients who consumed Kan Jang also recovered more rapidly overall, and had decreased nasal secretion and nasal congestion (Spasov *et al.*, 2004).

Paractin, a formulation consisting of 30 mg ADOs, was fed to rheumatoid arthritis (RA) patients 3 times a day for 14 week in a randomized, double blind, placebo controlled study (Burgos *et al.*, 2009). ADO treatment reduced the number and grade of swollen and tender joints, together with a reduction in the levels of rheumatoid factor (RF), IgM and IgA. *In vitro* studies showed that the ADO effect on relieving RA symptoms could also be due to its ability to reduce proliferation, induce cell cycle arrest and apoptosis in human primary rheumatoid arthritis fibroblast like synoviocytes (RAFLSs) extracted from rheumatoid arthritis patients. RAFLSs are known to contribute to inflammation and cartilage destruction by secreting pro-inflammatory cytokines and metalloproteases (Bartok & Firestein, 2010). Upon ADO treatment in RAFLs, expression of anti-apoptotic protein Bcl-2 was decreased, whereas pro-apoptotic Bax was upregulated; cytochrome c was also released leading to the cleavage of pro-apoptotic caspase-3. (Yan *et al.*, 2011)

### 1.7. Andrographolide and Immunostimulation

Although ADO is known to be anti-inflammatory, some studies have actually demonstrated that it can induce the immune system (table 8.5) through increasing the proliferation of lymphocytes. Human immunodeficiency virus (HIV) positive patients who took 10 mg/kg of ADO had a statistically significant 23% increase in the number of CD4<sup>+</sup> lymphocytes which corresponded to no change in the HIV viral mRNA levels.(Calabrese *et al.*, 2000). Proliferation of phytohemagglutinin (PHA) induced human peripheral blood lymphocytes (HPBL) was significantly increased by about 5% when ADO was added, but decreased by 16.4% in the presence of Kan Jang. ADO and Kan Jang also increased the amount of pro-inflammatory cytokine IFN- $\gamma$  secreted in the absence of PHA, and TNF- $\alpha$  in the presence of PHA. Neopterin, which is an indication of lymphocyte activation, and  $\beta$ -2-microglobulin ( $\beta$ 2MG), which is a component of the MHC class I molecule which is responsible for antigen presentation, were increased upon treatment in the absence of PHA;  $\beta$ 2MG levels were also increased in the presence of PHA after treatment (Panossian *et al.*, 2002). Non-PHA induced HPBL were also induced to proliferate upon ADO treatment, with an increase in IL-2 secretion (Kumar *et al.*, 2004).

Interestingly, lymphocyte proliferation was insignificant in mice immunized with sheep red blood cells (SRBC), but SRBC specific antibody titres, which is representative of the humoral response, as well as hemolytic plaque forming cells and delayed type hypersensitivity response, which are measures of cell mediated immunity, were increased upon treatment with ADO or ethanol extract of *A. paniculata* (APE) (Puri *et al.*, 1993). Mice gavaged with either ADO or APE and then immunized with inactivated *Salmonella typhimurium* also showed enhancements in humoral and cell-

mediated immunity as evidenced by huge increases in serum IgG specific for *Salmonella*, as well as the amount of IFN- $\gamma$  secreted by splenocytes (Xu *et al.*, 2007). Synthesis and secretion of the macrophage migration inhibitory factor (MIF), which is an important pro-inflammatory cytokine that has several functions including upregulating Toll like receptor 4 and prostaglandin E<sub>2</sub> expression (Calandra & Roger, 2003), is also increased upon ADO treatment, although other NF- $\kappa$ B inhibitors such as gliotoxin and oridonin have a more significant effect. This effect in MIF is probably due to the increase in superoxide anion, and is likely to be mediated via the phosphatidylinositol-3-kinase/Akt/JNK pathway (Cho *et al.*, 2009).

## **1.8. Anti-cancer effects of andrographolide**

The six hallmarks of cancer as defined by Douglas Hanahan and Robert Weinberg are: the ability to sustain proliferative signalling; evading growth suppressors; activating invasion and metastasis; enabling replicative immortality; inducing angiogenesis and resisting cell death (Hanahan & Weinberg, 2011). ADO is able to counter these characteristics through inhibiting proliferation; inducing cell cycle arrest and cell death by apoptosis; decreasing metastasis and angiogenesis as well as triggering the anti-tumourigenic cytotoxic immune response (table 8.6). Some of these effects are focused on in the review below.

### **1.8.1. Inhibition of cellular proliferation and induction of apoptosis**

ADO was capable of inhibiting proliferation of various cancer cells, including cell lines from the colon, breast, central nervous system (CNS), lung, skin (melanoma), prostate, ovarian and renal systems (Kumar *et al.*, 2004; Nanduri *et al.*, 2004; Kim *et al.*, 2005). Cell cycle progression is mediated by the differing levels of cyclin-

dependent kinases (Cdks) and cyclins. Progression into the S and M phases are critical for the proliferation of cells, and cell cycle arrest is one of the ways in which ADO stops the proliferation of cancer cells. ADO was found to induce cell cycle arrest at the G<sub>0</sub>/G<sub>1</sub> phase (Rajagopal *et al.*, 2003; Satyanarayana *et al.*, 2004; Cheung *et al.*, 2005) as well as the G<sub>2</sub>/M phase (Li *et al.*, 2007).

Investigations on the levels of cyclins and cdks found that there was a corresponding upregulation of p27, a Cdk inhibitor (CKI) which inhibits activity of the cyclin-Cdk complex, as well as a decrease in Cdk 4 levels, which controls progression past late G<sub>1</sub> (Satyanarayana *et al.*, 2004). In Lovo cells, G<sub>1</sub> arrest corresponded with a decrease in cyclin D/Cdk 4 and cyclin A/Cdk 2 complexes which are the G<sub>1</sub>-Cdk and S-Cdk complexes respectively and upregulation of CKIs p21 & p16 which suppress G<sub>1</sub>-Cdk activities. p53 phosphorylation upon ADO treatment was responsible for the transcription of p21, while the increase in Rb/E2F complex prevented E2F from transcribing proteins required for cell cycle progression (Shi *et al.*, 2008).

Induction of apoptosis was observed in cells treated with ADO, with characteristic morphological changes such as plasma membrane blebbing, vacuolisation, DNA condensation and fragmentation (Cheung *et al.*, 2005; Kim *et al.*, 2005; Li *et al.*, 2007; Manikam & Stanslas, 2009). Flow cytometry studies also show treated cells to be Annexin V positive, which is a marker for early apoptosis, demonstrating translocation of phosphatidylserine from the inside leaflet to the outside (Gunn *et al.*, 2011). There are two possible pathways through which apoptosis could be induced: the extrinsic pathway which involves death receptor activation, leading to formation of the death receptor induced signalling complex (DISC) and cleavage of procaspase-

8, and downstream activation of caspase-3; and the intrinsic pathway, which involves cytochrome c release from the mitochondria which leads to formation of the apoptosome involving caspase-9 and downstream caspase-3 activation (Vermeulen *et al.*, 2005). Pro-apoptotic proteins and anti-apoptotic proteins play important roles in both pathways, as illustrated by figure 1.3. Cleavage of pro-apoptotic Bid by caspase-8 leads to Bax conformational change, oligomerization and mitochondria translocation of Bax, resulting in cytochrome c release from the mitochondria and loss of mitochondria membrane potential.

ADO induces apoptosis through the extrinsic pathway of caspase-8, (Kim *et al.*, 2005; Zhou *et al.*, 2006; Yang *et al.*, 2009b; Yang *et al.*, 2010), causing cleavage of pro-apoptotic proteins such as Bid, upregulation of Bax (Cheung *et al.*, 2005; Li *et al.*, 2007), Bax conformational change, and mitochondria translocation of Bax (Zhou *et al.*, 2006; Yang *et al.*, 2010), together with and decrease in anti-apoptotic Bcl-2 (Zhao *et al.*, 2008). This led to a decrease in the mitochondria membrane potential, with a corresponding release of cytochrome c (Cheung *et al.*, 2005; Yang *et al.*, 2009b) causing downstream caspase-9 and caspase-3 activation (Zhao *et al.*, 2008; Gunn *et al.*, 2011). Expression of p53, an important transcription factor responsible for pro-apoptotic genes such as Bax and the death receptor 4 (DR4), is also elevated (Li *et al.*, 2007; Sukardiman *et al.*, 2007; Shi *et al.*, 2008; Zhou *et al.*, 2008) upon ADO treatment. p53 upregulation was due to its phosphorylation on threonine 81 by JNK activation (Zhou *et al.*, 2008), leading to increased stabilization and decreased degradation.

JNK activation was caused by a drop in cellular glutathione (GSH) in the presence of ADO and buthionine sulfoximine (BSO), an inhibitor of cellular GSH biosynthesis. ADO increases GSH synthesis due to increased expression of glutamate cysteine ligase (GCL), but GSH synthesis is halted in the presence of BSO. This resulted in activation of the upstream apoptosis signal regulating kinase 1 (ASK1) and its downstream kinases (Ji *et al.*, 2011).



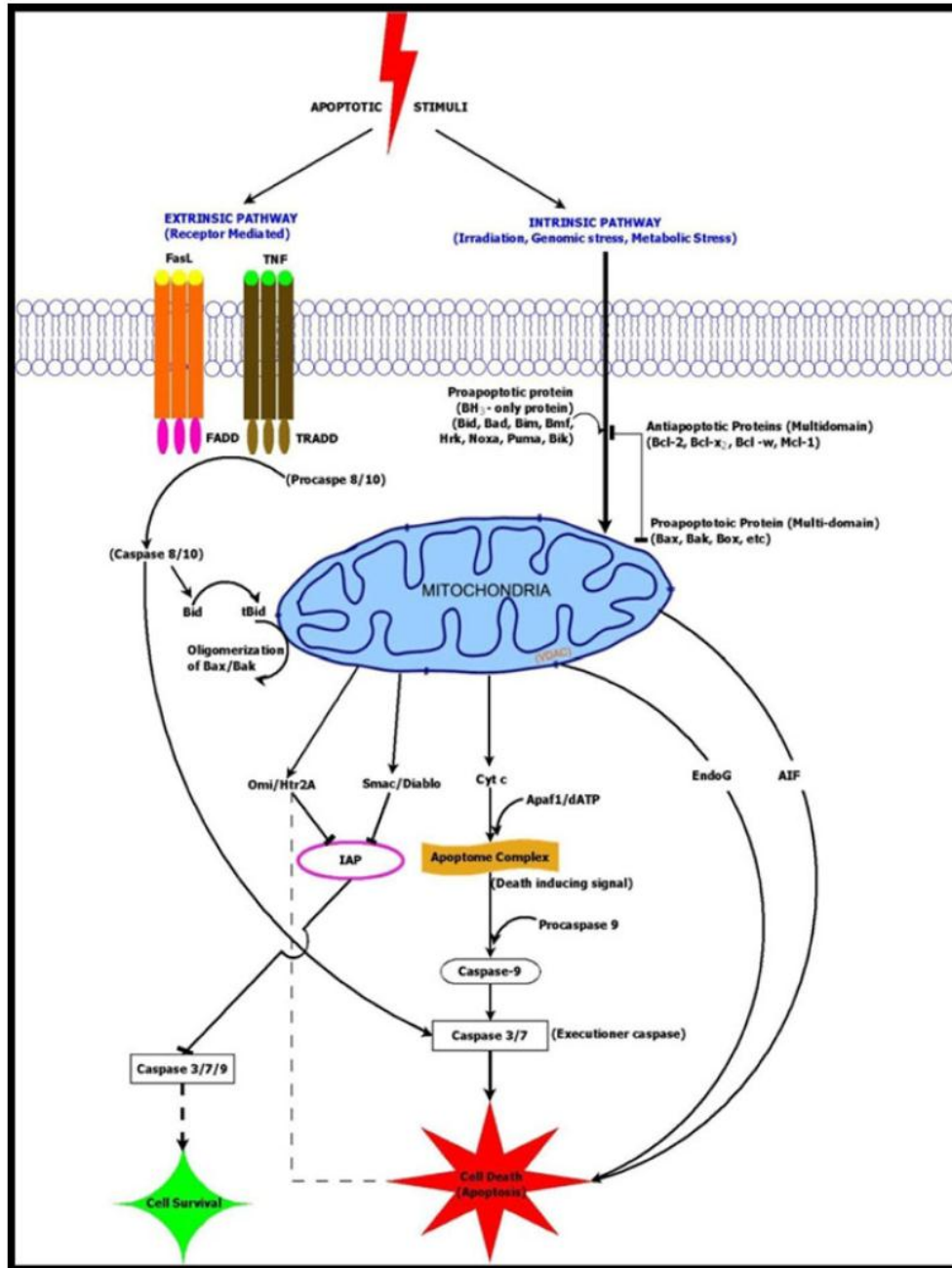


Figure 1.3 Extrinsic and intrinsic pathways of apoptosis and roles of proapoptotic and anti-apoptotic proteins. (Ola *et al.*, 2011). Permission granted courtesy of Springer.

### **1.8.2. Inhibition of tumour-promoting signalling**

Another anti-cancer mechanism through which ADO acts is inhibition of signalling pathways which are capable of causing tumour growth. IL-6 is an important cytokine which is an autocrine that promotes growth in human prostate cancer cells, and ADO suppression of IL-6 synthesis and expression led to the inhibition of downstream IL-6 signalling targets – STAT3, ERK1/2 and Akt. This caused the induction of apoptosis, inhibiting tumour growth, and migration of cancer cells (Chun *et al.*, 2010). Another important receptor involved in prostate cancer growth is the androgen receptor (AR), which is especially important for castration resistant prostate cancer survival. AR is upregulated in presence of dihydrotestosterone (DHT), and DHT is responsible for inducing prostate growth as well as progression of prostate cancer. In both the presence and absence of DHT, ADO could decrease AR synthesis and expression, as well as nuclear translocation of AR, inhibiting transcription of downstream genes such as the prostate-specific antigen (PSA); ADO also disrupted AR binding to heat shock protein 90, reducing the stability of AR. These effects on AR combined to induce apoptosis and reduce cell viability (Liu *et al.*, 2011).

ADO is capable of suppressing constitutive activation of signal transducers and activators of transcription-3 (STAT3), a transcription activator, as well as IL-6 induced STAT3 activation. Upon activation, STAT3 is phosphorylated and translocates to the nucleus to initiate transcription of genes involved in cell cycle progression such as cyclin D1 and c-Myc (Quesnelle *et al.*, 2007). ADO suppression of STAT3 is due to its inhibition of Janus activated kinase (JAK) 1 and 2 signalling, causing a decrease in STAT3 association with gp130, and decrease in nuclear

translocation. This led to sensitization of various cancer cell lines that were previously resistant to doxorubicin (Zhou *et al.*, 2010).

Although activation of the immune system is important to protect the host from infection, chronic inflammation is known to lead to carcinogenesis, due to release of reactive oxygen species and nitric oxide, which can lead to cellular mutagenesis. During inflammation, NF- $\kappa$ B, a pro-survival signalling pathway, is activated. ADO is immunosuppressive and known to be able to inhibit the NF- $\kappa$ B signalling pathway in immune cells (Xia *et al.*, 2004), and ADO treatment on Ras-transformed cancer cells and tumour growth inhibited the pro-survival signalling pathways Akt and NF- $\kappa$ B, sensitizing them to radiation (Hung *et al.*, 2010). NF- $\kappa$ B inhibition by ADO was similarly replicated in an oral squamous carcinoma hamster model and Tb human tongue squamous cell carcinoma cells, resulting in cell cycle arrest, increase in apoptosis and decrease in cancer cell proliferation (Wang *et al.*, 2011).

### **1.8.3. Inhibition of migration**

One of the hallmarks of cancer progression is the loss of adhesion and acquisition of the ability to metastasize from the site of the primary tumour. Thus, one of the approaches to treat cancer is to target the metastatic capability of the tumour, and the anti-cancer candidate ADO is able to inhibit migration and invasion of lung (Lee *et al.*, 2010) and colorectal cancer cells (Shi *et al.*, 2009; Chao *et al.*, 2010a) by various mechanisms.

Src is an oncogenic tyrosine kinase controlling various signalling pathways, and transformation of cells with the constitutively active mutant v-Src results in change in

cellular morphology, loss of adhesion and increase in invasion ability. In ADO treated v-Src transformed cells, morphology transformation, decrease of the adhesion molecule E-cadherin and actin filament disorganization is inhibited. This is due to decreased v-Src protein expression due to increased ubiquitination, leading to a cellular decrease in tyrosine phosphorylation. Increased phosphorylation of ERK1/2 mediates v-Src transformation of cells, and it is also inhibited upon ADO treatment. Hence, ADO can inhibit oncogenic transformation of cells (Liang *et al.*, 2008).

Cleavage of cell adhesion to the extracellular matrix by the matrix metalloproteases (MMP) is one of the steps for tumour cells to acquire mobility. One of the mechanisms by which ADO is anti-metastatic is its ability to inhibit the activity, synthesis and protein expression of MMP-7. One of the transcription factors responsible for synthesizing MMP-7 is the AP-1 complex, and AP-1 DNA binding is lowered upon ADO treatment. This is due to inhibition of the PI3K signalling pathway, which lowered c-Jun and c-Fos nuclear translocation, make up the AP-1 complex (Shi *et al.*, 2009; Lee *et al.*, 2010). MMP-2 activity was also decreased without affecting its expression, and ERK signalling, which is responsible for promoting invasion, was inhibited (Chao *et al.*, 2010a).

In the initial process of metastasis, cancer cells leave the primary tumour site to enter circulation in the bloodstream, and they bind to endothelial cells in the vessel walls through adhesion molecules such as E-selectin with the aid of oligosaccharides such as sialyl Lewis<sup>x</sup> (Sle<sup>x</sup>) in order for them to undergo extravasation. ADO is known to decrease gastric cancer cells adhesion to the TNF- $\alpha$  induced endothelium through

downregulating E-selectin expression on endothelial cells and its binding partner  $Sle^x$  (Jiang *et al.*, 2007).

#### **1.8.4. Induction of cytotoxic immune response**

Induction of the cytotoxic immune response is an important mechanism for control of cancer progression, since cytotoxic ADO and the ethanol extract of *A. paniculata* (APE) can induce an increase in natural killer (NK) cell activity, antibody-dependent cell-mediated cytotoxicity (ADCC) and antibody-dependent complement-mediated cell cytotoxicity (ACC) in Ehrlich Ascites Carcinoma (EAC) tumour bearing mice. Mitogens such as concanavalin A, phytohaemagglutinin, and in some cases, poke weed mitogen or lipopolysaccharide, together with ADO and APE enhanced the proliferation of splenocyte, thymocyte and bone marrow derived cells. Cytokines such as IL-2, which controls T cell proliferation, and IFN- $\gamma$ , which enhances MHC class I presentation of antigens and has anti- tumour activity, were also upregulated (Sheeja & Kuttan, 2007b). Similar results were seen for B16F10 metastatic melanoma tumour bearing mice (Sheeja & Kuttan, 2010), and EL4 thymoma cells (Sheeja & Kuttan, 2007a).

ADO can also be used in combination with other forms of anti-cancer therapy such as chemotherapy, radiotherapy and hyperthermia treatment to augment the immune system. Treatment using ADO in combination with these other therapies results in increased white blood cell count, decreased tumour volume, upregulation of pro-inflammatory cytokine production (IL-2, GM-CSF, TNF- $\alpha$ ), and decreased myeloperoxidase levels. Myeloperoxidase levels are associated with tumour development (Sheeja & Kuttan, 2008).

In addition to the above effects, ADO also has other anti-neoplastic effects. One of the treatments to inhibit uncontrolled proliferation of promyelocytic leukaemia cells is to induce differentiation of these cells through activating the retinoic acid receptor pathway to form mature granulocytes. In addition to inducing apoptosis of these cells, ADO is capable of inducing differentiation in a retinoic acid receptor independent manner at the low dose of 4.5  $\mu\text{M}$  (Manikam & Stanslas, 2009), causing them to have a restricted reproductive capability. Short treatments with ADO can also reduce levels of hypoxia inducible factor-1  $\alpha$  (HIF-1 $\alpha$ ) in non small cell lung cancer (NSCLC) through inhibiting the transforming growth factor –  $\beta$  signalling pathway, leading to increased proteolytic degradation of HIF-1  $\alpha$ . This inhibits vascular endothelial growth factor (VEGF) signalling, hence inhibiting cancer growth (Lin *et al.*, 2011)

In summary, ADO is capable of acting as cytotoxic agent either on its own, or in combination with different chemotherapy agents such as 5-fluorouracil (FU) and tumor necrosis factor (TNF)-related apoptosis inducing ligand (TRAIL); it can induce cytotoxicity in cancers which may be resistant to classical therapies; or apoptosis in cancer cells. It is also capable of inhibiting pro-tumourigenic signalling pathways, angiogenesis as well as migration. Cancer cell sensitivity to chemotherapy could also be restored in multidrug resistant cancer cell line by ADO treatment, possibility due to lower expression of the efflux glycoprotein P-170 (Han *et al.*, 2005).

# **Chapter 2**

# **Materials and Methods**

## **2. Materials and Methods**

### **2.1. Maintenance of cell lines**

#### **2.1.1. Media and growth conditions**

A-431 human skin epithelial carcinoma cells (CRL-1555), HeLa (CCL-2) and N9 microglia were obtained from ATCC, and cultured in Dulbecco's Modified Essential Medium (DMEM) (Gibco, Singapore).

DMEM was supplemented with fetal bovine serum (FBS) (Gibco, Singapore), 2 mM L-glutamine (Gibco, Singapore), 0.1 mM non-essential amino acids (Gibco, Singapore), 5 mM HEPES buffer (pH 7.2-7.5) (Gibco, Singapore) and 1X antibiotic-antimycotic (Gibco, Singapore). All cells were grown at 10% FBS (v/v) with DMEM with the exception of A-431, which was grown with 5% FBS in DMEM. Cells that were serum-starved were grown in DMEM with all the above supplements except FBS. Cells were routinely grown at 37 °C with 5 % CO<sub>2</sub>.

Cells were dislodged from the culture flasks by incubation with 0.25 % trypsin-EDTA in phosphate buffered saline (PBS) (Gibco, Singapore) for approximately 10 min, and trypsin was inactivated with the addition of complete media. Cells were then pelleted at 1500 rpm at room temperature for 5 min, resuspended in fresh media and seeded accordingly.

#### **2.1.2. Cryopreservation of cell lines**

A confluent flask of cells was trypsinised and pelleted. The cell pellet was then resuspended in a solution with 90 % FBS and 10 % DMSO as the cryoprotectant and frozen at -80 °C, and in liquid nitrogen for long term storage.



## 2.2. Antibodies

The primary antibodies used are: anti-EGFR (Clone F4, Sigma, Singapore); anti-phosphorylated EGFR (BD Bioscience, San Jose, California, USA), anti-TfR (OKT9, monoclonal hybridoma), anti-CD204 (AbD Serotec, Oxford, UK), anti-early endosomal antigen-1 (Santa Cruz Biotechnology, California, USA), anti- $\beta$ -actin (Sigma, Singapore), anti-vesicle associated membrane protein-3 (VAMP-3), VAMP-8 (Synaptic Systems, Germany), anti-lysosomal associated membrane protein-1 (LAMP-1) (eBiosciences, San Diego, USA). Secondary fluorescence-conjugated antibodies were obtained from Jackson Laboratory, and secondary horse radish peroxidase conjugated antibodies were obtained from Thermo Scientific.

**Table 2.1 Catalogue of primary antibodies used**

Antibodies against	Clone (for mAb)	Company	Reference
Epidermal growth factor receptor (EGFR)	Clone F4	Sigma	-
Phosphorylated EGFR	74	BD Bioscience	-
Phosphorylated EGFR (serine 1046/ 1047)	N.A.	Cell Signaling	-
Epidermal growth factor receptor (EGFR), extracellular domain.	Clone LA1	Millipore	-
Epidermal growth factor receptor (EGFR), extracellular domain.	Clone 29.1	Sigma	
Transferrin Receptor	OKT9	monoclonal hybridoma	(Goding & Burns, 1981)
CD204	Clone 2F8	AbD Serotec	-
early endosomal antigen-1	N.A.	Santa Cruz Biotechnology	-
anti- $\beta$ -actin		Sigma	-
anti-vesicle associated membrane protein-3 (VAMP-3)	N.A.	Synaptic Systems	-
anti-vesicle associated membrane protein-8 (VAMP-8)	N.A.	Synaptic Systems	-

Mouse anti-lysosomal associated membrane protein-1 (LAMP-1)	eBioH4A3	eBiosciences	-
Rabbit anti-lysosomal associated membrane protein-1 (LAMP-1)	N.A.	Thermo Scientific	-
CD36	CRF D-2712	BD Bioscience	-
MARCO	ED31	AbD Serotec	-
phosphorylated ERK1/2	N.A.	Cell Signalling	-
ERK1/2	N.A.	Cell Signalling	-
Phosphorylated JNK	N.A.	Cell Signalling	-
JNK	N.A.	Cell Signalling	-
Phosphorylated MAPK p38	N.A.	Cell Signalling	-
p38 MAPK	N.A.	Cell Signalling	-

### 2.3. Other Reagents

ADO of purity  $\geq 95\%$  was purchased directly from Calbiochem, resuspended in DMSO to give a stock solution of 50 mM and stored at  $-20\text{ }^{\circ}\text{C}$ . Alexa-fluor 488 labelled transferrin and alexa-fluor 555 EGF were purchased from Molecular Probes, resuspended in sterile water to give a final concentration of 2 mg/ml (transferrin) or 200  $\mu\text{g/ml}$  (EGF). Human recombinant EGF was purchased from Roche Applied Science, resuspended in sterile water to give a stock solution of 0.5 mg/ml. Holo-transferrin was purchased from Sigma and resuspended in sterile water to give a stock solution of 2 mg/ml. Carboxylate modified fluorescent green 1  $\mu\text{m}$  latex beads for phagocytosis assays were purchased from Sigma-Aldrich.

### 2.4. Cellular Analysis

#### 2.4.1. Cell Viability Assay

Cell viability was assessed by MTT (3-(4,5-dimethylthiazol-2-yl)-2,5-diphenyltetrazolium bromide) (Sigma) as previously described (Li *et al.*, 2007; Pannecouque *et al.*, 2008). Briefly, cells were seeded into a 96 well microplate and routinely cultured. Cells were then exposed to ADO (0-160  $\mu\text{M}$ ) for 24 h. The amount

of DMSO (1% v/v) in each well was standardised across all samples. 20  $\mu$ l of tetrazolium dye solution (5 mg/ml in phosphate buffered saline, PBS) was added to each well and incubated for 1 h with shaking in the dark. Cells were then lysed overnight in the presence of lysis buffer at 37 °C to dissolve the formazan crystals. The absorbance was then read using a microplate reader (Tecan Gemini Infinite 200) at 540 nm, and with reference filter at 690 nm to deduct for absorbance due to cell debris.

## **2.4.2. Indirect Immunofluorescence**

### **2.4.2.1. Steady State Studies**

Immunofluorescence microscopy was performed as described previously (Wong *et al.*, 1998; Wong *et al.*, 1999). Briefly, cells grown on coverslips were treated for 4 h with DMSO (0.2% v/v) or ADO and fixed in 4% (w/v) paraformaldehyde on ice. After fixing, the cells were then permeabilized with 0.1% (w/v) saponin (Sigma) in PBS, and stained with the corresponding primary antibodies and secondary fluorescence-conjugated antibodies (Jackson Immunoresearch). The coverslips were mounted using fluorescence mounting medium (Vector Laboratories). Conventional images were taken with the fluorescent microscope (Olympus BX60).

### **2.4.2.2. Endocytosis Studies**

Cells were serum starved when labelled epidermal growth factor (EGF) was used in the experiment. The cells were pretreated with DMSO (0.2% v/v) or ADO for 30 min, then incubated with mouse antibody EGFR (Clone 29.1, Sigma, Singapore), or 1.6  $\mu$ g/ml Alexa Fluor 555- labelled epidermal growth factor (EGF) (Invitrogen, Singapore) or mouse anti transferrin receptor OKT9 for 1 h on ice, to allow the

antibody or ligand to bind to cell surface receptors. Cells were then replaced into media containing DMSO (0.2% v/v) or ADO, washed and fixed at the appropriate time points, then stained and mounted in the manner stated above. Confocal microscopy was carried out using the Olympus FV500 confocal microscope, and images obtained were processed using the Olympus Fluoview software.

#### **2.4.2.3. Phagocytosis Immunofluorescence Assay.**

Cells were incubated in Opti-MEM (Invitrogen) for 3 h and then treated with ADO for 3 h. Green fluorescent protein (GFP) expressing bacteria were then added to the cells for 10 min to allow for phagocytosis to occur. The bacteria were then washed off by PBS, and the cells were fixed with 4% (w/v) paraformaldehyde on ice for 25 min prior to washing with PBS. Fixed cells (200 cells) were randomly selected, and the number of bacteria remaining on the coverslip, as well as the number of cells was enumerated. The number of bacteria per cell was expressed as a percentage of the vehicle control.

#### **2.4.3. Fluorescence-activated Cell Sorting (FACS)**

##### **2.4.3.1. Quantification of cell surface receptors**

Cells were pretreated with DMSO (0.2% v/v) or ADO, and harvested using 2 mM EDTA. Cells were then quantified using a haemocytometer, and  $1 \times 10^6$  cells from each sample were used. Cells were blocked using 0.5 % bovine serum albumin (BSA) in PBS for 20 min, and probed with primary antibodies for 1 h, washed, and probed with secondary antibodies for 1 h. Cells were washed, fixed with 2% (w/v) paraformaldehyde and analysed using the Cytomics FC 500 Series Flow Cytometry Systems (Beckman Coulter).

#### **2.4.3.2. Endocytosis Assay**

Cells were first pretreated with DMSO (0.2% v/v) or ADO for 4 h, detached from the plate using 2 mM EDTA, and then incubated with anti-EGFR (Clone 29.1, Sigma, Singapore) or OKT9 on ice for 1 h. The cells were then washed and replaced in complete media with DMSO or ADO and incubated at 37 °C. At the appropriate time points, remaining surface bound antibody was washed off cells with an acid wash (pH 2.0). The cells were then fixed with methanol, stained with anti-mouse FITC (Jackson ImmunoResearch, West Grove, Pennsylvania, USA) and analysed using the Cytomics FC 500 Series Flow Cytometry Systems (Beckman Coulter). The percentage of internalised EGFR was calculated by the following formula: mean fluorescence intensity from intracellular EGFR/ (mean fluorescence intensity from total EGFR) x 100.

#### **2.4.3.3. Quantification of intracellular receptors**

Cells were first pretreated with DMSO (0.2% v/v) or ADO for 3 h, fixed for 25 minutes on ice using 4% (w/v) paraformaldehyde, washed 3 times, followed by permeabilization with 0.2% (w/v) saponin in PBS for 30 min at room temperature. Cells were then incubated with the appropriate primary antibodies, washed, centrifuged, incubated with the appropriate secondary antibodies, washed and analysed.

## **2.4.4. Western Blot Analysis**

### **2.4.4.1. Steady-state studies**

Cells were pretreated with DMSO (0.2% v/v) or ADO for 4 h, harvested by 2 mM EDTA and lysed for 1 h using 1% (v/v) Triton X-100, supplemented with 2x complete protease inhibitor cocktail (Roche, Indianapolis, Indiana, USA) and 2 mM phenylmethanesulphonylfluoride, in PBS. Protein concentration was read using the Bradford assay (Bio-Rad), resolved on an SDS-PAGE gel and transferred to a nitrocellulose membrane (Bio-Rad). Blots were then blocked with 5 % (w/v) skimmed milk in PBS containing 0.1% (v/v) Tween-20 and probed using the primary antibodies and secondary antibodies at room temperature in blocking buffer. The secondary antibodies used were either anti mouse or rabbit conjugated horse radish peroxidase IgG antibodies (Thermo Scientific), depending on the serotype of the primary antibody used. The immunoreactive bands were visualised using chemiluminescent substrate (Thermo Scientific) and exposed to X-ray film (Thermo Scientific). The resulting blot was then scanned and band signals were quantified using ImageJ and normalised to the appropriate control.

### **2.4.4.2. Kinetics studies**

Cells were incubated on ice with the primary antibody against the protein of interest for 1 h, washed, and replaced in complete media with DMSO (0.2% v/v) or ADO, incubated at 37 °C in the CO<sub>2</sub> incubator for varying time-points. Cells were then detached from the plate using 2 mM EDTA and lysed. The lysate was then separated on a SDS-PAGE gel and transferred onto a nitrocellulose membrane (Bio-Rad). The blots were then blocked with 5 % (w/v) skimmed milk in PBS and 0.1% (v/v) Tween-

20 and probed using the appropriate horse radish peroxidase conjugated secondary antibody.

#### **2.4.4.3. L-cysteine blocking assay**

ADO was incubated with 5mM L-cysteine in DMEM at 37 °C for 1 h and the resultant mixture was added to A-431 cells and incubated for 4 h, before the cells were washed, lysed and analysed by Western blot.

#### **2.4.5. Reverse-transcription polymerase chain reaction (RT-PCR)**

Cells were pretreated with DMSO (0.2% v/v) or ADO for 4 h. Total RNA was extracted using TRIzol reagent (Invitrogen) following the manufacturer's instructions. First strand synthesis was performed using 7 µg of total RNA, oligo dT primer and M-MLV Reverse Transcriptase (Promega) following the manufacturer's instructions and polymerase chain reaction (PCR) performed using the GeneAmp PCR System 9700 (Applied Biosystems) using the following cycling conditions: 94 °C for 2 min; 94 °C for 15 s, 60 °C for 15 s, 72 °C for 30 s and repeated for 22 cycles; 72 °C for 5 min. The corresponding PCR product was then analysed by agarose gel electrophoresis.

Primers: EGFR forward primer 5'-ATGCAAATAAAACCGGACTGAAGG-3'

EGFR reverse primer 5'-ACGTGGTGGGGTTGTAGAGCA-3'

β- actin forward primer

5'-GAACCCTAAGGCCAACCGTGAAAAGATG-3'

β- actin reverse primer 5'-GGCCAGCCAAGTCCAGACGCAG-3'

#### **2.4.6. Recycling Assay**

Cells were pretreated with DMSO (0.2 % v/v) or ADO and starved in serum free DMEM for 4 h. Cells were then incubated with Alexa Fluor 488 conjugated transferrin (Invitrogen) for 1 h in a water bath at 17 °C in the presence of the compound to allow transferrin to be trapped in the recycling compartment. Residual surface transferrin was then washed off with ice cold acetic acid wash (pH 3.5) and the cells were then washed with DMEM and PBS. Cells were then replaced in the CO<sub>2</sub> incubator in PBS, with holo-transferrin and either DMSO or ADO, to allow for the trapped transferrin to be recycled. PBS was collected at selected time points and the cells in the dish lysed. Amount of fluorescent transferrin in PBS and cell lysates was quantified using the microplate reader (Tecan Gemini Infinite 200) using an excitation wavelength of 480 nm and emission wavelength of 520 nm. The percentage of intracellular transferrin was calculated by the following formula:

fluorescence from lysate/ (fluorescence from lysate + fluorescence from PBS) x 100.

#### **2.4.7. Phagocytosis Assay**

##### **2.4.7.1. Vybrant Phagocytosis Assay**

The assay was conducted based on the protocol of the Vybrant phagocytosis assay (Invitrogen). Briefly, cells seeded in 96-wells were incubated with 25 µl of either anti-CD36, or anti-CD204 or anti-MARCO antibodies in media on ice for 1 h in media, before 25µl of K-12 fluorescent *E. coli* bioparticles with the appropriate amount of antibodies were added in and allowed to internalise for 1 h at 37 °C. The bioparticles were removed and trypan blue was added to the wells for 1 min to quench the fluorescence of extracellular particles. Trypan blue was then removed and the amount



of bioparticles engulfed by cells measured using the Tecan Gemini Infinite 200 plate reader using 480nm for excitation and 520nm for emission.

#### **2.4.7.2. Suspension Phagocytosis Assay**

Cells were treated with varying concentrations of ADO for 3 h, then incubated with fixed green fluorescent protein (GFP) expressing bacteria and ADO for 10 min. The mixtures were washed with PBS, spun down at 1500 rpm for 5 min at 4 °C and fixed in 2% (w/v) paraformaldehyde for 30 min. The amount of internalised bacteria was read using the Cytomics FC 500 Series Flow Cytometry Systems (Beckman Coulter) with gating for cells.

#### **2.4.8. p38 MAP Kinase assay**

Cells were starved overnight in serum-free DMEM, and then treated with ADO for 4 h, or 100ng/ml recombinant EGF for 15 min. Cells were then rinsed 1x with cold PBS and processed according to the instructions in the p38 MAP kinase assay kit (Cell Signalling Technology, Beverly, Massachusetts, USA). Briefly, cells were lysed and immunoprecipitated with immobilized phospho-p38 MAPK antibody overnight. The beads were washed and then incubated with ATF-2 fusion protein and ATP for 30 min at 30 °C to allow for p38 MAPK to phosphorylate ATF-2. Levels of phosphorylated ATF-2 was then detected using western blot analysis.

#### **2.4.9. CD204 secretion assay**

Cells were seeded overnight in a 96-well plate, washed once in OPTI-MEM, and then treated in OPTI-MEM with ADO for 8 h. Cells were then dislodged by 2 cycles of incubation with 2 mM EDTA for 10 min followed by 5 times of washing. Secreted

CD204 was then fixed with 4% (w/v) paraformaldehyde for 20 min followed by washing. Wells were then blocked overnight with 10 % (w/v) BSA in PBS. Wells were then rinsed with 0.05% (v/v) Tween-20 in PBS, and 2  $\mu\text{g/ml}$  anti-CD204 antibody was then added for an hour. Primary antibody was then rinsed off with 0.05% (v/v) Tween-20 and 1:500 anti-rat Cy3-conjugated secondary antibody was added for 1 h. Excess secondary antibody was then rinsed off and the plate was read using the Tecan Gemini Infinite 200 plate reader using 555nm for excitation and 580nm for emission.

# **Chapter 3**

## **Andrographolide affects receptor trafficking in A-431 cells**

### **3. Andrographolide affects receptor trafficking in A-431 cells**

#### **3.1. Abstract**

ADO, an active component of *Andrographis paniculata*, is known to affect the levels of cell surface receptors present on dendritic cells after activation with lipopolysaccharide. Hence, we were interested to investigate if ADO could affect receptor trafficking in general. We used the epidermoid carcinoma cell line, A-431, as a model as it over-expresses two receptors which have different trafficking pathways. The epidermal growth factor receptor (EGFR), is known to endocytose and move to the lysosomes for degradation, whereas the transferrin receptor (TfR) endocytoses and recycles constitutively back to the cell surface. We found that ADO changed the degradation rates of EGFR and TfR; it decreased surface levels of EGFR through increasing EGFR internalisation, and accumulated EGFR in a lysosomal associated membrane protein-1 (LAMP-1) positive compartment.

#### **3.2. Introduction**

ADO is the main active constituent of the plant *Andrographis paniculata*. This versatile compound has been found to have hepatoprotective effects against toxic substances (Sheeja & Kuttan, 2006), and it is also anti-inflammatory in nature, as it can suppress inflammation by inhibiting the nuclear translocation of NF- $\kappa$ B (Singha *et al.*, 2007; Bao *et al.*, 2009). Previously, it has also been demonstrated to be an anti-cancer compound, as it can cause apoptosis in hepatocellular carcinoma cells (Yang *et al.*, 2009b), as well as induce cell cycle arrest in colorectal carcinoma cells (Shi *et al.*, 2008). Furthermore, ADO affects dendritic cell maturation by inhibiting the

upregulation of I-A<sup>b</sup>, CD40 and CD86 upon lipopolysaccharide induction of dendritic cells (Iruretagoyena *et al.*, 2005). This suggested that ADO may have an effect on the trafficking of these molecules to the cell surface, and thus we hypothesised that the anti-neoplastic effect of ADO could be due to the ability of ADO in regulating cell surface expression and trafficking of growth-regulating receptors such as the epidermal growth factor receptor (EGFR) and the transferrin receptor (TfR). These two receptors are of interest as both are known to be upregulated in cancers. In particular, EGFR has been known to be upregulated in various cancers involving the head and neck (Gold *et al.*, 2009), lung (Dy & Adjei, 2009), gliomas (Kesari *et al.*, 2006) and ovaries (Lafky *et al.*, 2008); while TfR is known to be overexpressed in breast cancer (Habashy *et al.*, 2009). As such, EGFR and TfR have become prime targets in the development of cancer therapies (Lepelletier *et al.*, 2007; Capdevila *et al.*, 2009), and hence they are also the focus of our current study. In addition, these two receptors follow different pathways upon internalisation into the cell. Hence, observations of the effects of ADO on these two receptors would be useful in the detection of how ADO may differentially affect trafficking of these receptors within the cell. Furthermore, the trafficking of these receptors have been extensively studied, making it much easier to establish the membrane compartments which ADO affects.

### **3.2.1. Epidermal Growth Factor Receptor (EGFR)**

EGFR is a 170 kDa transmembrane receptor tyrosine kinase that has been extensively characterised. It is an important player in activating signaling pathways for cell growth. In its inactive state, it is known to localise on the plasma membrane to cholesterol-rich lipid rafts, which are detergent resistant regions that are distinct from caveolae (Pike, 2005). Upon the binding of EGF to EGFR, the tyrosine kinase

receptors dimerize and autophosphorylate, forming the active state where it triggers the Ras- mitogen associated protein kinase (MAPK) pathway for cell proliferation. The receptors are then internalised into the cells for downregulation. In the classical pathway, upon the dimerization and phosphorylation of the receptors, they move into clathrin coated pits. Cbl, a ubiquitin E3 ligase, then binds at and ubiquitinates the receptors and the proteins associated with EGFR, epsin and EPS15 (Le Roy & Wrana, 2005). The ubiquitination of EGFR is important for the sorting of the receptors to the endosomes for degradation. Upon entry into the cell, the receptor then moves to the early endosomes. It is then either recycled back up to the cell surface, or moves to the multi vesicular body (MVB) and then to the late endosomes and lysosomes for degradation through association with the endosomal sorting complex required for transport (ESCRT).

The notion that EGFR is capable of clathrin independent endocytosis has been explored in various studies recently. Caveolae, which are lipid rich rafts with associated caveolin-1 and the absence of clathrin, were found to contain EGFR (Sigismund *et al.*, 2005). However, although EGFR is associated with caveolae, there is no concrete evidence to demonstrate that caveolae are important for EGFR internalisation (Sigismund *et al.*, 2008; Madshus & Stang, 2009). Another clathrin independent mode of EGFR internalisation is via circular dorsal ruffles, which recruits large amounts of surface EGFR into membrane ruffles with the aid of dynamin, phosphatidylinositol-3-kinase and EGFR activation (Orth *et al.*, 2006; Orth & McNiven, 2006). This mode of internalisation usually occurs in the presence of high amounts of EGF (30 ng/ml). Although EGFR can be internalised in a clathrin-

independent manner, the primary mode of internalisation is likely to be mainly via clathrin coated pits as it is the most rapid mode of internalisation (Sorkin & Goh, 2009).

### **3.2.2. Transferrin Receptor**

TfR, is a 95kDa transmembrane receptor that is one of the important proteins involved in the uptake of iron (Daniels *et al.*, 2006). Two TfR binds transferrin, which binds to two ferric ions, and like EGFR, is endocytosed in clathrin-coated pits. It then moves to the sorting endosomes, where the iron ions are released due to the lower pH of the endosomes, to the endocytic recycling compartment, and back to the plasma membrane (Maxfield & McGraw, 2004). TfR was chosen as a marker of the recycling pathway as it is known to constitutively recycle.

The aim of this part of the work is to elucidate the effects of ADO on receptors critical for cell proliferation and survival in the human epidermoid carcinoma A-431 cells. A-431 was chosen as it is a cancer cell line, and it expresses our receptors of interest at high levels – epidermal growth factor receptor (EGFR) (Wrann & Fox, 1979) and transferrin receptor (TfR) (Hopkins & Trowbridge, 1983). In this study, we show that ADO causes the downregulation of EGFR from the cell surface as well as the inhibition of EGFR and TfR degradation.

### 3.3. Results

#### 3.3.1. Andrographolide inhibits growth and downregulates surface EGFR

In order to understand the effect of ADO on cell proliferation, A-431 cells were exposed to varying concentrations of ADO for 24 h and analysed by the MTT cytotoxicity assay. As expected from previous work on several other cancer cell lines such as colon cancer (Rajagopal *et al.*, 2003; Kumar *et al.*, 2004), prostate cancer (Kim *et al.*, 2005), liver cancer, (Li *et al.*, 2007), leukaemia (Cheung *et al.*, 2005), cervical cancer (Zhou *et al.*, 2006), and promyelocytic leukaemia cells (Manikam & Stanslas, 2009), ADO could inhibit cancer cell growth. In our experiment, growth of A-431 was inhibited significantly from 60  $\mu$ M onwards (Figure 3.1). Since EGFR is known to be one of the receptors important for cell growth and proliferation of cancer cells, we went on to investigate if surface levels of EGFR were affected upon treatment with ADO at concentrations and incubation times that are not known to cause apoptosis. This was to ensure that the effects observed on EGFR are specific to ADO, and are not due to downstream events from apoptosis. Approximately 30% of surface EGFR was downregulated upon ADO treatment at both 50  $\mu$ M and 100  $\mu$ M (Figure 3.2). Similarly, downregulation of approximately 30% of surface EGFR also occurs for treatment of A-431 at concentrations of 5  $\mu$ M and 15  $\mu$ M ADO for 48 h (Figure 3.3). The longer timepoint of 48 h was chosen to ensure that the effects of ADO were also true at lower doses.



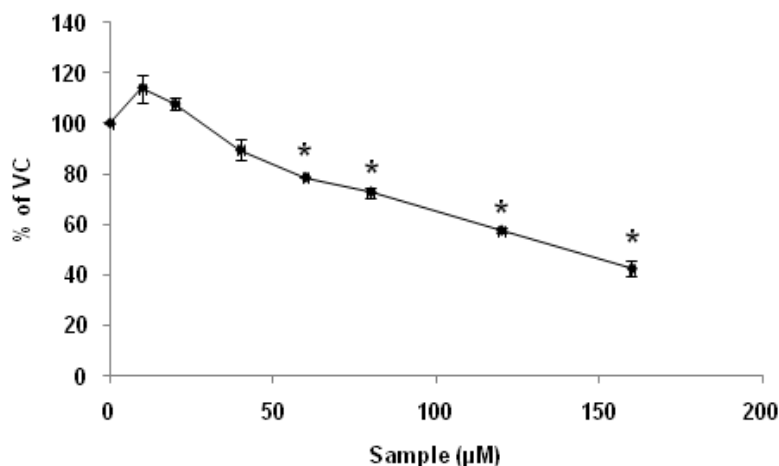


**Figure 3.1 Assessment of cell viability upon ADO treatment.** A-431 cells were treated with varying concentrations of ADO for 24h, and cell viability assessed by MTT assay. Values from each concentration were compared to the untreated cells and expressed as mean  $\pm$  standard deviation from two independent experiments. Vehicle control, VC; andrographolide, ADO. \*  $P < 0.05$  relative to vehicle control.

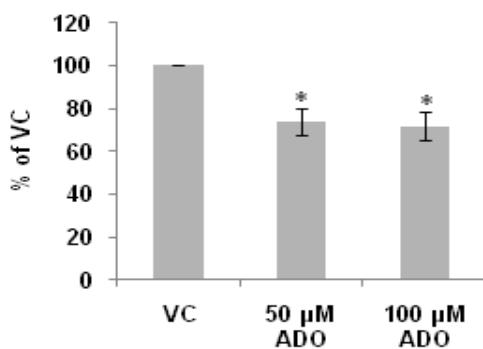


**Figure 3.2 Surface expression of EGFR after ADO treatment.** A-431 cells were treated with various concentrations of ADO for 4 h and then analysed by flow cytometry for surface EGFR. Mean fluorescence intensity of surface receptor levels is expressed as a percentage of vehicle control (VC)  $\pm$  SD of at least two experiments. Vehicle control, VC; andrographolide, ADO. \*  $P < 0.05$  relative to vehicle control.

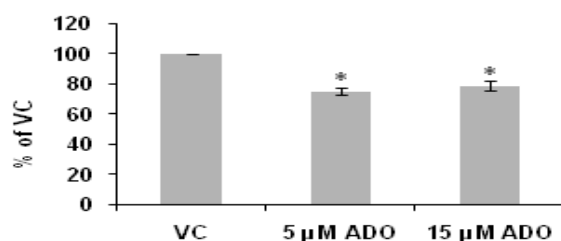


**Figure 3.3 Surface expression of EGFR after 48 h of ADO treatment.** A-431 cells were treated with various concentrations of ADO for 48 h and then analysed by flow cytometry for surface EGFR. Mean fluorescence intensity of surface receptor levels was expressed as a percentage of vehicle control (VC),  $\pm$ SD of at least two experiments. Vehicle control, VC; andrographolide, ADO. \*  $P < 0.01$  relative to vehicle control.

Since surface EGFR was downregulated by ADO, it was possible that ADO could have decreased the total amount of EGFR in A-431 cells. However, as shown in A-431 cells treated with ADO for 4 h and analysed by western blot (Figure 3.4), the total amount of EGFR was not decreased, but significantly increased by around 15% upon treatment with 100  $\mu$ M ADO.

In order to ascertain if the change in total amount of EGFR was due to increase in EGFR mRNA transcripts, total RNA was extracted from cells treated with 50  $\mu$ M and 100  $\mu$ M ADO for 4 h and analysed by RT-PCR. From the results, it is evident that there was no change in the amount of EGFR mRNA at the transcriptional level (Figure 3.5).

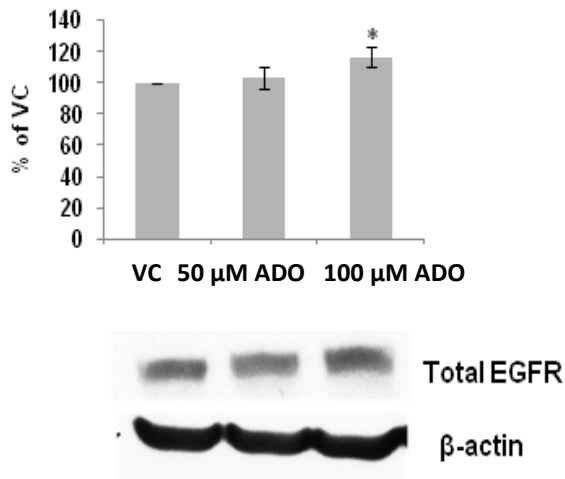


**Figure 3.4 Western blot analysis of ADO effect on total EGFRs in A-431.** A-431 cells were treated with various concentrations of ADO for 4 h and then analysed by Western blot for total EGFRs. Blots are representative of at least two experiments. Intensity of Western blot bands were quantified and normalised to  $\beta$ -actin, then expressed as a percentage of VC  $\pm$  SD of at least two experiments. Vehicle control, VC; andrographolide, ADO. \* $P < 0.005$  relative to vehicle control.

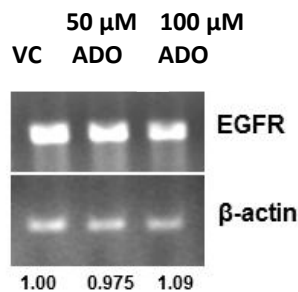
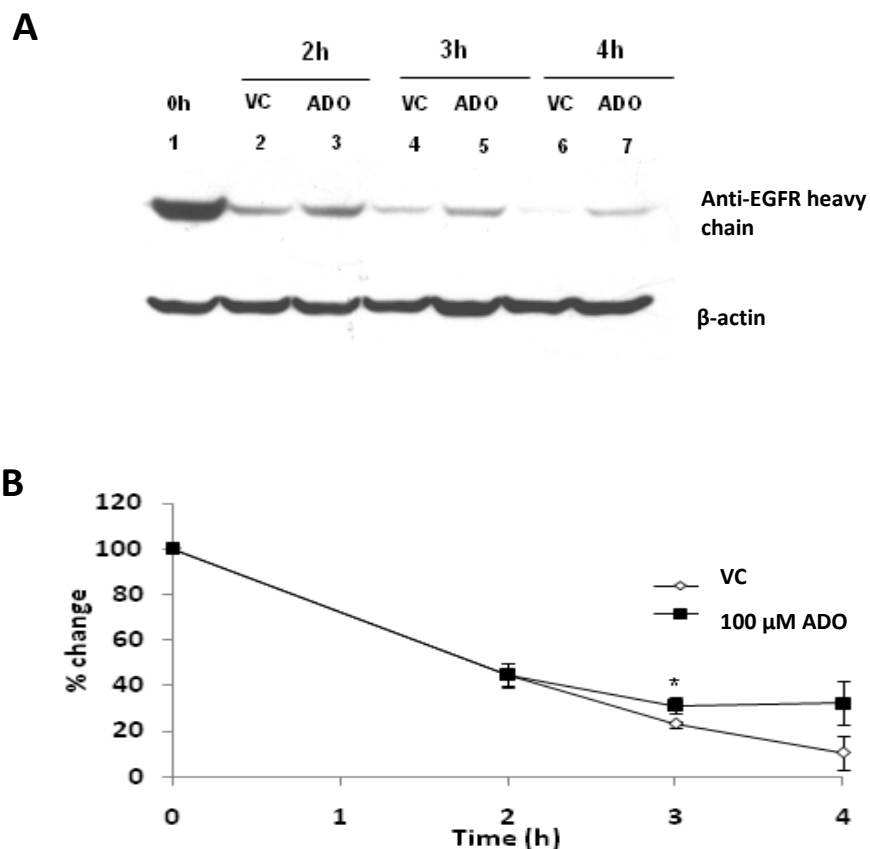


**Figure 3.5 Reverse-transcription polymerase chain reaction (RT-PCR) of EGFR mRNA transcripts.** A-431 cells were treated with various concentrations of ADO for 4 h and analysed by RT-PCR. Results are representative of two experiments. Vehicle control, VC; andrographolide, ADO.

### **3.3.2. Andrographolide changed the rate of degradation of both EGFR and TfR**

As the ADO-induced upregulation of EGFR was not due to an increase in EGFR mRNA transcripts, it is possible that ADO inhibits trafficking of EGFRs to the lysosomes for degradation in A-431 cells. To determine whether this occurs, surface EGFRs of A-431 cells were labelled with mouse EGFR-specific monoclonal antibody and internalised into the cell at various time points either in the presence or absence of ADO. Cells were then lysed and analysed by Western blot using horse radish peroxidase conjugated anti-mouse antibodies to detect the heavy and light chain of the EGFR-specific antibodies. The degradation rate of the EGFR-specific antibodies was used as a marker for determining the rate of EGFR trafficking to the late lysosomes for degradation. Significant changes in the degradation rate upon ADO treatment were observed at 3 and 4 h (Figure 3.6A, lanes 4–7, and B), and degradation was inhibited by approximately 22%. Thus, ADO delayed trafficking of EGFRs from the cell surface to the lysosomes for degradation. To ascertain whether this inhibition of degradation was specific for EGFR or if it affects general receptor trafficking from the cell surface, a similar degradation assay for TfR was run with anti-TfR antibody.

Interestingly, TfR degradation was inhibited significantly at 4 h and up to approximately 47% at 6 h (Figure 3.7A, lanes 4–7, and B). Thus, our results indicate that ADO induces the accumulation of both EGFRs and TfRs in intracellular membrane compartments of A-431 cells.



A. **Figure 3.6 ADO changed the rate of degradation of EGFR.** A-431 cells were incubated with primary antibody on ice for 1 h, treated with DMSO or ADO for the various time points at 37°C and then subjected to Western blot analysis for IgG;  $\beta$ -actin was used as a loading control. Blots are representative of at least three experiments. The intensity of the Western blot bands were quantified and normalised to  $\beta$ -actin, and expressed as a percentage of the initial amount of antibody at 0 h  $\pm$  SD of at least two experiments (A and B). Internalised EGFR was degraded more slowly in ADO-treated cells. VC, vehicle control; ADO, andrographolide, EGFR, epidermal growth factor receptor; .

- A. Western blot of internalised EGFR.  
 B. Quantification of degraded internalised EGFR. \*,  $p < 0.05$  relative to 0 h.

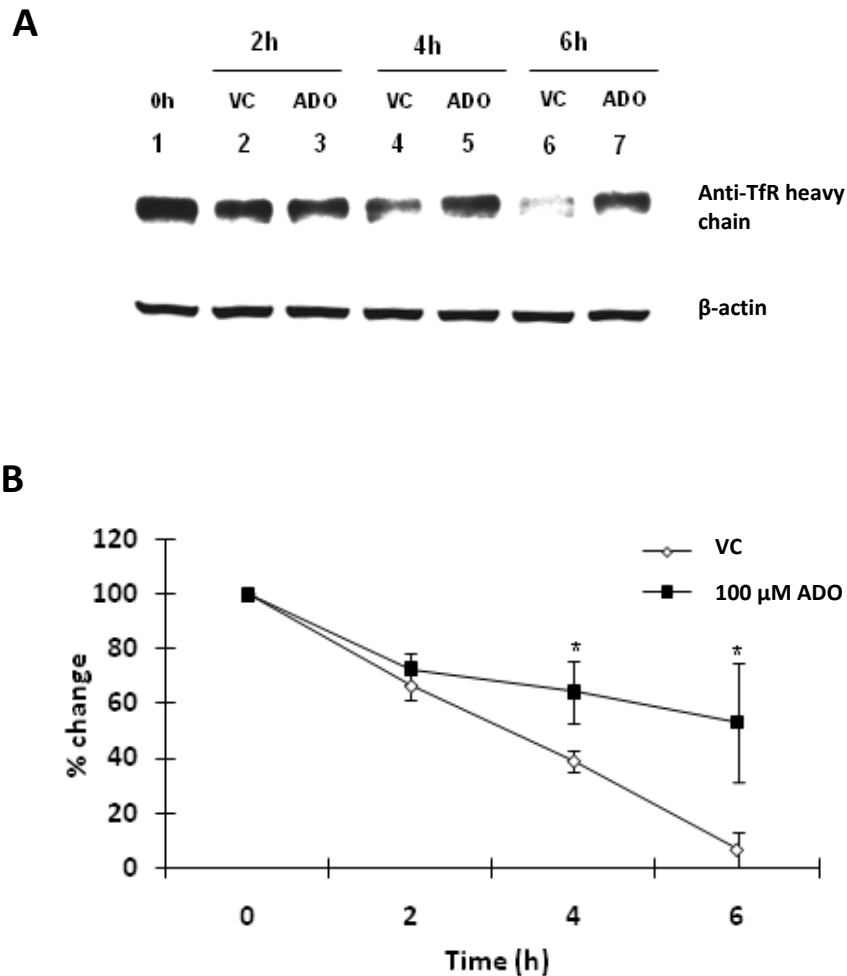


**Figure 3.7 ADO changed the rate of degradation of TfR.** A-431 cells were incubated with primary antibody on ice for 1 h, treated with DMSO or ADO for the various time points at 37°C and then subjected to Western blot analysis for IgG;  $\beta$ -actin was used as a loading control. Blots are representative of at least three experiments. The intensity of the Western blot bands were quantified and normalised to  $\beta$ -actin, and expressed as a percentage of the initial amount of antibody at 0 h  $\pm$  SD of at least two experiments (A and B). Internalised TfR accumulated in ADO-treated cells although degradation is not inhibited. VC, vehicle control; ADO, andrographolide, TfR, transferrin receptor.

B. Western blot of internalised TfR.

C. Quantification of degraded internalised TfR. \* $P < 0.05$  relative to vehicle control.

### **3.3.3. Andrographolide induced the accumulation of EGFRs into an intracellular LAMP-1- and VAMP-8-positive but VAMP-3-negative membrane compartment**

The intracellular localisation of cell surface internalised EGFR and TFR in A-431 cells upon ADO treatment was examined by immunofluorescence microscopy. A-431 cells were treated with ADO for 4 h, fixed and then stained for EGFR. As can be seen, EGFR accumulates in compact membrane structures in the perinuclear region, and this effect is slightly more apparent upon 100  $\mu$ M ADO treatment (Figure 3.8A, panel c). Upon the addition of EGF, which was utilised to drive the surface EGFR into the cell, the ADO induced accumulation of EGFR became more pronounced in comparison to the vehicle control (Figure 3.8A, panels e and f). Similarly, internalised surface EGFR is also accumulated at the perinuclear region upon treatment with 5  $\mu$ M and 10  $\mu$ M of ADO for 28 h (Fig. 3.8B).

To confirm that the EGFR accumulated at the compact structures are originated from the cell surface and not newly synthesised EGFR which were retained in intracellular compartments such as the Golgi, surface EGFR of A-431 cells were labelled with anti-EGFR antibody, internalised into the cell for various time points in the absence or presence of ADO, fixed and analysed by immunofluorescence microscopy. As anticipated, the perinuclear compact membrane structure (PCM) was also apparent (Figure 3.8C), thus showing that the EGFR accumulated at the perinuclear compact structure in the presence of ADO are cell surface EGFR internalised from the cell surface.

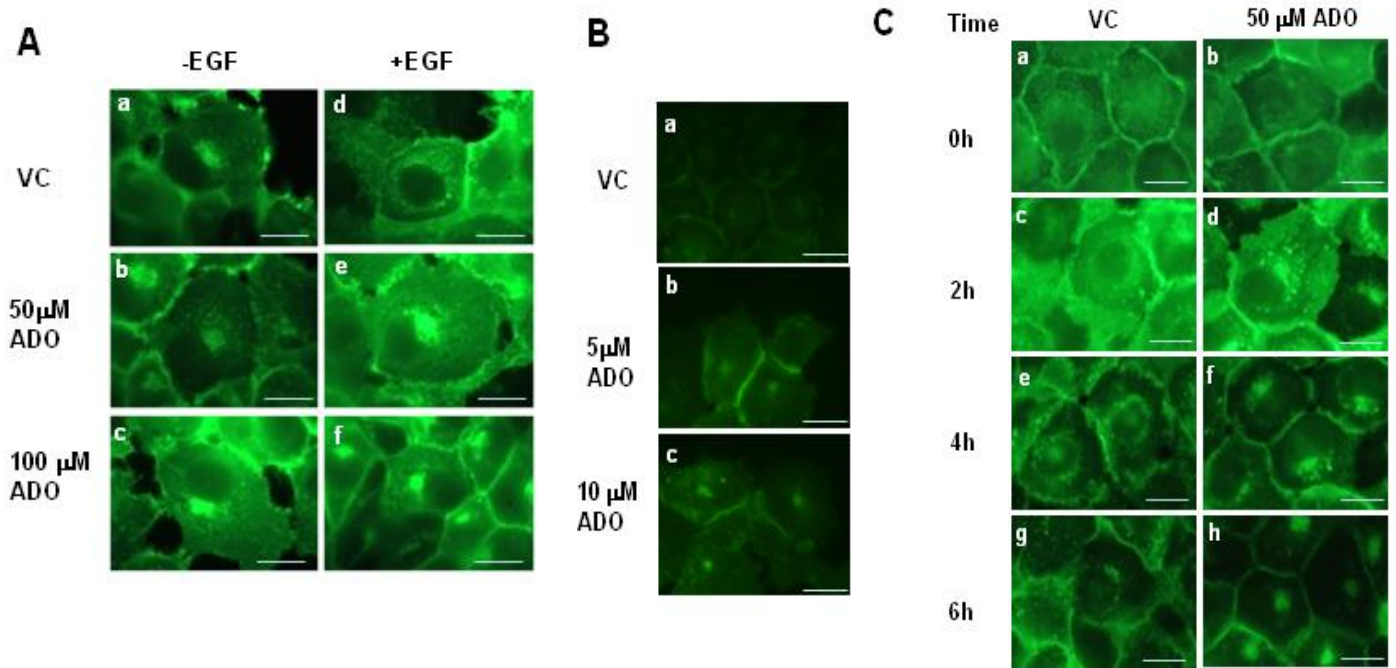


**Figure 3.8 ADO affected the intracellular distribution of EGFRs.**

- A. A-431 cells were treated with various concentrations of ADO for the 4 h in the presence or absence of 100 nM EGF, then fixed and stained with antibody (29.1) against EGFR. Scale bars are representative of 10 μm.
  - B. Effect on EGFR by ADO internalised from the cell surface for 4 h after 24 h treatment. Scale bars are representative of 10 μm.
  - C. Effect on EGFR by ADO internalised from the cell surface for various treatment timepoints. Scale bars are representative of 10 μm.
- VC, vehicle control; ADO, andrographolide; EGFR, epidermal growth factor receptor; EGF, epidermal growth factor.



Co-localisation studies were then carried out to determine the compartment that EGFR is accumulated in. Under steady-state conditions, where A-431 cells were treated with ADO for 4 h and then fixed and stained for EGFR together with a compartmental marker, EGFR did not co-localise well with the vesicle associated membrane protein-3 (VAMP-3) in both cells treated with ADO without (Figure 3.9, panels a-i) and with EGF (Figure 3.9, panels j-r) even though there was some overlap in EGFR and VAMP-3 antibody staining. This is as the shape of the structures staining for VAMP-3 and the ADO induced EGFR clump is different. Confocal 3D convolution and XZ/YZ projection imaging further confirmed that EGFR and VAMP-3 do not co-localise in the PCM structures (Figure 3.10). VAMP-3 is a soluble NSF attachment receptor (SNARE) that resides within the early and recycling endosomes (Hong, 2005). The co-localisation of EGFR was better with vesicle associated membrane protein -8 (VAMP-8) (Figure 3.11), a SNARE that resides in both the early and late endosomes (Wong *et al.*, 1998; Antonin *et al.*, 2000) in A-431 cells. As can be seen, EGFR in both the vehicle control and ADO treated cells have structures that are similar to VAMP-8.

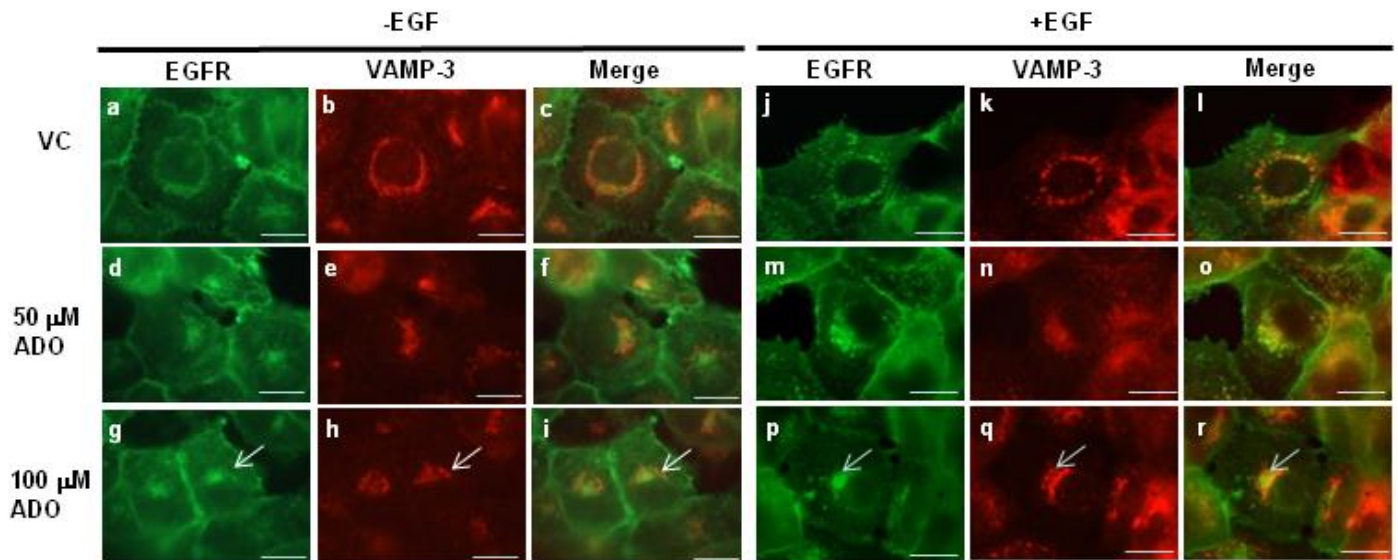


**Figure 3.9 Intracellular distribution of EGFRs in ADO treated cells.** A-431 cells were treated with various concentrations of ADO for the 4 h in the presence or absence of 100 nM EGF, then fixed and stained with antibody against EGFR and co-localised with VAMP-3. Scale bars are representative of 10  $\mu\text{m}$ . Arrows point to the overlapping EGFR and VAMP-3 compartments. VC, vehicle control; ADO, Andrographolide; EGF, epidermal growth factor; EGFR, epidermal growth factor receptor.

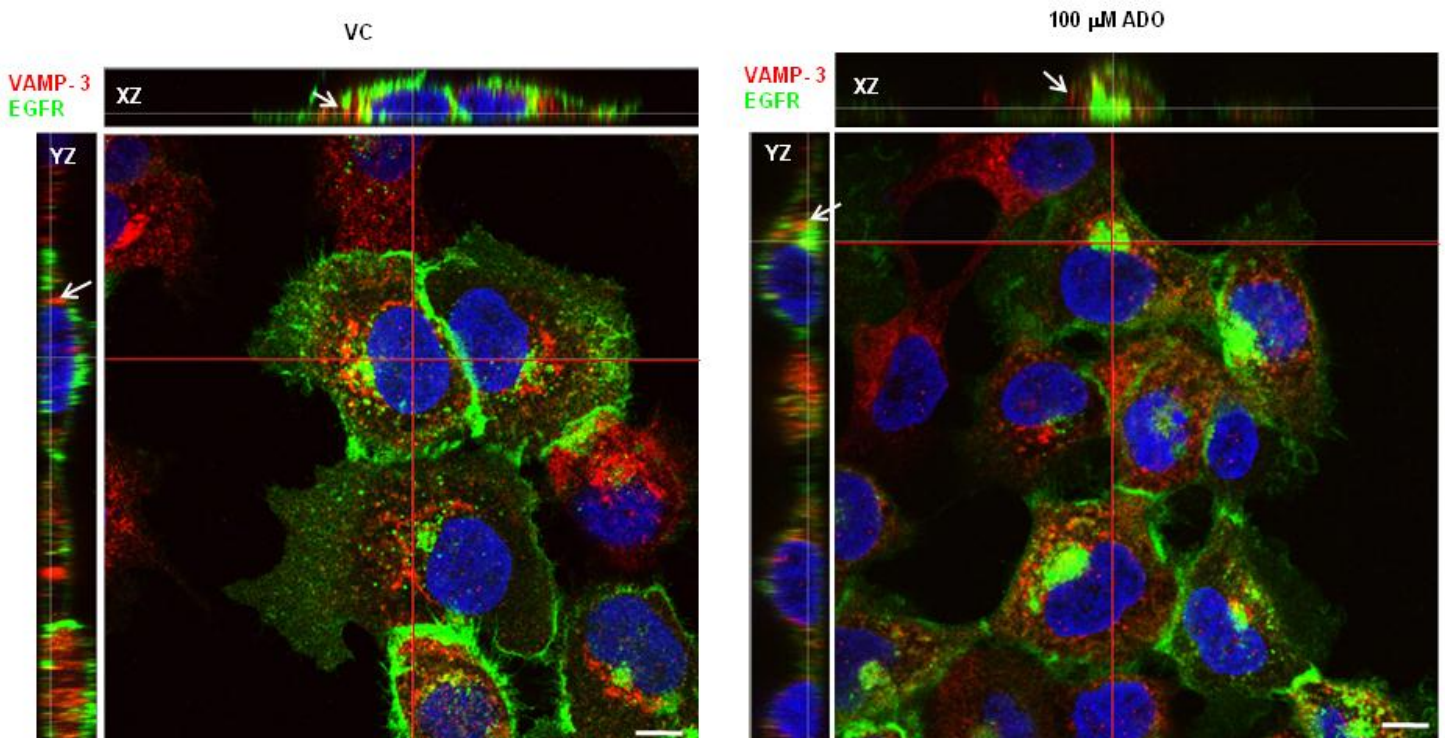


**Figure 3.10 X-Z/Y-Z projection of EGFR with VAMP-3 after ADO treatment.** A-431 cells were incubated with anti-EGFR on ice, treated with 100  $\mu\text{M}$  ADO for 4 h at 37°C, and then fixed and stained with anti-VAMP-3 antibody. Photomicrographs are representative of at least two independent experiments, and were taken with the Olympus FV 1000 confocal microscope at 100x magnification. Scale bars represent 10  $\mu\text{m}$ . Arrows point to the lack of co-localization between EGFR and VAMP-3. VC, vehicle control; ADO, Andrographolide; EGF, epidermal growth factor; EGFR, epidermal growth factor receptor.

Similar results were also obtained for TfR. A-431 cells treated with ADO for 4 hours which were then fixed and stained for TfR show that TfR accumulates at the PCM structures (Figure 3.12A, panel c). Similarly, TfR forms a clump under steady state conditions upon treatment with 5  $\mu$ M and 10  $\mu$ M ADO for 24 h (Fig. 3.12B, panels b and c). Internalised surface TfR (labelled with anti-TfR antibody) was also found to accumulate at the perinuclear region upon ADO-treatment (Figure 3.12C, panels d and f). Cells were then treated with ADO under steady state conditions for 4 h, fixed and stained for TfR, together with either VAMP-3 and VAMP-8. We observed that TfR co-localises well with VAMP-8 (Figure 3.12E), but did not co-localise as well with VAMP-3 (Figure 3.12D) in the PCM structures.

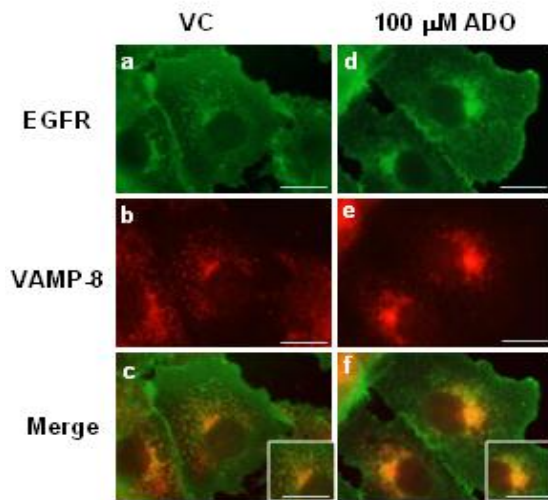


**Figure 3.11 ADO enhances EGFR co-localization with VAMP-8.** A-431 cells were incubated with primary antibody on ice, treated with 100  $\mu$ M ADO for 4 h, fixed and stained with VAMP-8 antibody. The perinuclear clump of EGFRs co-localised well with VAMP-8 for both vehicle control (VC) and ADO treatment. Inset image shows enlarged image of EGFR and VAMP-8 co-localisation. Scale bars are representative of 10  $\mu$ m. VC, vehicle control; ADO, andrographolide. EGFR, epidermal growth factor receptor.

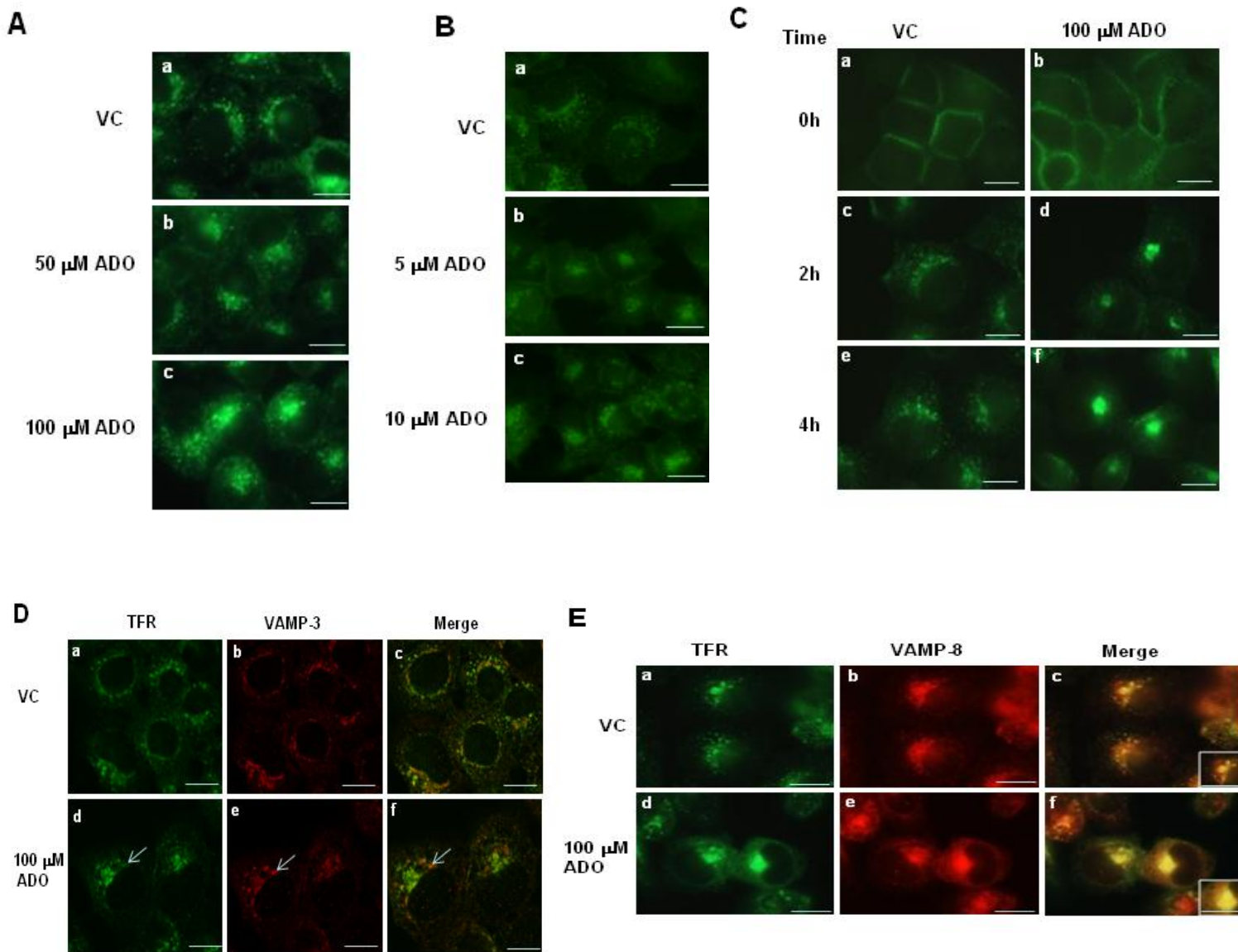


**Figure 3.12 ADO affected intracellular distribution of TfRs.** ADO affected the intracellular distribution of TfRs. A-431 cells were treated with various concentrations of ADO for 4 h (A), or 24 h (B), then fixed and stained with antibodies; or they were incubated with primary antibody on ice, and then treated with various concentrations of ADO at 37°C, fixed and stained (C, D, E). Primary antibodies used were against TfR (monoclonal), VAMP-3 (polyclonal), and VAMP-8 (polyclonal), and secondary antibodies were FITC-conjugated anti-mouse IgG and Cy-3 conjugated anti-rabbit IgG. Photos are representative of at least two independent experiments, and were taken with the Olympus BX60 (A, B, C, E) and Leica TS5 confocal microscope (D) at 100x magnification. Scale bars represent 10  $\mu\text{m}$ .

- A. Effect of ADO on steady state TfRs after the 4 h treatment.
- B. Effect of ADO on steady state TfRs after the 24 h treatment.
- C. Effect of ADO on TfRs internalised from the cell surface. The time points tested were 2 h and 4 h.
- D. The perinuclear clump of TfRs did not co-localise well with VAMP-3.
- E. The perinuclear clump of TfRs co-localised well with VAMP-8. Inset image shows enlarged image of TfR, VAMP-8 co-localisation. Vehicle control, VC; andrographolide, ADO. EGFR, epidermal growth factor receptor; TfR, transferrin receptor; VAMP, vesicle-associated membrane protein.

In order to further characterise the compartment which EGFR is present in upon andrographolide treatment, surface EGFR of A-431 cells were labelled with Alexa Fluor-conjugated EGF, internalised, fixed at various time-points and then co-localised with lysosomal associated membrane protein-1 (LAMP-1), a commonly used marker for late endosomes and lysosomes (Eskelinen *et al.*, 2003). As can be seen, EGFR is present in the PCM structures in ADO treated cells at the 2 and 4 hours time-point (Figure 3.13A, panels j and p). This is consistent with the earlier result which demonstrates that EGFR degradation is inhibited upon ADO treatment (Figure 3.6). Internalised EGF also co-localised well with LAMP-1 at 2 and 4 hour time-points in the presence of ADO (Figure 3.13A, panels l and r). Furthermore, confocal 3D convolution and X-Z/Y-Z projection imaging showed that co-localisation between EGF and LAMP-1 in the PCM structures occurs both for the vehicle control (though to a lesser extent) and ADO-treated cells (Figure 3.13B, C). This is not surprising as it has been known that EGFR trafficked to the late endosomes and lysosomes for degradation (Le Roy & Wrana, 2005). Hence, this demonstrates that ADO accumulates EGFR in the late endosomes and lysosomes.

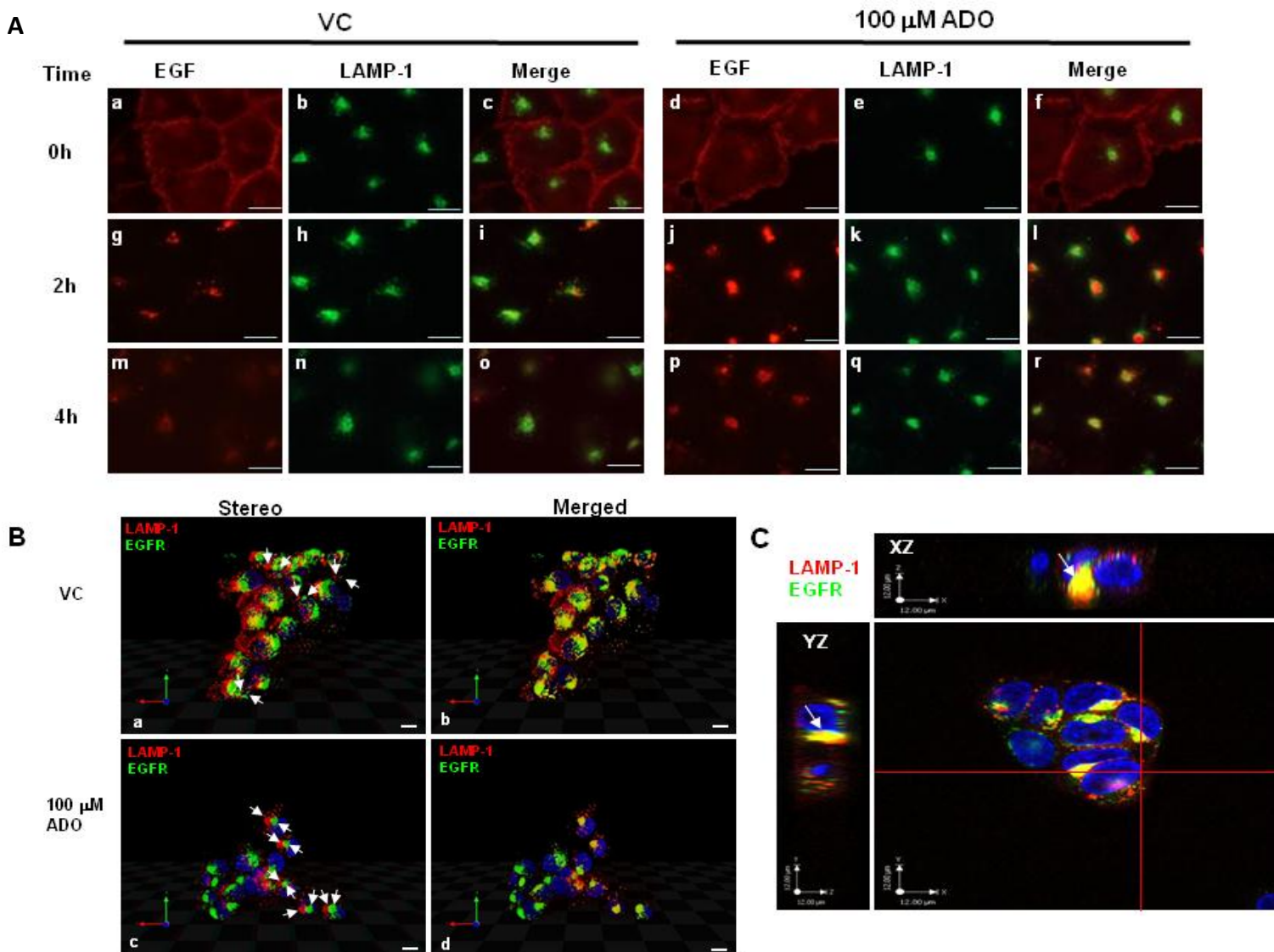


**Figure 3.13 Epidermal growth factor receptor (EGFR) accumulated in an intracellular membrane compartment that co-localises with LAMP-1 upon treatment with ADO.** Cells were incubated with labelled EGF on ice, treated with various concentrations of ADO, then fixed and stained with antibody against LAMP-1 (monoclonal). Photos are representative of at least two independent experiments. Vehicle control, VC; andrographolide, ADO.

- A. Internalised labelled EGF co-localised with LAMP-1. The time points tested were 2 h and 4 h. Images were taken using Olympus BX60. Scale bars represent 10  $\mu\text{m}$ .
- B. Stereo three-dimensional convolution image of EGF co-localisation with LAMP-1. Images were taken using the confocal microscope Olympus Fluoview 500. Stereo three-dimensional rendering was performed using the velocity visualization software from Improvion. Scale bar represents 5  $\mu\text{m}$ . Arrowheads point to co-localization between EGFR and LAMP-1
- C. X-Z/Y-Z projection of EGF co-localisation with LAMP-1. Images were taken using Olympus Fluoview 500. X-Z/Y-Z projection was performed using the velocity visualization software from Improvion. Scale bar represents 12  $\mu\text{m}$ . LAMP-1, lysosomal-associated membrane protein-1. Arrow points to the co-localization between EGFR and LAMP-1

#### **3.3.4. Downregulation of surface EGFR upon andrographolide treatment was not due to the inhibition of receptor recycling but due to the enhanced internalisation of EGFR from the cell surface of A-431 cells**

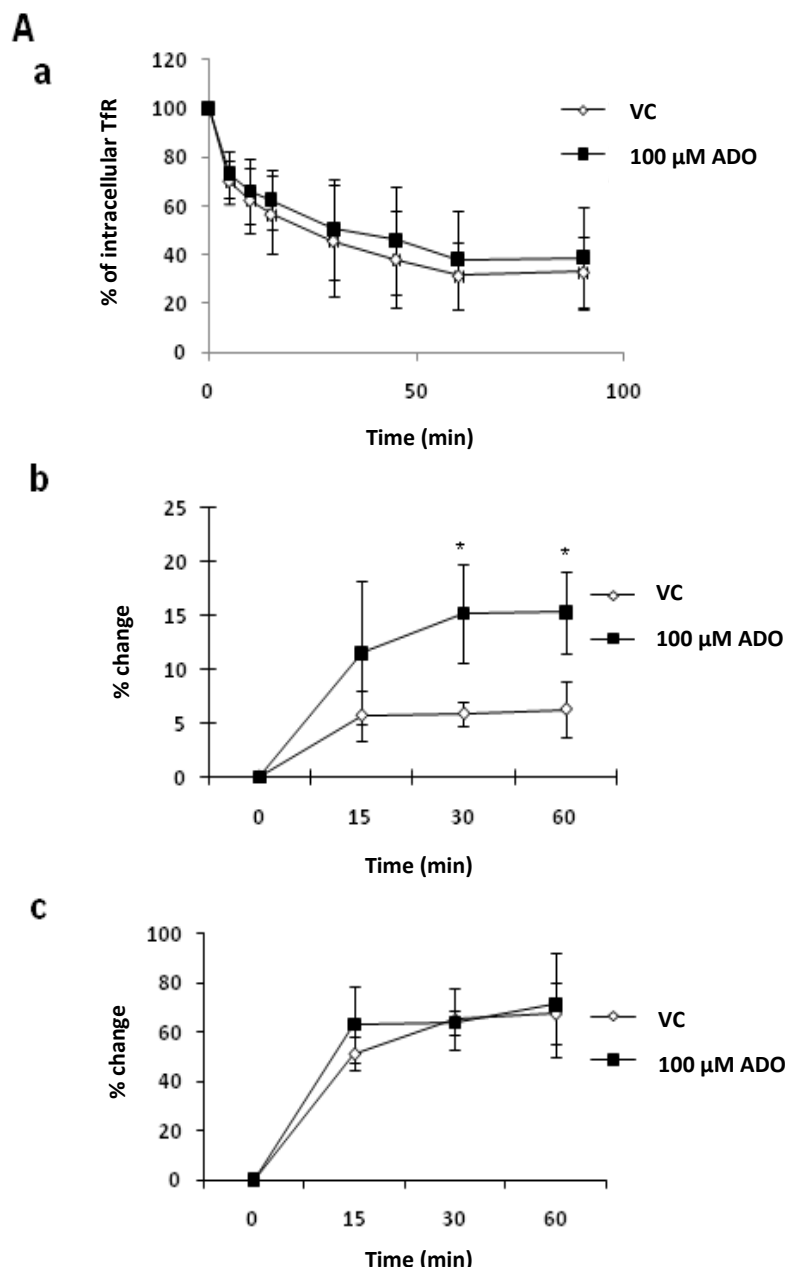
In view of our observation that ADO downregulates expression of cell surface EGFR and accumulates EGFR in intracellular membrane compartments, there is a possibility that ADO could also regulate recycling of EGFR to the cell surface in A-431 cells. The recycling pathway is responsible for recycling receptors from the endocytic recycling compartment back to the cell surface (Maxfield & McGraw, 2004), and therefore inhibition of this pathway could act as a contributing factor to the inhibition in degradation of both EGFR and TfR. To examine this possibility, cells were serum starved and either untreated or pretreated with ADO for 4 h. Cells were then incubated with labelled transferrin for 1 h, washed and then further incubated for various time-points prior to media collection and quantification of recycled labelled transferrin. TfR is utilised here as a marker for the recycling pathway as it is constitutively recycled back to the cell surface. As can be seen, ADO did not significantly affect the recycling of TfR (Figure 3.14A, panel a) from the time-points of 0 to 90 minutes.

It was also possible that the change in the level of cell surface EGFR was due to a change in the rate of receptor internalisation into the cell. Hence, the rate of receptor internalisation was quantified by incubating cells with ADO for 4 h. Cell surface receptors were then incubated with anti-EGFR antibody for an hour on ice. Anti-EGFR antibody was then allowed to internalise by replacing cells in media and incubating them at 37 °C. At each time-point, the cells were washed with acid wash to



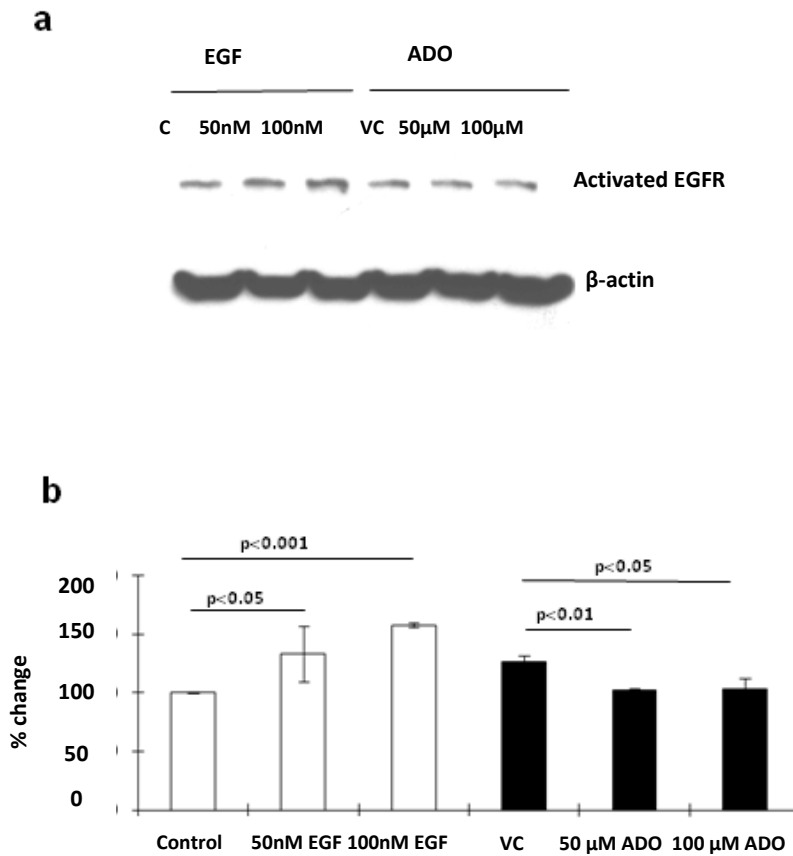
remove anti-EGFR antibody remaining on the cell surface. Cells were then fixed and stained with FITC-conjugated secondary antibodies and the amount of intracellular anti-EGFR antibody was then quantified by flow-cytometry. Interestingly, ADO was found to enhance the rate of EGFR internalisation from the cell surface (Figure 3.14A, panel b). The increase in the rate of internalisation of EGFR accounts for the decrease in the amount of surface EGFR upon ADO treatment. However, it is worth noting that the effect of ADO on receptor internalisation seen here is EGFR-specific, as ADO does not significantly enhance internalisation of TfR from the cell surface (Figure 3.14A, panel c)

It was then interesting to find out if ADO could induce phosphorylation of EGFR so as to increase the internalisation rate, as EGFR is known to be endocytosed upon activation. Serum starved cells were treated in two separate groups – one group was pretreated with ADO for 4 hours, the other group was induced with EGF for 15 minutes. Both groups were then detached and lysed and analysed by western blot for activated EGFR. ADO did not change the phosphorylation levels of EGFR (Figure 3.14B).



**Figure 3.14 Andrographolide (ADO) did not affect the recycling pathway, but increased the internalisation of EGFR**

- A. (a) A-431 cells were pretreated with DMSO or 100 mM ADO for 4 h in serum-free DMEM, and then incubated with Alexa Fluor 488 labelled transferrin at 17°C. Unbound transferrin was then washed off and internalised transferrin allowed to recycle for 0–90 min. The amount of unrecycled transferrin in the cells was quantified and expressed as a percentage of total bound transferrin. Results are expressed as a mean percentage  $\pm$  SD from two independent experiments. (b) ADO increased the internalization of EGFR. A-431 cells were pretreated with DMSO or 100  $\mu$ M ADO for 4 h, and then incubated with anti-EGFR on ice for 1 h, before being placed in media and fixed at various time points. Cells were then stained with FITC-conjugated anti mouse IgG and read with the flow cytometer. Results are expressed as a percentage of the total amount of EGFR on the cell surface  $\pm$  SD from two independent experiments. \*  $P < 0.05$  relative to vehicle control. (c) ADO did not increase the internalization of TfR. A-431 cells were pretreated with DMSO or 100  $\mu$ M ADO for 4 h, and then incubated with anti-TfR on ice for 1 h, before being placed in the media and fixed at various time points. Cells were then stained with FITC-conjugated anti-mouse IgG and read with the flow cytometer. Results are expressed as a percentage of the total amount of TfR on the cell surface  $\pm$  SD from two independent experiments. VC, vehicle control; ADO, andrographolide; EGFR, epidermal growth factor receptor; TfR, transferrin receptor.

**B**

**Figure 3.14 ADO did not affect the recycling pathway, but increased the internalization of EGFR**

B. ADO did not induce the phosphorylation of EGFR. For the EGF group, A-431 cells were deprived of serum and then treated with various concentrations of EGF for 15 min. For the ADO group, A-431 cells were deprived of serum and treated with DMSO or ADO for 4 h, then lysed and used for Western blot analysis. Blots were probed for activated EGFR;  $\beta$ -actin was the loading control. The intensity of the activated EGFR bands was quantified, normalised to  $\beta$ -actin bands, and expressed as a percentage of the control  $\pm$  SD of at least two experiments. Blots are representative of at least two experiments. (a) Western blot of phosphorylated EGFR. (b) Quantification of phosphorylated EGFR. VC, vehicle control; ADO, andrographolide; EGFR, epidermal growth factor receptor.

### 3.4. Discussion

Thus far, no work has been carried out to determine if ADO modulates receptor trafficking, particularly receptors that are implicated in cancer progression like EGFR and those important for cell survival like TfR. Here, we demonstrate that ADO can affect receptor trafficking. Although the concentration of ADO utilised in this paper is higher than the concentration used in most papers, the effect of ADO observed on A-431 cells at 100  $\mu\text{M}$  for 4 h similarly occurs at 5  $\mu\text{M}$  or 10  $\mu\text{M}$  upon 24 h treatment. We have also observed downregulation of close to 30% of cell surface EGFR at 5  $\mu\text{M}$  of ADO for 48 h (Figure 3.3), as well as the formation of the PCM for EGFR and TfR using 5  $\mu\text{M}$  and 10  $\mu\text{M}$  for 24 h (Figure 3.8B, Figure 3.12B). Thus, it is possible to conclude that the effect of ADO at a higher concentration for a shorter time point is similar to the lower concentration for a longer time point. We have chosen to work with a shorter time-point and a higher concentration to ensure that the effects observed on receptor trafficking are not downstream events of cells dying due to long hours of drug treatment. In comparison to other studies, the effects of ADO on EGFR and TfR at 10  $\mu\text{M}$  upon 24 h treatment is similar to the concentrations of ADO utilised on human colorectal carcinoma Lovo cells (Shi *et al.*, 2008) to inhibit cell growth, and is also much lower than 50  $\mu\text{M}$  treatment for 24 h used to induce apoptosis in HeLa and HepG2 cells (Zhou *et al.*, 2006). Hence, the effects of ADO on receptor trafficking are most probably events that are not downstream effects of cell death.

Comparisons of the effective concentrations on EGFR and TfR at 24 h to those found in *in vivo* pharmacokinetics studies using normal therapeutic dosages reveal that it

may be necessary to use higher dosages of ADO to see the anti-cancer effect *in vivo*. This is as plasma concentrations of ADO in humans treated with Kan Jang at the daily therapeutic dosage of 1 mg ADO/ kg body weight/ day, which is an approximation of 60 mg of ADO, gave a peak of 3.8  $\mu\text{M}$  (Panossian *et al.*, 2000), which is slightly lower than the effective concentrations of 5 and 10  $\mu\text{M}$ . But it is possible to attain much higher plasma concentrations than the 3.8  $\mu\text{M}$  achieved with a higher dosage as preliminary pharmacokinetics studies in mice treated at 150 mg ADO/kg have been found to yield maximal plasma concentrations of 20  $\mu\text{M}$  to 30  $\mu\text{M}$  (Stanslas *et al.*, 2001b). However, in the process of dosage optimisation to achieve the anti-cancer effect of ADO, it is important to bear in mind results from previous clinical trials and toxicity tests. The  $\text{LD}_{50}$  of ADO in mice was found to be more than 4000 mg ADO/kg/day (Chen *et al.*, 2009), while a small clinical trial conducted in both HIV positive and negative volunteers utilising higher dosages of 5 mg ADO/kg body weight and 10 mg ADO/ kg body weight 3 times a day to test for toxicity did show some adverse effects in the form of rash and diarrhoea, but did not affect liver enzymes – aspartate transaminase (AST) and alanine transaminase (ALT) levels significantly in normal subjects during the medication period (Calabrese *et al.*, 2000). Hence, dosage optimisation within the range of 60 mg to 300 mg daily is needed to achieve the anti-cancer effects of ADO in humans without adverse effects.

Here, we have demonstrated that ADO downregulates cell surface EGFR and also inhibits the degradation of both EGFR and TfR, causing them to accumulate in the late endosomes (Figure 3.15). Upon activation with its ligand, EGFR self-phosphorylates and is internalised at an increased rate from the cell surface upon

ADO treatment (Figure 3.14A, panel b), where it moves into the early endosomes and progresses to the late endosomes. Interestingly, from our observations, the downregulation of cell surface EGFR is not dose-dependent (Figure 3.2). It may be possible that the effect of ADO on the trafficking machinery involved in internalising cell surface EGFR is saturated at 50  $\mu\text{M}$  for 4 h and 5  $\mu\text{M}$  for 48 h. In the presence of ADO, the degradation of EGFR is slowed down such that it accumulates in the VAMP-8 positive compartment. Similarly, TfR constitutively internalises from the cell surface where it either enters the recycling endosomes to travel back to the plasma membrane, or it enters the late endosomes. Upon entry to the late endosomes, it also accumulates in a VAMP-8 positive compartment in the presence of ADO, similar to EGFR (Figure 3.15). It can be inferred that the VAMP-8 and LAMP-1 positive compartment that EGFR is accumulated in is the late endosomal compartment, as VAMP-8 is known to be found in both early and late endosomes (Antonin *et al.*, 2000), whereas LAMP-1 is expressed in both the late endosomes and lysosomes (Eskelinen *et al.*, 2003). The accumulation of EGFR in the late endosome is expected as EGFR traffics rapidly from the cell surface into the late endosomes for degradation upon internalisation. Here, we propose that ADO acts in two ways to cause the accumulation of receptors – the increase in the internalisation rate of EGFR from the cell surface, and also the inhibition of movement into the lysosomes from late endosomes for degradation. The increase in internalisation rate is not the sole reason for receptor accumulation as TfR does not internalise more rapidly upon treatment, but its degradation is inhibited. Hence, the inhibition in the movement of receptors into the lysosomes is more likely to be a greater contributor. In addition, we have also ruled out the possibility that ADO inhibits some lysosomal enzymes upon treatment for 4 h (data not shown), although it is possible that the endosomal sorting

complex required for transport (ESCRT) machinery, which is responsible for receptor downregulation by trafficking receptors from the endosomes/ multivesicular bodies to the lysosomes (Kirisits *et al.*, 2007; Saksena & Emr, 2009), is affected by ADO. Both EGFR and TfR also differ at the time-point where the accumulation of receptors is obvious (Figure 3.6, 3.7). This most likely due to the difference in the pathways in EGFR and TfR, as EGFR is delivered directly for degradation after internalisation, whereas a large pool of TfR undergoes a few rounds of recycling to the cell surface before being sent for degradation (Daniels *et al.*, 2006). Hence, it would take a longer time for TfR accumulation to be obvious. TfR accumulation was also more distinct as it took longer for it to be degraded, hence the cells could be treated for 6 h.

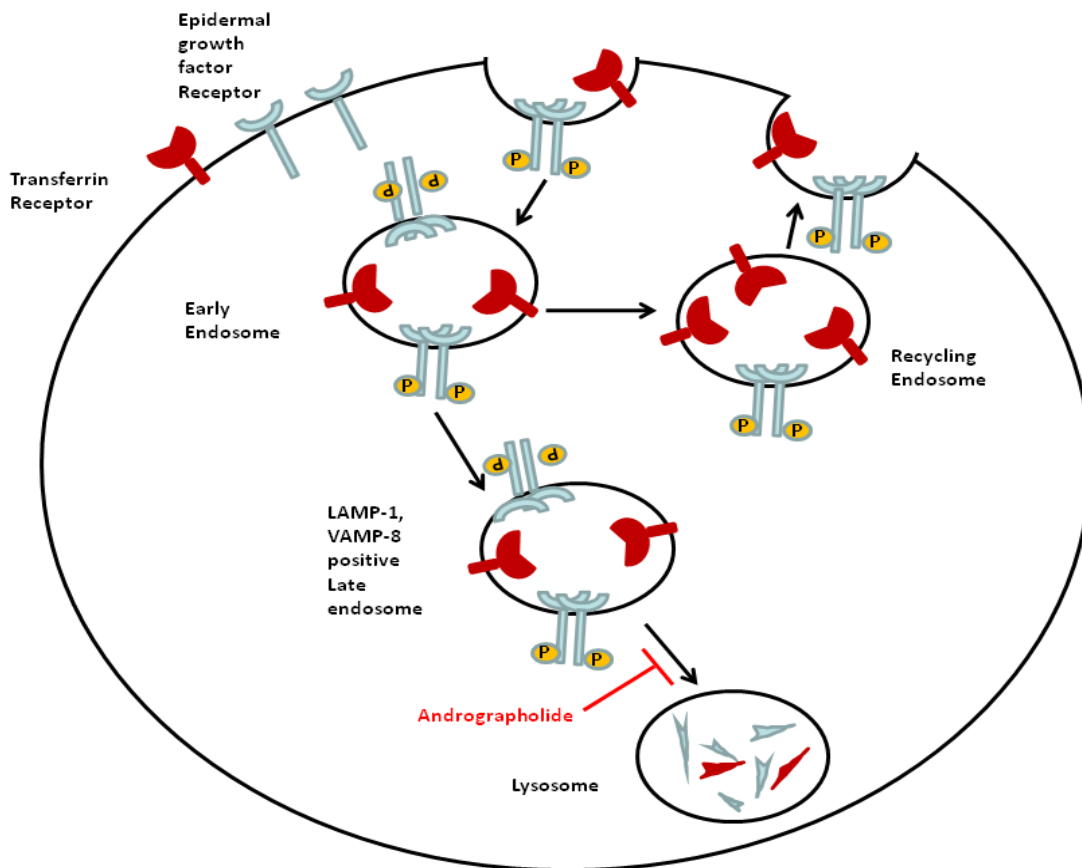


**Figure 3.15 Proposed mechanism of andrographolide (ADO)-induced inhibition of receptor degradation in late endosomes.** Monomeric EGFR dimerizes upon binding of a ligand, following which the tyrosine kinases autophosphorylate, and enter the cell by endocytosis. Similarly, TfR enters the cell by endocytosis constitutively, and a portion of both EGFR and TfR receptors are recycled back to the surface. Receptor trafficking from the late endosome to the lysosome is inhibited after ADO treatment. EGFR, epidermal growth factor receptor; TfR, transferrin receptor.



The inhibition of protein trafficking to the lysosome for degradation is detrimental to cell survival (Figure 3.1). Lysosomes are acidic, hydrolase containing organelles in the cell responsible for protein degradation and recycling (Eskelinen *et al.*, 2003), and proteins are trafficked to lysosomes either from autophagosomes or late endosomes (Nixon *et al.*, 2008). Failure to efficiently break down proteins targeted for degradation is known to be associated with the disruption of cellular function. Recently, it was shown that the inhibition of rhodopsin trafficking to lysosomes resulted in its accumulation in late endosomes. This accumulation caused the death of photoreceptor cells, leading to blindness (Chinchore *et al.*, 2009). Hence, inhibiting protein trafficking to the lysosome is a possible mechanism for ADO to induce cell death.

It may also seem paradoxical that ADO inhibits cell growth despite the accumulation of internalised EGFR (Figure 3.6), as lysosomal degradation is thought to be one of the modes of downregulating EGFR mediated signalling. However, it has been demonstrated in MDA-MB-468 breast cancer cells, which overexpress EGFR, that internalised EGFR is capable of activating caspase-3 to induce cell death (Hyatt & Ceresa, 2008). As A-431 is known to express caspase-3 (Mese *et al.*, 2000), it is possible that the accumulation of EGFR in the late endosomes by ADO may then result in cell death by the activation of caspase-3.

Finally, the downregulation of surface EGFR upon ADO treatment (Figure 3.2) due to the increase in the rate of internalisation of receptors (Figure 3.14A, panel b) is also another mechanism by which ADO could cause cell death. Previously, it was

demonstrated that knockdown of EGFR by siRNA in human glioma cells has been shown to result in a decrease in cell survival (Kang *et al.*, 2005). This is expected as EGFR is also a receptor that is known to be upstream of the mitogen associated protein kinase (MAPK) and phosphatidylinositol 3-kinase (PI3K) signalling cascades that control cell proliferation (Hynes & Lane, 2005), and thus downregulation of surface EGFR could inhibit tumour proliferation in the presence of growth factors.

Currently, there are two main classes of anti-cancer agents targeting EGFR (Hynes & Lane, 2005; Zhang *et al.*, 2007). The first class is made up of monoclonal antibodies such as cetuximab and panitumumab, which target the extracellular domain of EGFR to inhibit ligand binding. Reversible and irreversible tyrosine kinase inhibitors such as gefitinib and erlotinib form the second class, and they inhibit the activation of EGFR, and hence the downstream cell proliferation signalling pathways (Yap *et al.*, 2009; Zahorowska *et al.*, 2009). We have shown here for the first time that ADO, a small chemical compound which does not belong to these two classes of anti-cancer agents, can be used to target EGFR. Another emerging small molecule in the area of anti cancer therapy is the major catechin found in green tea (–)-epigallocatechin gallate (EGCG) (Yang *et al.*, 2009a). EGCG has not only been found to inhibit activation of EGFR and its downstream signaling pathways (Shimizu *et al.*, 2008), but it is also capable of downregulating EGFR by inducing its internalisation (Adachi *et al.*, 2008). However, in contrast to ADO, EGFR internalised upon EGCG treatment is recycled to the cell surface upon removal of EGCG. Hence, the ability of ADO to increase the internalisation of cell surface EGFR and accumulate them in the late endosomes is unique.

ADO has been shown previously to be anti-cancer in nature, as it induces cell cycle arrest at the G2/M phase in HepG2 cells (Li *et al.*, 2007), and at the G0/G1 phase in HL-60 leukemic cells (Cheung *et al.*, 2005). It can also induce apoptosis in cancer cells in a caspase-3 (Zhao *et al.*, 2008) and -8 dependent manner (Zhou *et al.*, 2006) as well as inhibit NF- $\kappa$ B binding of DNA by forming a covalent bond with the reduced 62 cysteine of p50 (Xia *et al.*, 2004; Hidalgo *et al.*, 2005). The immunosuppressive property of ADO through its effect on NF- $\kappa$ B would be useful for its utilisation as an anti-cancer drug, especially as NF- $\kappa$ B has emerged in the recent years as a target for cancer therapy (Baud & Karin, 2009). NF- $\kappa$ B activation has been implicated in cancers such as breast, colon, liver, prostate, cervical and acute lymphocytic leukaemia, and its prolonged activation results in increased cell survival and proliferation, tumour metastasis and angiogenesis, factors which are involved in cancer progression (Baud & Karin, 2009). Our work on EGFR and TfR here has added a new dimension to the utilisation of ADO as an anti-cancer drug, as well as provided an understanding into how ADO regulates receptor trafficking in the cell.

# **Chapter 4**

## **Andrographolide increases surface EGFR downregulation through activation of p38 MAPK**

## **4. Andrographolide increases surface EGFR downregulation through activation of p38 MAPK**

### **4.1. Abstract**

We have shown that ADO is capable of downregulating surface EGFR by increasing the rate of endocytosis. As EGFR is an important initiator of cell signalling pathways, it is possible that the ADO effect on EGFR trafficking could also affect EGFR-induced signalling pathways such as the mitogen activated protein kinase (MAPK) pathways. Our studies show that ADO is capable of upregulating the phosphorylation state of all three MAPKs – ERK 1/2, p38 MAPK and SAPK/JNK. In particular, the increased phosphorylation of p38 MAPK led to an increase in its activity, and phosphorylation of EGFR at the serine 1046/1047 residues. This phosphorylation is responsible for inducing the increase in EGFR internalisation.

### **4.2. Introduction**

One of the many mechanisms of ADO which modulates its anti-inflammatory effect is the ability to reduce levels of surface receptors, specifically inhibiting upregulation of the surface receptors I-A<sup>b</sup>, CD40 and CD86 in lipopolysaccharide stimulated dendritic cells (Iruretagoyena *et al.*, 2005). Previously, we also demonstrated that ADO downregulated surface epidermal growth factor receptor (EGFR) and caused the accumulation of endocytosed EGFR by affecting its degradation (Tan *et al.*, 2010). As receptor trafficking and signaling activation are closely related events, we were interested to further understand the effect that ADO has on EGFR trafficking and its downstream signaling pathways.

EGFR is a key receptor tyrosine kinase responsible for controlling signaling pathways that mediate cellular proliferation. Upon the binding of its ligand, epidermal growth factor (EGF), the receptors dimerize, autophosphorylate and activate several mitogen activated protein kinase pathways (MAPKs), which include the extracellular signal regulated kinase 1 and 2 (ERK 1/2), the p38 mitogen activated protein kinase (p38 MAPK) and stress activated protein kinase/c-Jun N-terminal activated kinase (SAPK/JNK). Phosphorylated EGFR is then internalised largely via endocytosis and degraded in the late endosomes to downregulate the signalling. However, it is known that internalised EGFR continues signalling in the endosomes. Hence, we postulated that the accumulation of intracellular EGFR could possibly affect downstream MAPK signalling.

#### **4.2.1. MAPK Pathways**

There are three major families of MAPKs – ERK1/2, p38 MAPK and JNK. They are serine/threonine kinases, and are activated upon dual phosphorylation of the conserved threonine and tyrosine residues in the threonine-X-tyrosine (TXY) motif within the conserved activation loop by their upstream MAPKK and MAPKKKs. Protein scaffolds bring these proteins into close proximity so that phosphorylation can occur (Pimienta & Pascual, 2007). The MAPKs are important signalling proteins as they dissociate from the scaffold and translocate to the nucleus upon activation, then they phosphorylate transcription factors (TFs) which control genes responsible for proliferation (ERK1/2), cellular response to stress and apoptosis (p38 MAPK and JNK) (Table 4.1). Phosphorylation of TFs enhances their transcription activity (Turjanski *et al.*, 2007). In turn, mitogen kinase phosphatases (MKPs) regulate

MAPK activity by dephosphorylating the TXY motif after a certain period of activation (Pimienta & Pascual, 2007). Hence, if ADO affects the activation of any of these MAPKs, it could affect cell fate.

MAPK	Transcription factors phosphorylated
ERK 1/2	Sap-1a, ELK-1, SMAD-1, SMAD-2,3, SMAD4, MAF-A, p53, c-Myb, SP1, c-Myc, c-Fos
p38 MAPK	ATF-2, c-Fos, ELK-1, c-Jun, p53, p73, MEF 2A, C, STAT-4,
JNK	c-Jun, ATF-2, ELK-1, JunD, ELK-3, p53, c-Myc, HSF-1, NFAT4.

**Table 4.1** Transcription factors phosphorylated by different MAPKs. (Adapted from (Turjanski *et al.*, 2007))

Several studies have investigated the effect of ADO on MAPK pathways with various contradicting results due to different cell types, ligands and incubation times used. However, ADO treatment in cancer cells generated a consistent upregulation of MAPK signalling: For cancer cell lines the increase in phosphorylated MAPK were: ERK1/2, p38 MAPK and JNK in liver carcinoma Hep3B cells (Ji *et al.*, 2007); JNK in the presence of glutathione synthesis inhibitor in Hep3B cells (Ji *et al.*, 2011); JNK in HepG2 cells (Zhou *et al.*, 2008) and ERK1/2 in colon carcinoma CT26 cells were found to be activated upon ADO treatment (Chao *et al.*, 2010b).

#### 4.2.2. Crosstalk between MAPK signalling and receptor endocytosis

Conventionally, receptors were thought to activate downstream signalling molecules such as the MAPKs, and receptor endocytosis was then initiated to traffic receptors for degradation to attenuate receptor-induced signalling. Thus, endocytosis was

thought of mainly as a process to downregulate signalling. However, recent studies have led to a paradigm shift in how signalling and endocytosis interact; signalling molecules such as the MAPKs are now known to be important players in regulating the endocytic process. For instance, while p38 MAPK activates the stress response pathway, it is also known to phosphorylate EGFR on serines within the region of 1002 – 1020, as well as 1046/1047, causing its internalisation from the cell surface (Frey *et al.*, 2006; Zwang & Yarden, 2006; Sorkin & Goh, 2009). Conversely, proteins involved in trafficking such as the growth factor receptor-bound protein 2 (Grb2), which is commonly known to induce internalisation of receptor tyrosine kinases such as EGFR, can also activate signalling cascades through the Ras proteins (Sorkin & von Zastrow, 2009). Thus, to obtain a more holistic picture of ADO regulation of receptor trafficking, there is a need to understand how ADO regulates MAPK signalling. Specifically, we sought to understand the underlying mechanism by which ADO regulates MAPK signalling and its corresponding effect on EGFR trafficking. We demonstrate that ADO is capable of upregulating phosphorylation of MAPKs, in particular extracellular regulated kinase (ERK) 1/2, p38 MAPK and c-Jun N terminal Kinase (JNK) in an EGF independent manner. The activation of p38 MAPK induced phosphorylation of EGFR at serine residues 1046/1047, causing its internalisation from the cell surface, and inhibition of p38 MAPK activity restores levels of surface EGFR downregulated by ADO.



### **4.3. Results**

#### **4.3.1. Andrographolide upregulates the MAPK signalling pathways independently of EGF**

Downregulation of EGFR signalling is mediated by endocytosis and degradation of phosphorylated EGFR. As we previously showed that EGFR is internalised from the cell surface and accumulated intracellularly, we were interested to determine whether this accumulation affected the EGFR signalling pathways, particularly the major MAPK pathways which regulate cell proliferation and apoptosis. Cells were pretreated with ADO in serum-free media for 4 h prior to incubation with 100 nM EGF (to induce MAPK signalling) and lysis at various time points. Interestingly, ADO is able to upregulate phosphorylation of MAPKs ERK1/2, p38 MAPK and p46 of SAPK/JNK (Figure 4.1 A – D, lanes 1 and 2) even in the absence of EGF. As anticipated, total phosphorylation of EGFR remained unchanged. Thus, ADO can induce EGF-independent MAPK signalling in A-431 cells.

Next, we were interested to understand the manner in which ADO induces MAPK signalling. MAPK signalling is highly dynamic due to its induction by upstream MAPKKs as well as regulation by protein phosphatases, and hence, there is a short time frame during which the MAPKs will be activated. This activation typically decreases shortly after due to dephosphorylation by the MKPs. Thus, we investigated the timepoint at which ADO induced MAPK signalling by incubating ADO with A-431 cells for varying timepoints in serum-free media. Cells were then lysed and the phosphorylation level of EGFR and the MAPKs analysed. As was expected, total EGFR phosphorylation was unchanged, whereas the phosphorylation of p38 MAPK

and p46 of SAPK/JNK was upregulated upon ADO treatment with increasing incubation times beginning at 1 h, and p42 of ERK at 2 h (Figure 4.2A). The MAPK activation was sustained till the endpoint of 4 h. This phenomenon was not limited to A-431, but was similarly replicated in the human cervical carcinoma cell line HeLa after 4 h treatment with ADO in serum-free media (Figure 4.2B) hence demonstrating that ADO induction of MAPK pathways is not cell line specific.

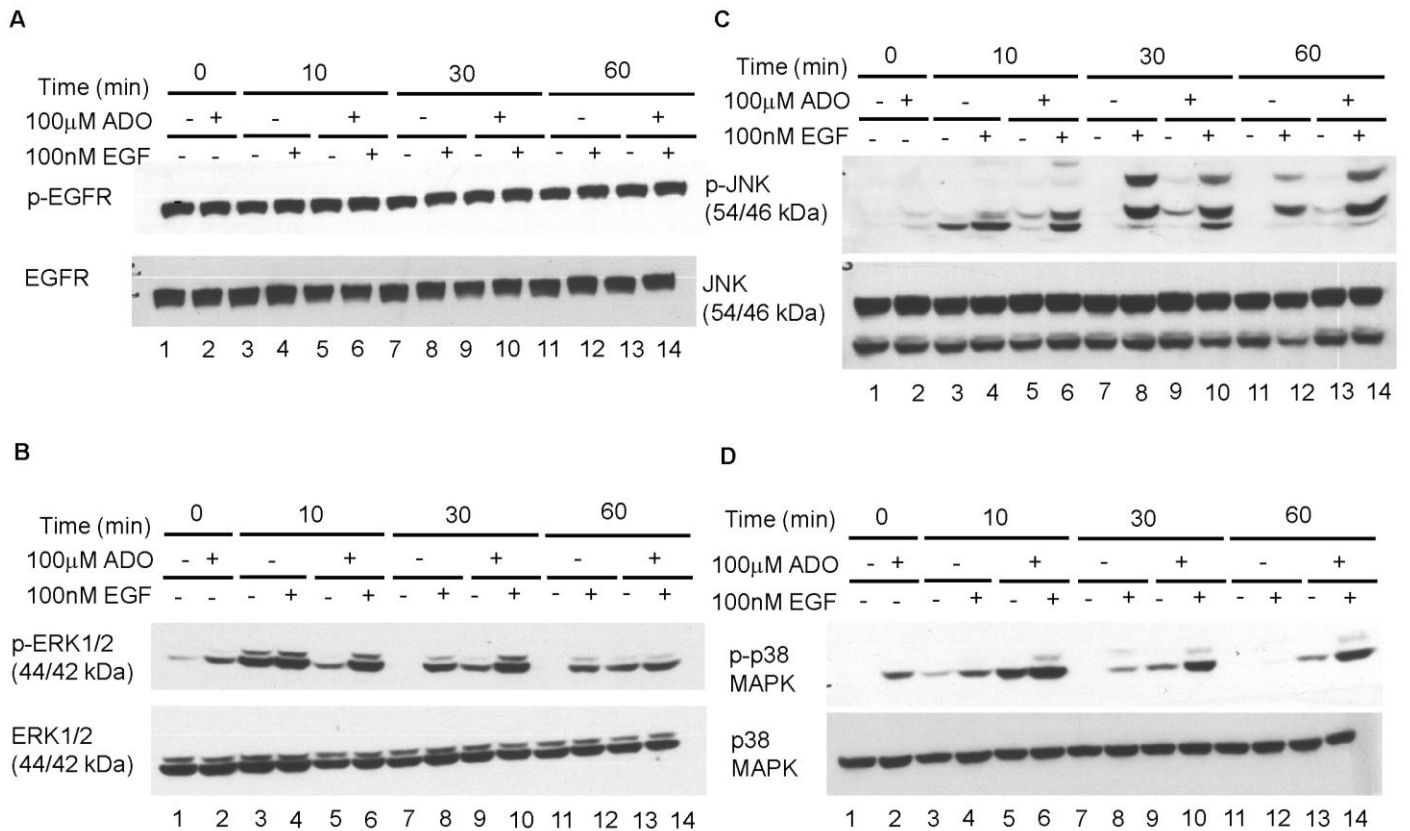


**Figure 4.1 Andrographolide up-regulates the MAPK signalling pathways independently of EGF.** A-431 cells were starved overnight in serum-free media, pre-treated with DMSO or 100  $\mu$ M ADO for 4 hours in serum-free media, and then either activated with 100 nM EGF for varying timepoints (A); or treated with DMSO or 100  $\mu$ M ADO for varying time-points, lysed (B) and used for western blot analysis. VC, vehicle control; ADO, andrographolide. Phosphorylation of EGFR and major MAPK signalling pathways was determined using anti-phosphorylated EGFR (BD Biosciences) and total EGFR (A), phospho-ERK1/2 and total ERK1/2 (B), phospho-JNK and total JNK (C), and phospho-p38 MAPK and total p38 MAPK (D) antibodies. Blots are representative of at least two independent experiments.

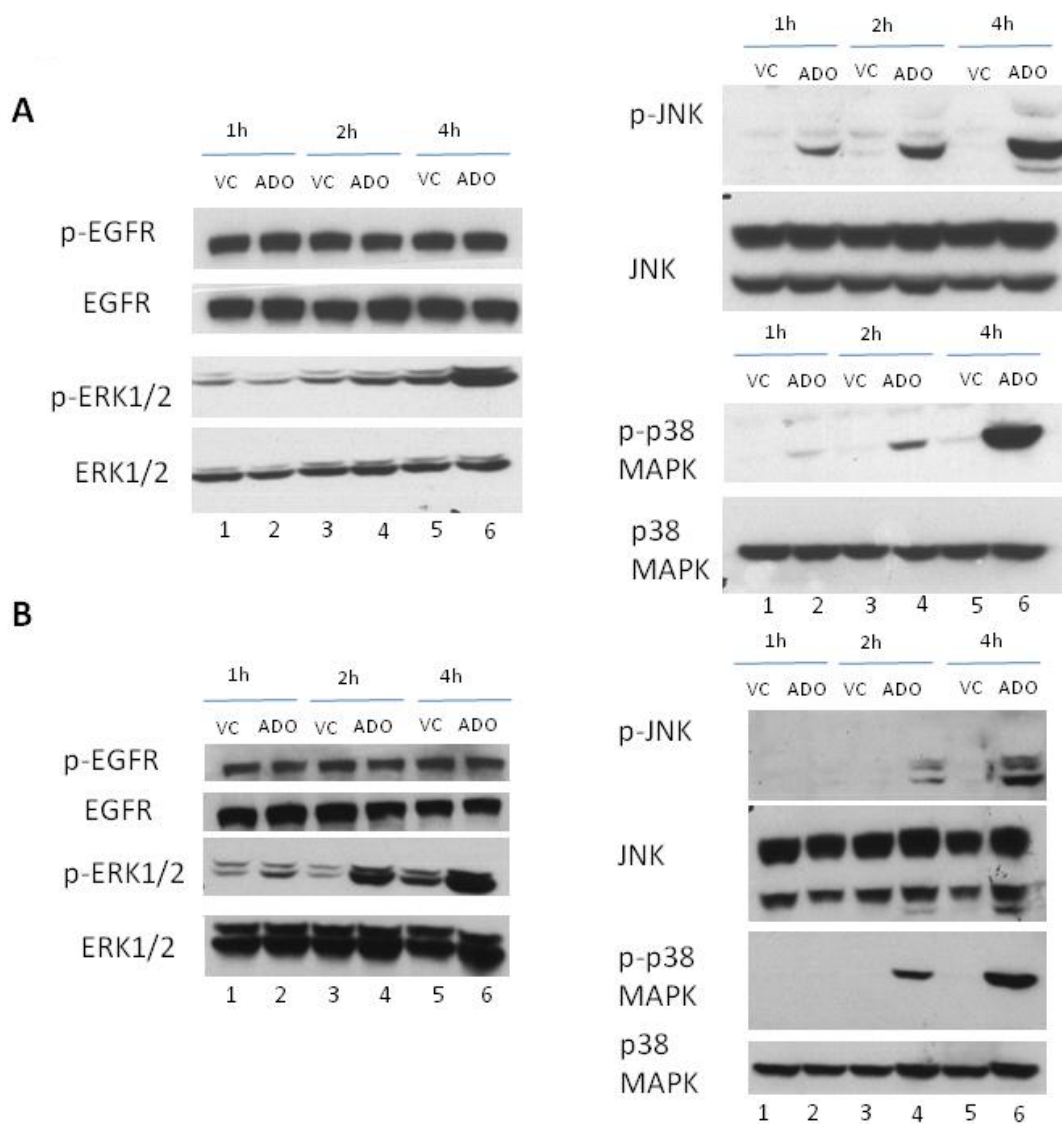


**Figure 4.2 Andrographolide upregulates MAPK signalling pathways phosphorylation independently of EGF in A-431 (A) and HeLa (B) cells.** Cells were starved overnight in serum-free media, pre-treated with DMSO or 100  $\mu$ M ADO for varying timepoints in serum-free media, lysed and analysed by western blot. VC, vehicle control; ADO, andrographolide. Phosphorylation of EGFR and major MAPK signalling pathways were determined using the same antibodies as figure 1. Blots are representative of at least two independent experiments.

### **4.3.2. JNK and p38 MAPK activity regulate ADO induced EGFR internalisation**

Although phosphorylation of MAPKs is usually closely associated with the upregulation of MAPK activity, we wanted to be certain that ADO does not only upregulate the levels of phosphorylated MAPKs, but also increases their activity. Hence, we used a p38 MAPK activity assay to check for ADO effect on p38 MAPK activity. Cells were pretreated with ADO for 4 h, lysed and phosphorylated p38 MAPK was incubated with its downstream signalling target, recombinant ATF-2 protein. Levels of ATF-2 phosphorylation were then analysed by western blot. As anticipated, p38 MAPK is activated upon ADO treatment (Figure 4.3A).

As p38 MAPK is known to induce EGFR internalisation (Vergarajauregui *et al.*, 2006; Zwang & Yarden, 2006) by inducing EGFR phosphorylation, we postulated that the p38 MAPK activation by ADO could be responsible for regulating EGFR downregulation from the cell surface. Hence, we investigated the effect of MAPK inhibitors (MAPKi) on EGFR internalisation from the cell surface. A-431 cells were incubated with anti-EGFR antibody on ice, and the antibody was allowed to internalise at 37 °C for 4 h either in the absence or presence of ADO and MAPKi which were added together. ADO caused the accumulation of EGFR at the perinuclear region, and this accumulation was reduced in the presence of p38 MAPKi and JNKi, but not ERKi (Figure 4.3B).

We were then interested to determine if continued p38 MAPK activity was required for accumulation of EGFR. EGFR antibody was internalised in the presence of ADO

for 3 h to allow for p38 MAPK activation, and p38 MAPKi was then added for an hour. Cells were then fixed and visualized. After 1 h of treatment, p38 MAPKi can still inhibit the accumulation of EGFR at the perinuclear region, indicating that continued phosphorylation of EGFR by p38 MAPK is important for the accumulation of EGFR (Figure 4.3C).

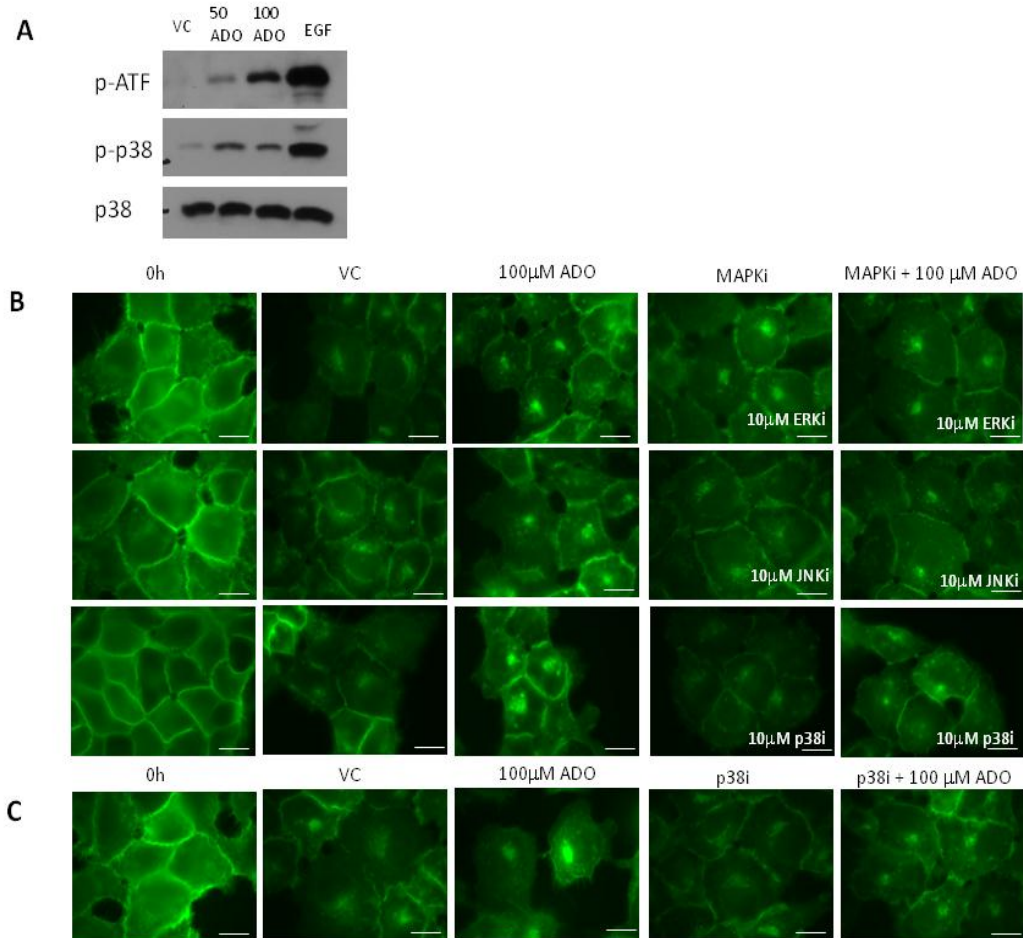


**Figure 4.3 Andrographolide enhances endocytosis of EGFR via activation of the p38 MAPK.** Cells were incubated with anti-EGFR 29.1 mAb on ice for 1 h, then pre-treated with either DMSO, MAPKi in the presence or absence of 100  $\mu$ M ADO in media at 37 $^{\circ}$  C for 4 h (B), or pre-treated with DMSO or 100  $\mu$ M ADO in media for 3 h before p38 MAPKi was added for the last hour (C). VC, vehicle control; ADO, andrographolide; MAPKi, MAPK inhibitors; 50 ADO, 50  $\mu$ M ADO; 100ADO, 100  $\mu$ M ADO, EGF, 100 ng/ml EGF. Images are representative of at least two independent experiments. Scale bars are representative of 10  $\mu$ m.

A. ADO induced p38 MAPK phosphorylation results in increase of p38 MAPK kinase activity. Cells were starved overnight in serum-free media, and treated with ADO for 4 h or 100ng/ml of EGF for 15 minutes. Cells were then lysed and processed using the p38 MAPK kinase kit. Blots are representative of at least three independent experiments.

B. Inhibition of EGFR endocytosis by p38 MAPKi and JNKi.

C. Continual p38 MAPK kinase activity is required for EGFR accumulation.

We then went on to confirm if ADO induces the phosphorylation of EGFR on serine 1046/1047 in a p38 MAPK dependent manner. A-431 cells were pre-starved in serum-free media, treated with ADO for 4 h, lysed and analysed using western blot. As expected, the antibody specific for full-length phosphorylated EGFR showed no difference upon ADO treatment. However, the antibody specific only for EGFR phosphorylated on serine 1046/1047 showed increased phosphorylation at both 50 and 100  $\mu$ M ADO (Figure 4.4A). Addition of p38 MAPKi did not affect phosphorylation of p38 MAPK, but it inhibited ADO induced phosphorylation of EGFR on serine 1046 (Figure 4.4B). JNKi, in contrast, inhibited phosphorylation of JNK, but did not seem to affect phosphorylation of EGFR on serine 1046 (Figure 4.4C). Similar results were obtained for HeLa cells (data not shown).

Addition of MAPKi could partially rescue ADO downregulation of cell surface receptors. HeLa cells were used as it is easier to detect changes in EGFR surface levels as they express physiological levels of EGFR, as compared to A-431, which over-expresses EGFR. Cells were treated with ADO in the presence of either p38 MAPKi or JNKi for 4 h and analysed by flow cytometry for surface EGFR. ADO decreased surface EGFR by 25%, and addition of both p38 MAPKi and JNKi restored surface EGFR levels to approximately 95% after ADO treatment (Figure 4.5).



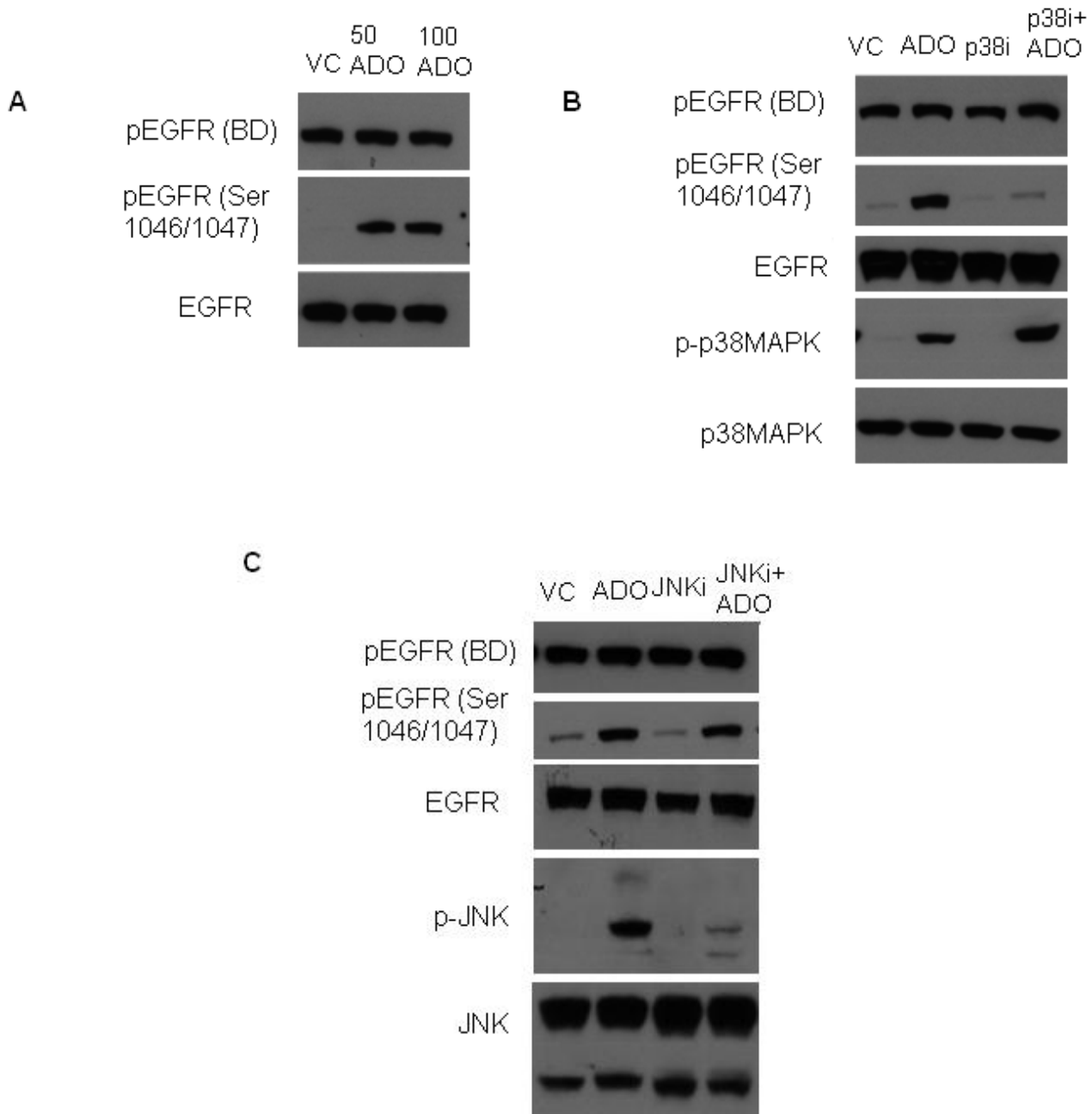


**Figure 4.4 Activated p38 MAPK phosphorylates EGFR in A-431 cells.** A-431 cells were starved overnight in serum-free media, pre-treated with DMSO or 100  $\mu$ M ADO for 4 hours in serum-free media in the presence or absence of 10  $\mu$ M MAPKi. VC, vehicle control; ADO, andrographolide; MAPKi, MAPK inhibitors, pEGFR, phosphorylated EGFR; 50 ADO, 50  $\mu$ M ADO; 100 ADO, 100  $\mu$ M ADO. Phosphorylation of EGFR and major MAPK signalling pathways were determined using the same antibodies as figure 1 with the exception of pEGFR serine 1046/1047. Blots are representative of at least two independent experiments.

- A. ADO causes phosphorylation of EGFR at serine 1046/1047 in A-431 cells.  
 B. p38 MAPKi inhibits ADO phosphorylation of EGFR at serine 1046/1047 in A-431 cells.  
 C. JNKi does not inhibit ADO phosphorylation of EGFR at serine 1046/1047 in A-431 cells.

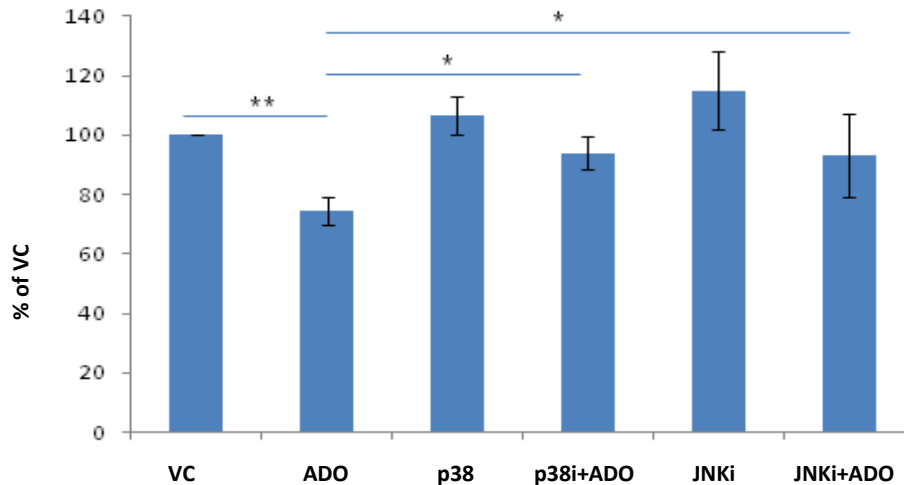


**Figure 4.5 Andrographolide induced p38 MAPK phosphorylates EGFR, causing downregulation of surface EGFR in Hela cells.** Hela cells were starved overnight in serum-free media, pre-treated with DMSO or 100  $\mu$ M ADO for 4 hours in serum-free media in the presence or absence of 10  $\mu$ M MAPKi. VC, vehicle control; ADO, andrographolide; MAPKi, MAPK inhibitors, pEGFR, phosphorylated EGFR. Phosphorylation of EGFR and major MAPK signalling pathways were determined using the same antibodies as figure 1 with the exception of pEGFR serine 1046/1047. Blots are representative of at least two independent experiments.

#### 4.4. Discussion

Activation of signalling pathways is a typical down-stream effect of ligand-receptor interaction, especially for growth receptors such as EGFR. The activated receptors are endocytosed and trafficked to the late endosome as a mechanism to downregulate signalling. However, in recent years, new evidence that proteins involved in signalling pathways can conversely regulate receptor trafficking and endocytosis has been emerging (Sorkin & von Zastrow, 2009). Earlier studies on p38 MAPK showed that it phosphorylates EGFR on threonine 669 (Winograd-Katz & Levitzki, 2006), residues 1002 – 1020 (Zwang & Yarden, 2006) and serine 1046/1047 (Adachi *et al.*, 2009a), and these residues are involved in the internalisation of EGFR. However, the exact mechanism of how phosphorylation of these residues induce EGFR endocytosis is not yet known (Sorkin & Goh, 2009). In a recent study, both p38 MAPK and EGF induced EGFR endocytosis was shown to be clathrin dependent, but p38 MAPK

mediated EGFR endocytosis was shown to require the di-leucine and YRAL motif to interact with adaptor protein-2 (AP-2) complex; whereas EGF induced EGFR endocytosis was Grb2 dependent (Grandal *et al.*, 2011). The di-leucine motif exists at residues 1010 – 1011, and hence it corresponds with the region of 1002 – 1020 as reported by Zwang *et al.* earlier on.

p38 MAPK activation is also known to increase endocytosis rates via enhancing the formation of the cytosolic guanyl-nucleotide dissociation inhibitor (GDI):Rab5 complex. GDI is responsible for sequestering Rab5 in the cytosol, away from membranes where it mediates endosomal fusion. GDI:Rab5 can either be directly involved in endosome formation, or it can increase recruitment of the Rab5 GTPase, to regions where endosomal formation is occurring (Cavalli *et al.*, 2001; Clague & Urbe, 2001). The  $\alpha$  isoform of p38 MAPK can also increase endocytosis by phosphorylating the Rab 5 effectors EEA-1 on threonine 1392 and Rabenosyn-5 on serine 215 within their FYVE domain, which is responsible for binding to the phosphatidylinositol-3 phosphate (PI(3)P) in endosomes, to induce increased membrane recruitment (Mace *et al.*, 2005). It would be interesting to uncover the mechanism through which ADO activates p38 MAPK for future studies.

Previous work on ADO has demonstrated that ADO upregulates the production of reactive oxygen species, hence leading to an increase in phosphorylation of the p46 and p54 subunit of JNK, and this increase was blocked by adding the antioxidant N-acetyl cysteine (Zhou *et al.*, 2008). We were interested to determine whether the ADO-induced phosphorylation of ERK1/2, p38 MAPK and JNK could be blocked by the addition of L-cysteine, and hence we pre-incubated ADO with 5mM of L-cysteine

for an hour before adding the resulting mixture to the cell culture. We chose L-cysteine to eliminate the possibility of the acetyl group playing any role in the reaction. L-cysteine is also capable of scavenging reactive oxygen species. In the presence of L-cysteine, ADO was no longer able to induce ERK1/2, p38 MAPK and JNK phosphorylation (Figure 4.6).

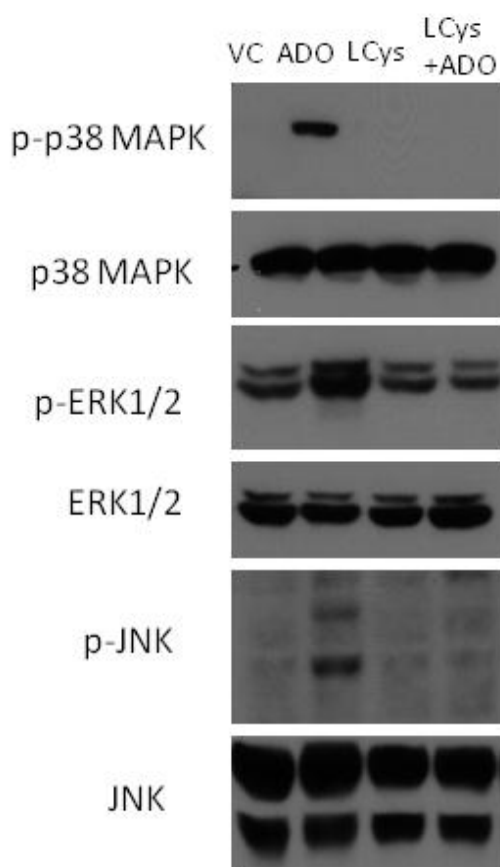


**Figure 4.6 L-cysteine inhibits MAPK induced signalling.** L-cysteine is capable of blocking the effect of ADO on MAPK signalling pathways. 100 $\mu$ M ADO was pre-incubated with L-cysteine for 1 h, then added to A-431 cells for 4 h and lysed for western blot analysis. VC, vehicle control; ADO, andrographolide; MAPKi, MAPK inhibitors. Phosphorylation of EGFR and major MAPK signalling pathways were determined using the same antibodies as Figure 4.1.

ADO is known to induce JNK activation via upregulation of free cellular glutathione, and chemical inhibition of free glutathione synthesis prevents ADO induced JNK activation (Ji *et al.*, 2011). Previously, ADO has also been shown to increase levels of hydrogen peroxide in HepG2 human hepatoma cells (Li *et al.*, 2007). This accumulation of hydrogen peroxide is most likely due to the increased activity of superoxide dismutase (SOD), hence reducing the overall levels of superoxide and increased levels of hydrogen peroxide. Although hydrogen peroxide can be decomposed by catalase (CAT) to give water and oxygen (Figure 4.7), and ADO upregulates CAT activity, hydrogen peroxide can be accumulated if its rate of production is higher than its rate of removal.

Hydrogen peroxide is known to activate the MAP3K molecule apoptosis signal-regulating kinase-1 (ASK-1), which is inhibited by complexing to thioredoxin [TrxR-(SH)<sub>2</sub>] (Saitoh *et al.*, 1998). In the presence of oxidative stress, the thiol group of thioredoxin is oxidised to form thioredoxin disulphide (TrxR-S<sub>2</sub>) and dissociates from ASK-1 (Yoshioka *et al.*, 2006), leading to recruitment of TNF receptor associated factor 2 and 6, resulting in phosphorylation of threonine 838 in the activation loop of human ASK-1 (Matsuzawa & Ichijo, 2008), allowing it to phosphorylate the downstream MAP2Ks, and eventually lead to JNK and p38 activation. ASK-1 is negatively regulated by phosphorylated Akt, which phosphorylates it at the serine 83 residue. As ADO induced JNK and p38 MAPK signalling is eliminated in the presence of the anti-oxidant L-cysteine, we speculate here that a possible mechanism of p38 MAPK activation could be through the ADO-induced increase in intracellular hydrogen peroxide levels, leading to activation of ASK-1, and downstream JNK and

p38 MAPK. The resultant active p38 MAPK then phosphorylates EGFR at serine 1046/1047 and induces its internalisation (Figure 4.8).

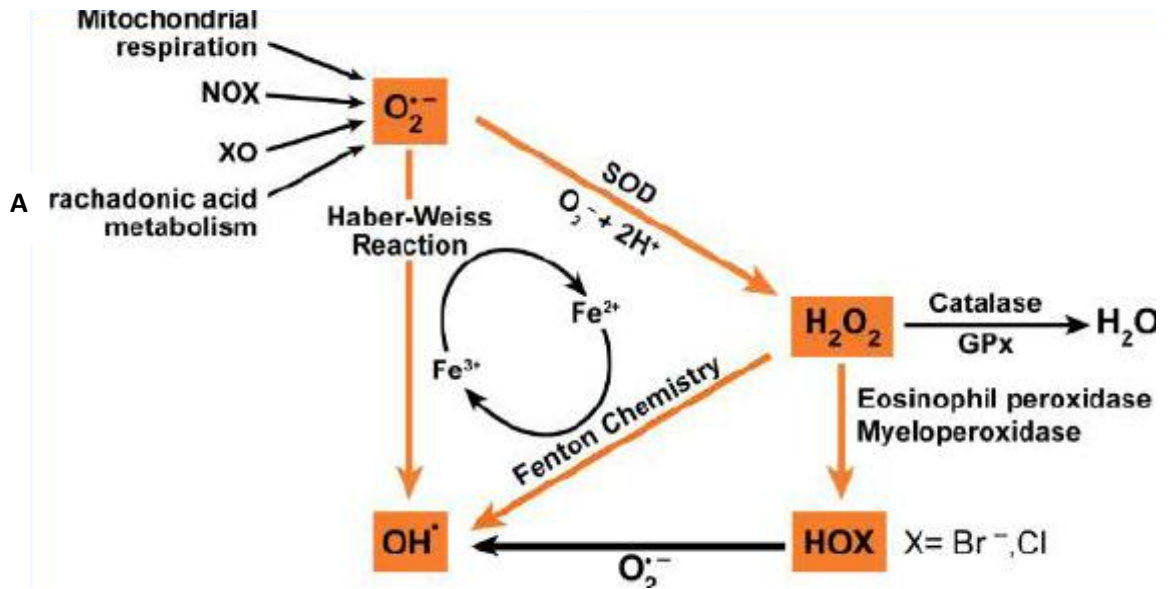


**Figure 4.7 Production and removal of reactive oxygen species (ROS)** (Comhair & Erzurum, 2010). Superoxide is removed by superoxide dismutase (SOD) to give hydrogen peroxide. Catalase then causes decomposition of hydrogen peroxide to give water and oxygen. Permission granted courtesy of Mary Ann Liebert.

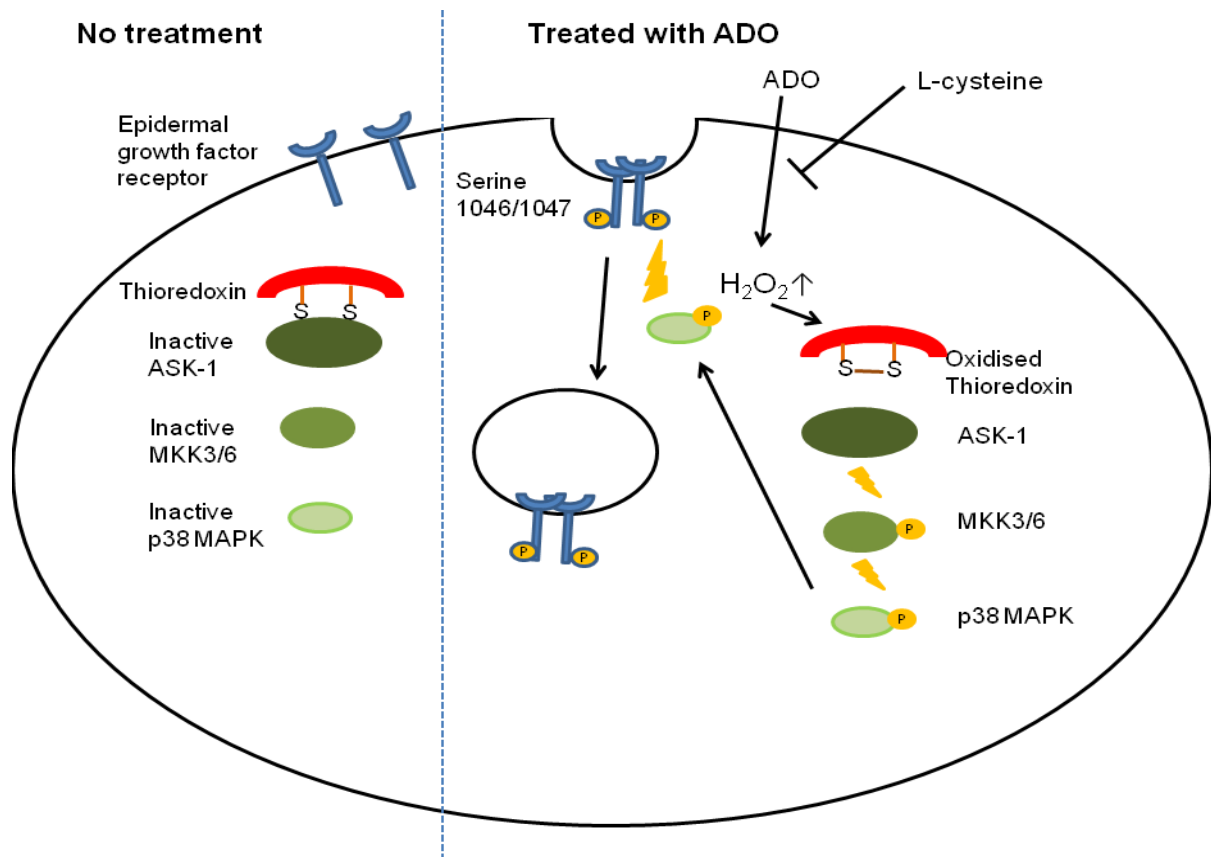


**Figure 4.8 Proposed model of ADO effect on p38 MAPK signalling and EGFR endocytosis.** In the absence of ADO, thioredoxin is in its reduced form, and acts to inhibit ASK-1, thus there is no activation of p38 MAPK. However, in the presence of ADO, hydrogen peroxide levels are up-regulated and this leads to the oxidation of thioredoxin. Thioredoxin dissociates from ASK-1 and this leads to its activation, causing MKK3/6 and p38 MAPK to be phosphorylated. p38 MAPK then moves to phosphorylate EGFR on serine 1046/1047, thus causing it to endocytose, reducing overall surface levels of EGFR. ADO elevation of hydrogen peroxide levels is inhibited in the presence of the anti-oxidant L-cysteine.

Conversely, phosphorylation of ERK1/2 is well known to activate cellular proliferation pathways and to inhibit apoptosis. However, it has been demonstrated that oxidative stress induced by hydrogen peroxide can lead to activation of ERK1/2 through activation of the Src kinase, or in a Ras-dependent or independent manner. Interestingly, ERK1/2 activation in some cases has been shown to be capable of inducing apoptosis in cells (McCubrey *et al.*, 2006).

The activation of the p38 MAPK, JNK and ERK1/2 may contribute to the reduction in cell survival upon ADO treatment, as they could induce apoptosis. Inhibition of p38 MAPK and JNK activation led to slight increases in cell viability, but inhibition of ERK1/2 did not induce significant change (Figure 4.9).

In summary, we have shown here that ADO downregulation of surface EGFR is due to its activation of p38 MAPK. ADO is not the only natural compound known to activate p38 MAPK and induce downregulation of surface EGFR. Other compounds such as epigallocatechin-3-gallate (EGCG) (Adachi *et al.*, 2009b), the active compound extracted from green tea, have been shown to induce p38 MAPK activation and cause EGFR phosphorylation at serine 1046/1047, causing downregulation of surface EGFR and inhibiting cell proliferation (Adachi *et al.*, 2008). This thus indicates the plausible use of dietary supplements to exert anti-carcinogenic effects to decrease surface levels of EGFR, and this could be an approach that is used in combination with current chemotherapy to reduce expression of EGFR in cancer cells.



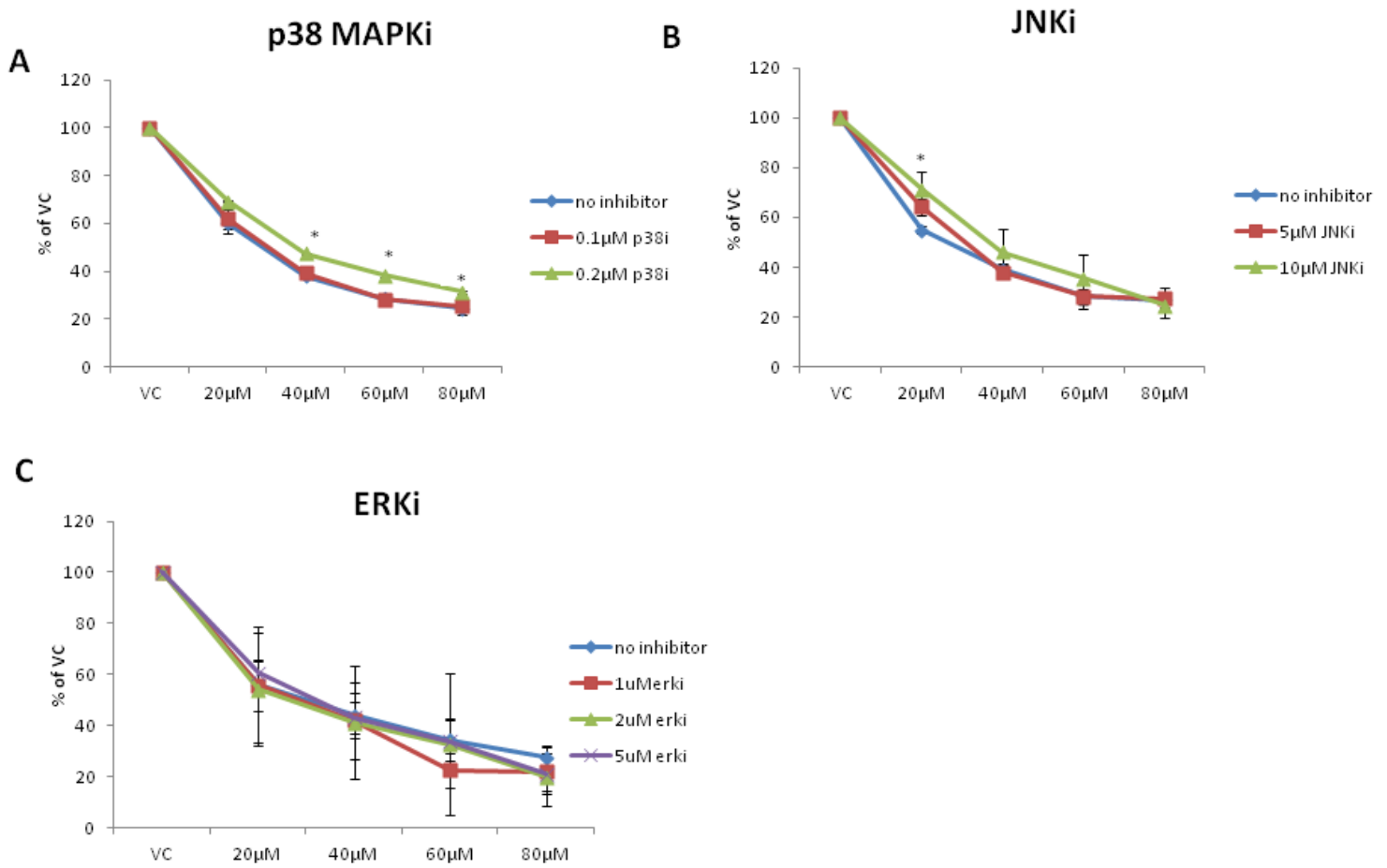


**Figure 4.9 MAPKi can partially restore cell viability in A-431 cells.** A-431 cells were treated for 24 h with varying concentrations of ADO in the presence or absence of MAPK inhibitors (MAPKi) and the amount of viable cells quantitated by the MTT assay. \*,  $p < 0.05$ .

# **Chapter 5**

## **Andrographolide regulates phagocytosis in microglia cells through downregulation of CD204**

## **5. Andrographolide regulates phagocytosis in microglia cells through downregulation of CD204**

### **5.1. Abstract**

It has been demonstrated in our earlier studies that ADO is capable of downregulating surface EGFR through phosphorylating EGFR on serine 1046/1047 residues. ADO is also known to inhibit dendritic cell maturation through suppressing important receptors such as CD40, CD80 and CD86. We postulated that one of the anti-inflammatory mechanisms of ADO could be due to its ability to decrease surface receptors of immune cells, hence we investigated the effect of ADO on surface scavenger receptor trafficking in N9 microglia cells. We found that ADO is capable of inhibiting phagocytosis by up to 50% through decreasing surface CD204, and this was mediated by inhibiting trafficking of CD204 to the cell surface.

### **5.2. Introduction**

Bacterial meningitis is the inflammation of the meninges, typically caused by *Streptococcus pneumoniae*, *Neisseria meningitidis* and in some cases, *Mycobacterium tuberculosis*. It occurs due to microbial penetration of the blood brain barrier (BBB) via interaction with receptors on the host endothelium (Kim, 2003). A lack of an immune response in this immunoprivileged area allows the microbes to rapidly multiply, resulting in the colonisation of the subarachnoid cavity. Bacteria in the cavity can then autolyse to release components such as pneumolysin, lipopolysaccharide, lipotechoic acid and bacterial DNA which then activate microglia, meningeal and perivascular macrophages through the toll like receptors. Pro-inflammatory cytokines such as TNF- $\alpha$  and IL-1 $\beta$  are then released, increasing BBB

permeability and causing the recruitment of leukocytes. Breakdown of the BBB then ensues, leading to brain edema and increased intracranial pressure. Inflammation of the CNS also results in the release of reactive oxygen species which causes neuronal injury and cell death (Gerber & Nau, 2010). Hence, 15 % of meningitis cases experience neurological sequelae in the form of seizures, loss of hearing as well as learning deficits (Saez-Llorens & McCracken, 2003).

ADO is a known anti-inflammatory agent which can also modulate neuroinflammation. It is capable of ameliorating the progression of EAE through inhibiting activation of dendritic cells, thereby downregulating the expression of MHC class II molecules on the cell surface, hence decreasing antigen presentation to T cells. T cells in turn proliferate to a smaller extent resulting in a decrease in IFN- $\gamma$  and IL-2 production (Iruretagoyena et al., 2006). Microglia activation by lipopolysaccharide (LPS) and the resultant release of proinflammatory factors was also specifically suppressed by ADO treatment (Wang *et al.*, 2004). Activation of OX-42 positive microglia and production of inflammatory markers in a rat model of cerebral ischaemia was similarly inhibited upon ADO treatment (Chan *et al.*, 2010).

ADO has been convincingly demonstrated to be an anti-inflammatory compound through its effects on the NF- $\kappa$ B signalling pathway – preventing binding of the p50 subunit of NF- $\kappa$ B to its target sequence (Xia *et al.*, 2004), as well as inhibiting phosphorylation of the upstream I $\kappa$ B kinase (IKK) complex, thus preventing downstream nuclear translocation of the p65 subunit of NF- $\kappa$ B (Bao *et al.*, 2009).

However, the possibility of a separate mechanism for the anti-inflammatory action of ADO still exists, as drugs are known to act on a variety of pathways. Interestingly, ADO was able to downregulate receptors from the cell surface such as CD40, CD80 and CD86 in dendritic cells (Iruetagoiena *et al.*, 2005), as well as the epidermal growth factor receptor (EGFR) in A-431 epidermoid carcinoma cells (Tan *et al.*, 2010) through phosphorylation of EGFR on the serine 1046/1047 residues. Although it does not decrease surface EGFR via affecting general cellular endocytosis mechanisms, it is possible that it could also lead to the lowered surface expression of other surface receptors. As scavenger receptors are important for the phagocytic uptake of antigens in antigen presenting cells (Husemann *et al.*, 2002), it is possible that ADO could inhibit inflammation by downregulating surface expression of scavenger receptors, hence affecting phagocytosis.

### **5.2.1. Scavenger Receptors**

Scavenger receptors (SRs) are an important class of receptors expressed on phagocytic cells which are responsible for the uptake and removal of a variety of foreign substances, such as cell debris and bacteria. They also play key roles in modulating lipid metabolism through the uptake of lipoproteins, and different scavenger receptors endocytose different forms of lipoproteins, which may be native or modified (acetylated or oxidized) (Ashraf & Gupta, 2011). SRs are divided into 8 classes (A – H) based on their different structural domains.

Class A scavenger receptors contain a common collagenous domain, and its members, which include the three isoforms of scavenger receptor A (SR-AI, II and III) and macrophage receptor with collagenous structure (MARCO) have a common cysteine rich region (Pluddemann *et al.*, 2007). SR-A binds to the lipopolysaccharide (LPS) found on the cell walls of bacteria (Doi *et al.*, 1993; Nakamura *et al.*, 2001), as well as other bacterial ligands on *Neisseria meningitidis*, and SR-A knock-out mice have higher rates of infection due to an inability to clear bacteria (Pluddemann *et al.*, 2006). Recombinant soluble MARCO consisting of the spacer, collagenous and cysteine rich domains similarly binds to LPS (Sankala *et al.*, 2002), and has been shown to bind to *Clostridium sordellii* (Thelen *et al.*, 2010) and *Neisseria meningitidis* (Mukhopadhyay *et al.*, 2006; Pluddemann *et al.*, 2009).

CD36 belongs to the SR class B family, and it contains loops with multiple glycosylation sites. It is known to bind to the lipoteichoic acid of *Staphylococcus aureus* (Stuart *et al.*, 2005), and has also been shown to be involved in the uptake of various bacteria such as *E. coli* K12 and K25, *Enterococcus faecalis*, *Klebsiella pneumoniae*, *Salmonella typhimurium* (Baranova *et al.*, 2008). Presence of CD36 is important for *Mycobacterium tuberculosis* infection of the host (Hawkes *et al.*, 2010).

We investigated the effect of ADO on phagocytic uptake of antigens by microglial cells. Microglia are resident macrophages of the brain (Muzio *et al.*, 2007), and are thought to be involved in the initiation of inflammation via their pattern recognition receptors. They are also capable of phagocytosing foreign materials and displaying

peptides on MHC class II for T cell activation. Here, we demonstrate that ADO is able to inhibit phagocytosis in microglial cells by downregulating cell surface expression of scavenger receptor CD204 and CD36. Our results suggest that ADO could alleviate inflammatory responses due to its ability in downregulating receptors that mediate non-opsonic phagocytic uptake of antigens and presentation by microglial cells.

### 5.3. Results

#### 5.3.1. Andrographolide regulates phagocytosis in microglial cells

ADO is well known for suppressing immune responses via inhibiting NF- $\kappa$ B activation, but we were interested to see if ADO could affect the immune response at another level. We postulated that ADO downregulation of surface scavenger receptors would affect phagocytic uptake of particulate antigens, and we investigated phagocytosis using fixed bacteria as an antigen. Bacteria were chosen as they express physiological ligands for scavenger receptors, and fixed bacteria were used to prevent bacteria growth and induction of microglia cell death.

Cells were treated with ADO for 3 hours, and allowed to phagocytose green fluorescent protein (GFP) *E. coli* bacteria for 10 minutes in the presence of the drug and fixed. The amount of phagocytosed bacteria was then quantified by flow cytometry. Interestingly, the inhibition in phagocytosis is dose-dependent (Figure 5.1A), and phagocytosis is inhibited up to 50% for 50  $\mu$ M of ADO. To visually confirm that phagocytosis was indeed down-regulated, microglia cells were allowed to phagocytose bacteria for 20 minutes before they were washed and fixed. Immunofluorescence was performed to check for the number of bacteria bound per cell with drug treatment. The number of bacteria binding to 200 cells for each concentration were then counted, and triplicates were performed for each concentration. Phagocytosis rates decreased by up to 50% at 50  $\mu$ M of ADO as shown in Figure 5.1B. Cell viability on the other hand, was unaffected upon treatment with ADO up to 120 $\mu$ M for 3 hours (data not shown). ADO is known to inhibit NF- $\kappa$ B activation, which is activated by lipopolysaccharide (LPS) through Toll like receptor



4 (Xia *et al.*, 2004). As LPS is known to induce an increase in phagocytosis in microglia and macrophages (Wu *et al.*, 2009; Sivagnanam *et al.*, 2010), there is a possibility that perturbing the LPS signalling pathway may in turn affect phagocytosis. In order to rule out the possibility that ADO affected phagocytosis rates through inhibiting the NF- $\kappa$ B pathway, we allowed N9 to phagocytose latex beads. Phagocytosis was similarly down-regulated up to 50% (Figure 5.1C), indicating that the ADO effect on phagocytosis was not dependent on the presence of LPS.

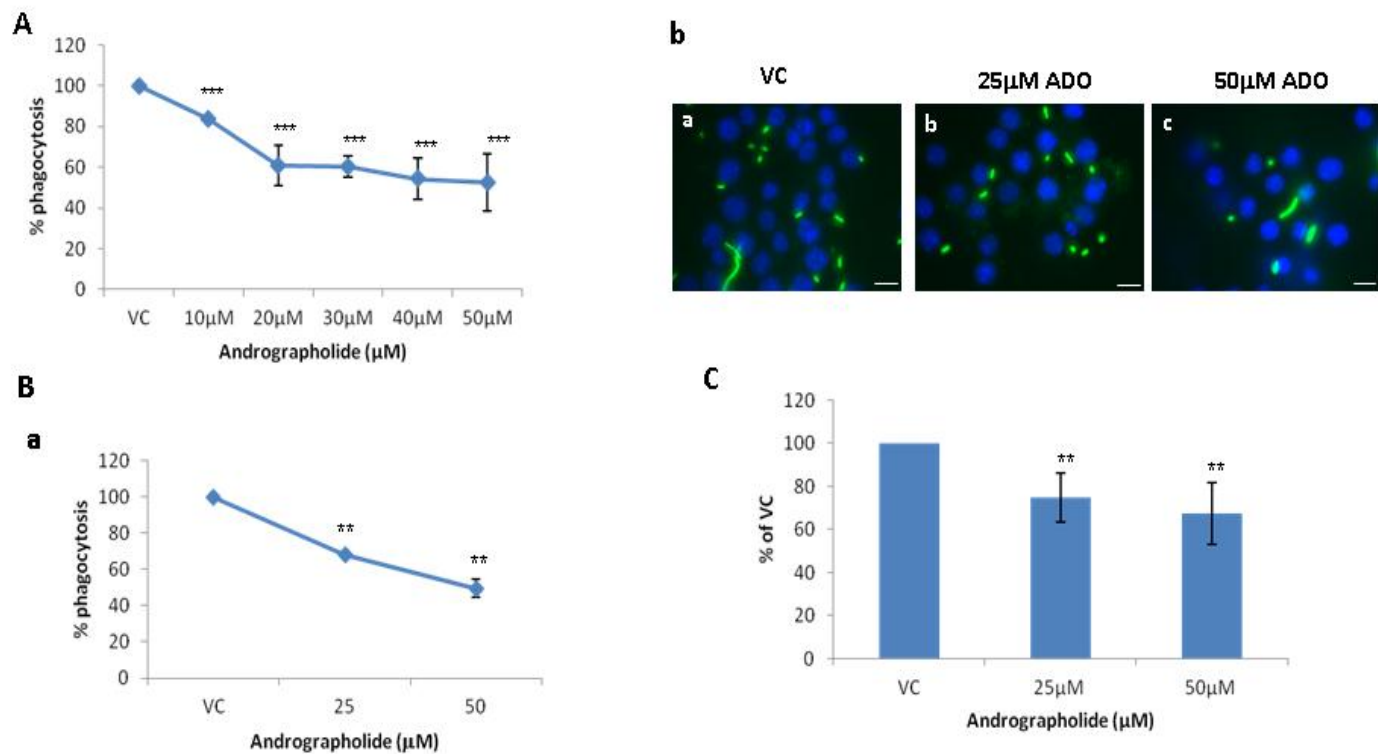


**Figure 5.1 ADO down-regulates phagocytosis in microglia.**

- A. Effect of ADO treatment on phagocytosis. N9 cells were treated for 3 hours with varying concentrations of andrographolide, incubated with fixed GFP expressing bacteria for 10 minutes, then fixed and analysed by flow cytometry. \*\*\*,  $P < 0.005$  relative to vehicle control; Graph is representative of at least 3 independent experiments.
- B. Visualisation of bacteria binding to microglia after andrographolide treatment.
- a. N9 cells were treated for 3 hours with varying concentrations of ADO, incubated with fixed GFP bacteria for 20 minutes and fixed. Triplicates of each concentration were used, and the number of bacteria binding to 200 cells was counted for each coverslip. Graph is representative of at least 2 independent experiments.
- b. Immunofluorescence photos of bacteria binding to N9 cells after 20 minutes. Pictures are representative of at least 2 independent experiments. Scale bars are representative of 10 μm.
- C. Effect of andrographolide treatment on phagocytosis of latex beads. N9 cells were treated for 2 hours with varying concentrations of ADO, incubated with 1μm polystyrene beads for 1 hour, then fixed and analysed by flow cytometry. \*\*,  $P < 0.001$  relative to vehicle control; Graph is representative of at least 3 independent experiments. VC, vehicle control; ADO, andrographolide; GFP, green fluorescent protein.

### **5.3.2. Andrographolide decreases the surface expression of CD204 and CD36**

Phagocytosis of bacteria is known to be mediated by scavenger receptors. As we have previously demonstrated that ADO is capable of downregulating expression of epidermal growth factor receptors (EGFR) on the surface of A-431 cells (Tan *et al.*, 2010), it was highly likely that andrographolide could have also down-regulated cell surface expression of scavenger receptors in N9 cells. To elucidate this drop in phagocytic activity, the surface expression of three scavenger receptors: class A scavenger receptors CD204, otherwise known as scavenger receptor A (SR-A), and MARCO (data not shown), as well as CD36, a class B scavenger receptor, were studied following drug treatment for 3 h. Interestingly, surface levels of CD36 and CD204 were reduced by about 20% upon 50 $\mu$ M ADO treatment (Figure 5.2A). However, the total receptor levels remained unchanged as shown by western blot (Figure 5.2B).

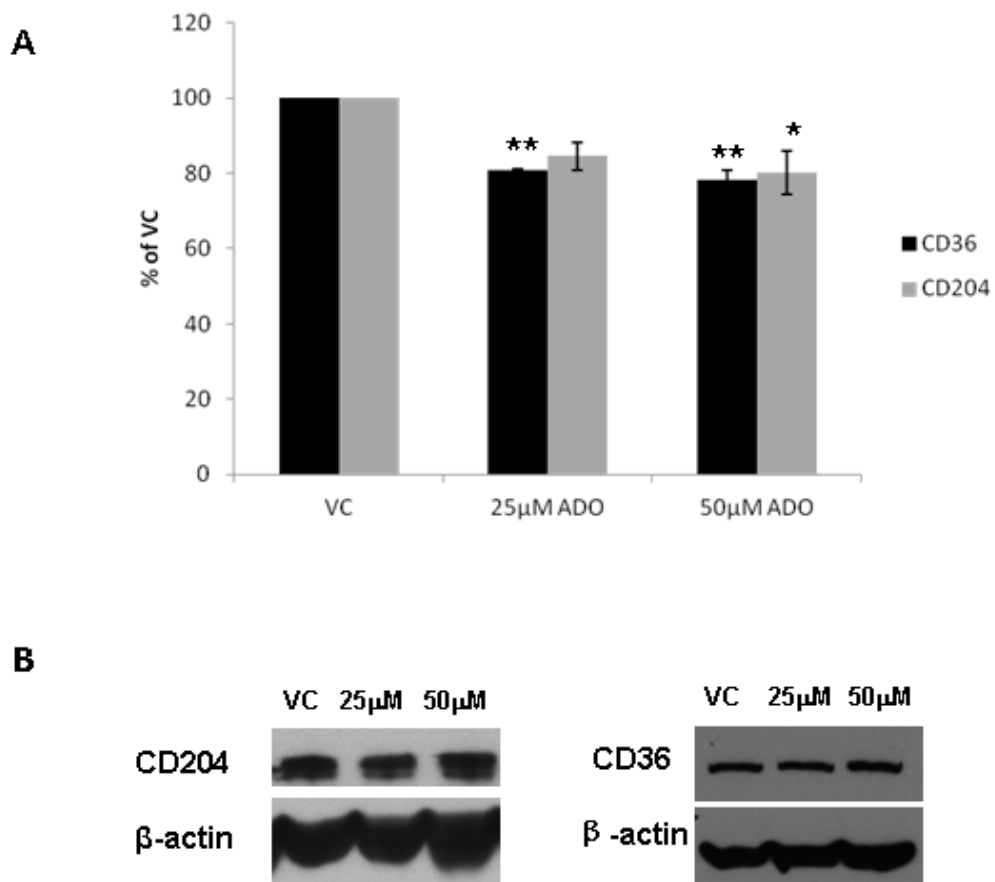


**Figure 5.2 ADO induces a decrease in surface expression of CD204 and CD36.**

- A. ADO downregulates cell surface receptor levels. N9 cells were treated for 3 hours with varying concentrations of ADO and stained with antibody against CD36 and CD204. Flow cytometry results are representative of at least 3 independent experiments. \*,  $P < 0.05$  relative to vehicle control; \*\*,  $P < 0.01$  relative to vehicle control.
- B. ADO does not affect total levels of receptors. N9 cells were treated for 3 hours with varying concentrations of ADO and lysed. CD36 and CD204 levels were analysed by non-reducing western blot. Blots are representative of at least 2 independent experiments. VC, vehicle control; ADO, andrographolide.

### **5.3.3. CD204 is important for phagocytosis of *E. coli* in N9 microglia cells**

Different SRs have varying domains that bind to different bacteria. As the SRs tested were down-regulated from the cell surface, we were interested to find out which receptors were responsible for the downregulation of phagocytosis of *E. coli* in N9. Hence, we blocked the receptors using inhibitory antibodies of varying concentrations for CD36, CD204 and MARCO, and assayed for phagocytosis levels using the Vybrant phagocytosis assay. Interestingly, only the CD204-specific antibody caused a significant drop of more than 50% in phagocytosis, indicating that it is the main scavenger receptor responsible for phagocytosis in N9 (Figure 5.3B). The drop in phagocytosis was the same for 5µg/ml and 20 µg/ml of antibody, showing that the capability of anti-CD204 antibody in blocking bacteria binding and phagocytosis was saturated at 5µg/ml.

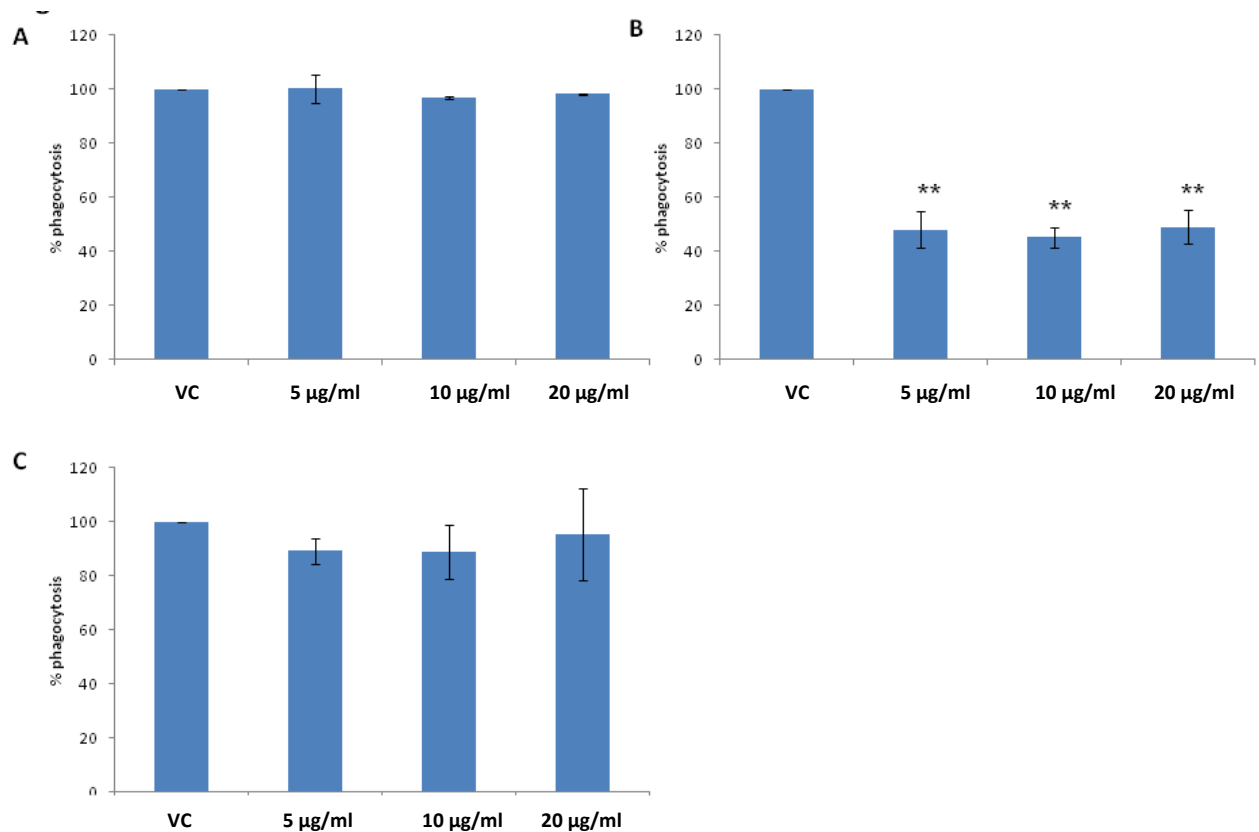
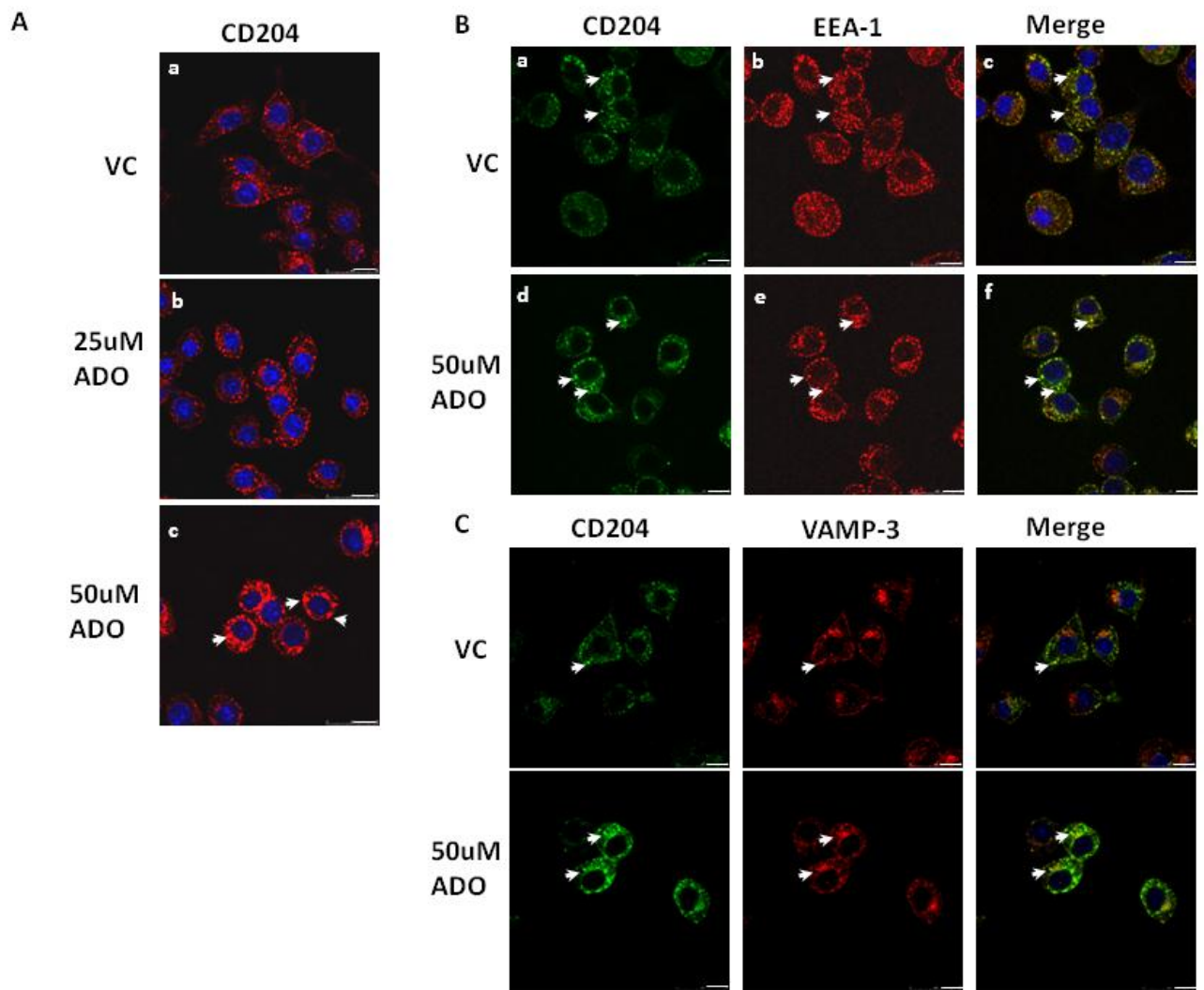


**Figure 5.3 CD204 is important for phagocytosis in N9 microglia cells.** N9 cells were incubated on ice with varying concentrations of antibody for an hour, and then incubated with fluorescent bioparticles from the Vybrant Phagocytosis Assay for an hour at 37 °C. The amount of bioparticles phagocytosed was then analysed by the fluorescent reader. Graphs are representative of at least 2 independent experiments. VC, vehicle control.

- A. Anti-CD36 does not block phagocytosis in N9 microglia cells.
- B. Anti-CD204 blocks phagocytosis in N9 microglia cells. \*\*,  $P < 0.01$  relative to vehicle control.
- C. Anti-MARCO does not block phagocytosis in N9 microglia cells.

#### **5.3.4. CD204 accumulates within the cell upon ADO treatment**

Since CD204 was important for N9 phagocytosis, and surface CD204 is downregulated upon ADO treatment, we were interested to identify the pathway of CD204 trafficking affected upon treatment. Hence, we observed the distribution of CD204 in N9 using immunofluorescence. Cells were treated with ADO for 3 h, fixed, permeabilized and stained for CD204. Intracellular endosomal structures containing CD204 seemed to be much larger upon ADO treatment, particularly for 50  $\mu$ M (Figure 5.4A). The cellular compartment which CD204 localises to specifically was then determined by co-localization study using different endosomal markers. Interestingly, CD204 partially co-localises with early endosomal antigen-1 (EEA-1), a marker of early endosomes, as well as VAMP-3, a marker of recycling endosomes, in both untreated (VC) and ADO treated cells upon confocal microscopy analysis (Figure 5.4B-D). Hence, it is likely that surface CD204 has been downregulated from the cell surface and accumulated within the early and recycling endosomes.





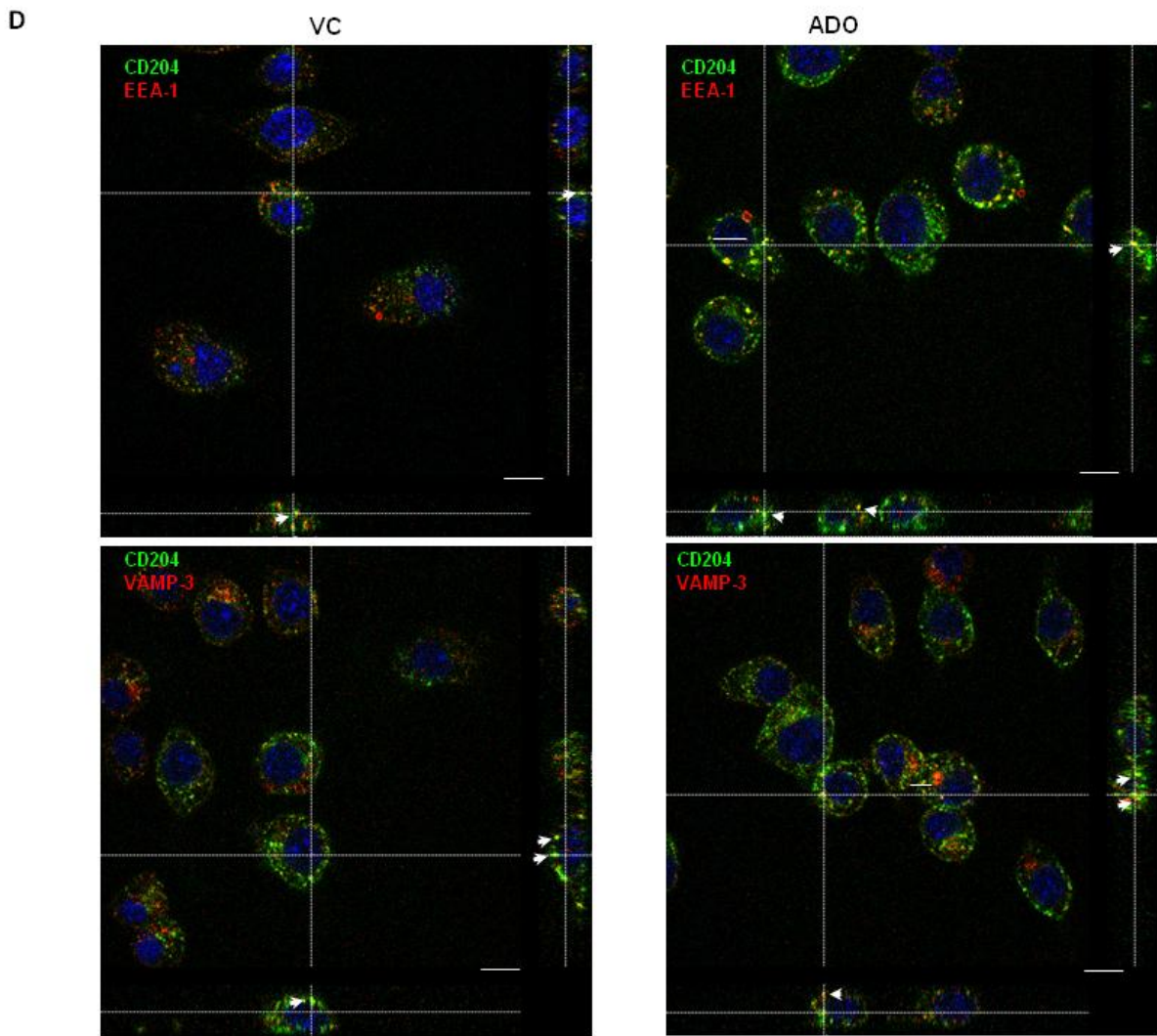


**Figure 5.4 ADO causes an accumulation of CD204 in intracellular endosomal compartments.** Images were taken using the Leica TCS SP5 confocal microscope, and are representative of at least 2 independent experiments. N9 cells were treated for 3 hours with varying concentrations of ADO and stained with anti-CD204 antibody (A) or together with an appropriate co-localizing antibody (B-D). Scale bars are representative of 10  $\mu$ m. VC, vehicle control, ADO, andrographolide.

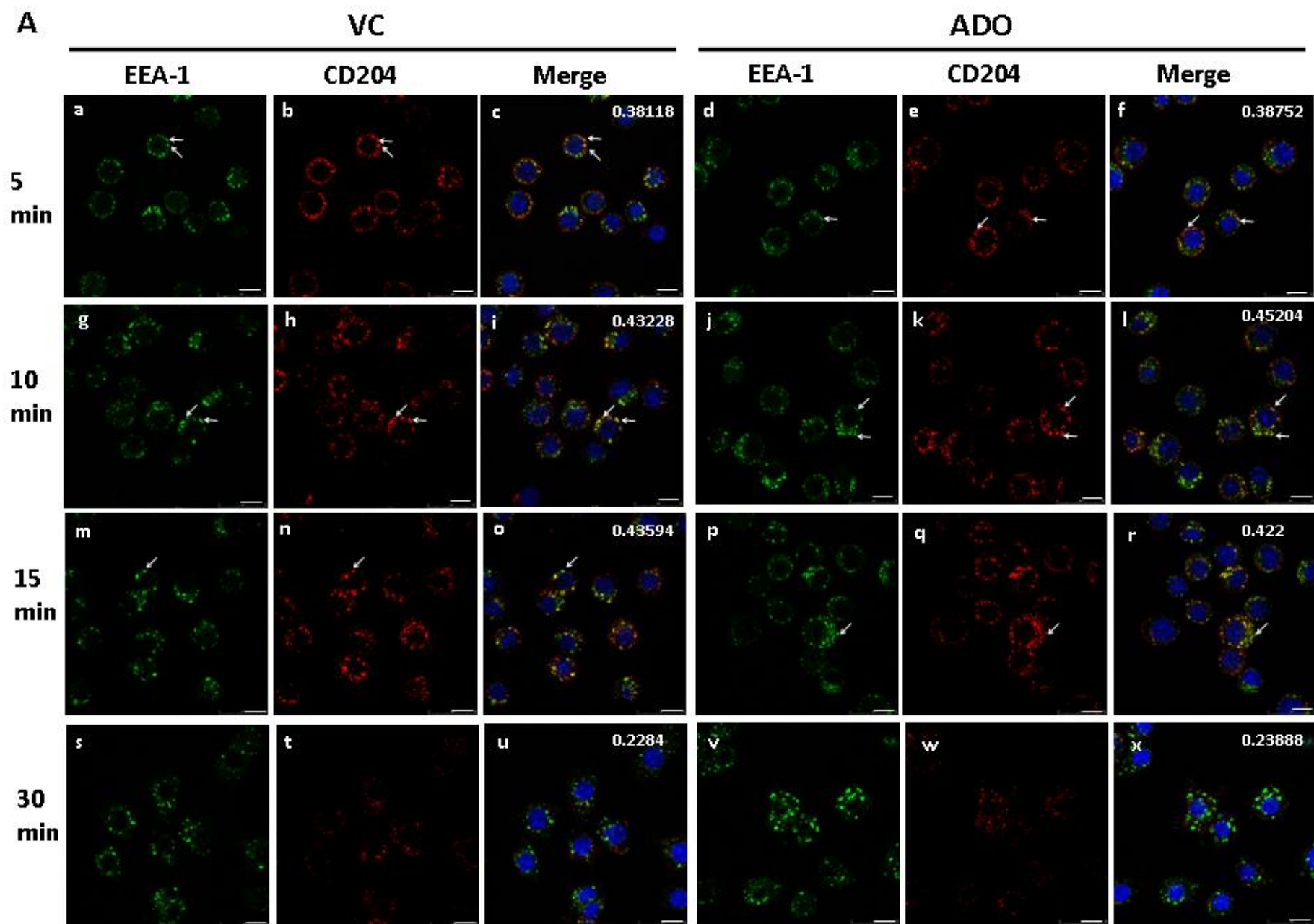
- A. CD204 accumulates within the cell upon andrographolide treatment. Arrows indicate the increased accumulation of CD204.
- B. CD204 co-localises with the early endosomal marker, EEA-1. Arrows indicate the increased accumulation of CD204.
- C. CD204 co-localises with the recycling endosomal marker, VAMP-3.
- D. Confocal analysis of CD204 co-localization with EEA-1 and VAMP-3, using X-Z/Y-Z projection of CD204 co-localization with EEA-1 or VAMP-3. X-Z/Y-Z projection was performed using the Leica LAS AF Lite. Arrows indicate the endosomal co-localization between CD204 and EEA-1 or VAMP-3.

### **5.3.5. ADO does not inhibit endocytosis or degradation of CD204**

As CD204 seems to accumulate within the cell, it was possible that the endocytosis or degradation rates of CD204 were changed upon treatment. We first investigated if there was any change in endocytosis rates of CD204 by immunofluorescence. CD204 antibody was allowed to bind to N9 on ice, and then endocytosed and fixed at different time points. Cells were then probed using EEA-1 as a marker for the early endosomes. Co-localisation of CD204 with EEA-1 was utilized to measure internalization of surface CD204 into the early endosomes. Interestingly, there did not seem to be any increase in the rate of endocytosis upon ADO treatment as is evident from the images (Figure 5.5A). We quantified the average amount of co-localisation using the Pearson's Correlation of five unique frames for each sample, at each specific time-point, and there is no significant difference between VC and ADO treated cells.

To ensure that the results from the immunofluorescence studies were reliable, levels of endocytosed CD204 in DMSO and ADO treated cells were also quantified by flow cytometry. FITC-conjugated CD204 was allowed to bind to N9 on ice and CD204-specific antibody was allowed to endocytose at 37 °C for different time points. CD204 remaining on the cell surface was then removed with acid wash, and cells were fixed. Similarly, there was no significant difference between VC and ADO treated cells (Figure 5.5 B).

Hence, we went on to investigate whether the increased accumulation of intracellular CD204 could be due to the ADO effect on degradation rate of CD204. N9 cells were pretreated with ADO, CD204 antibody was allowed to bind to the cell surface of N9 on ice, and then allowed to endocytose at 37 °C. The amount of remaining CD204 at various times was then quantified by western blot. However, the degradation of CD204 within the cell does not seem to be inhibited by ADO (Figure 5.5 C).



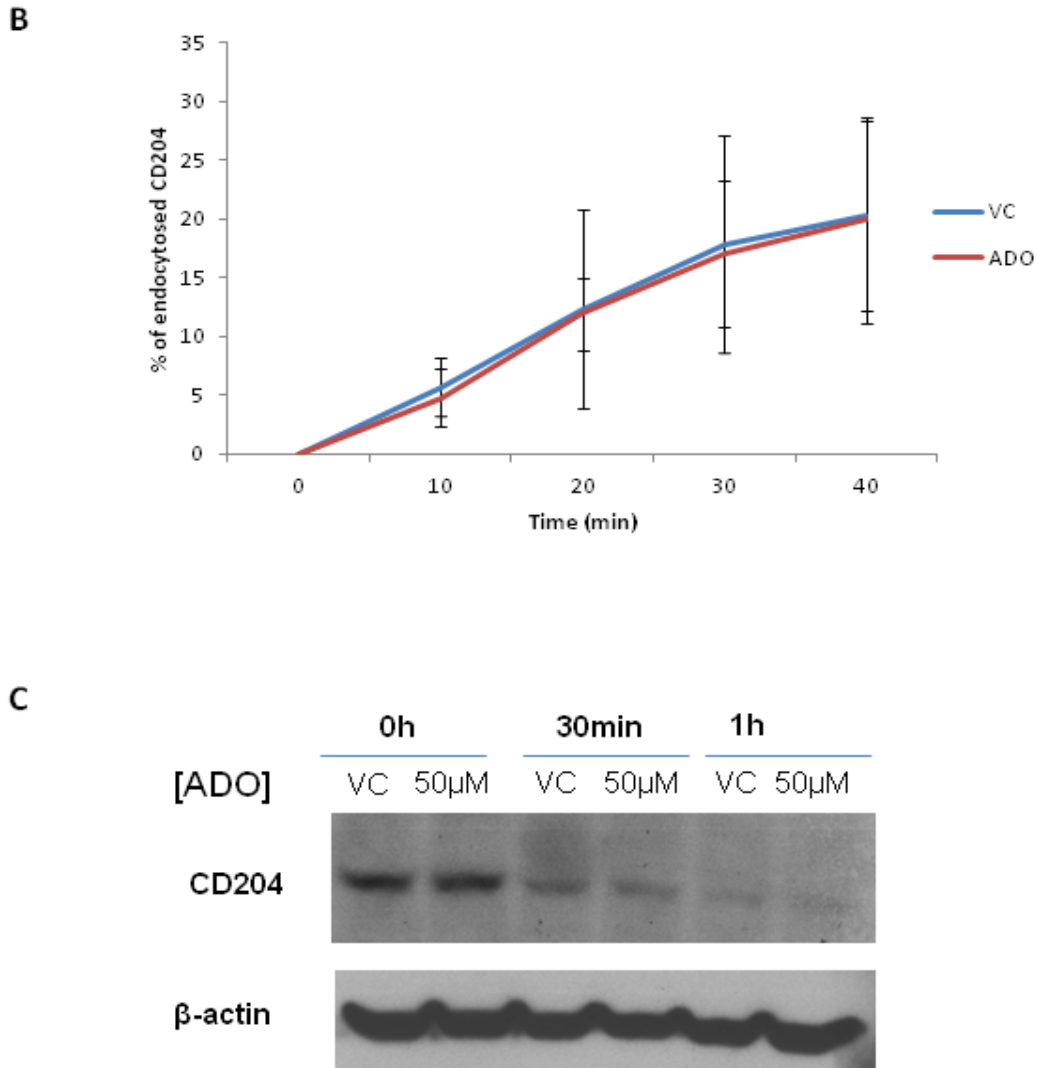


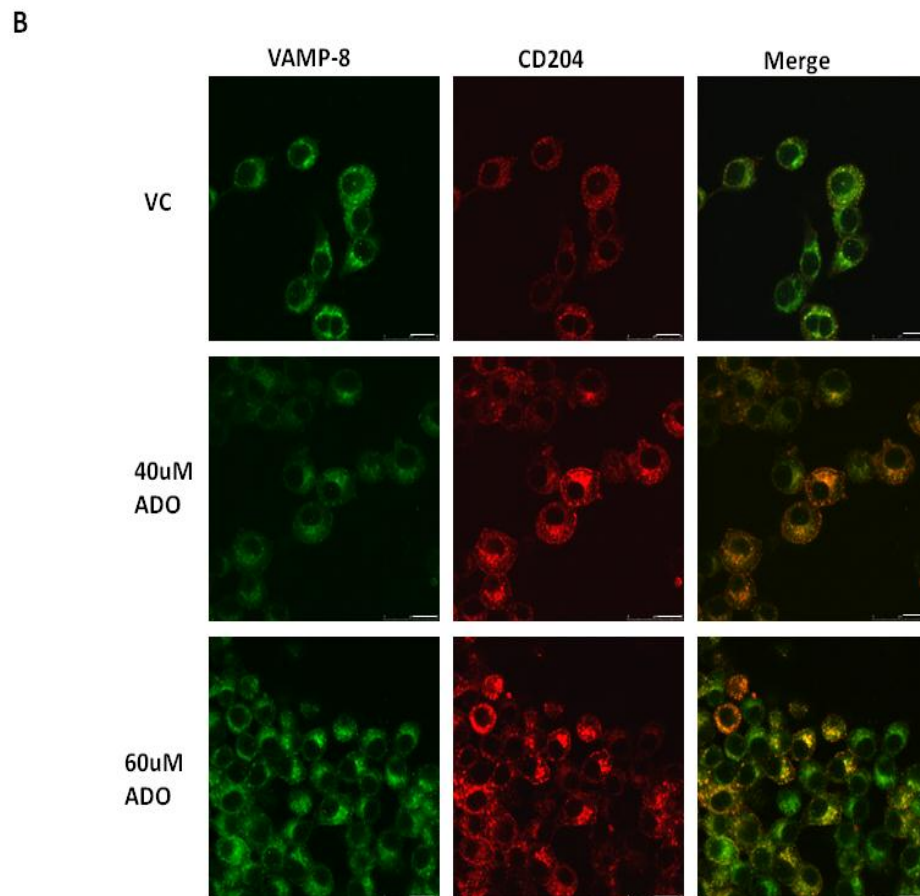
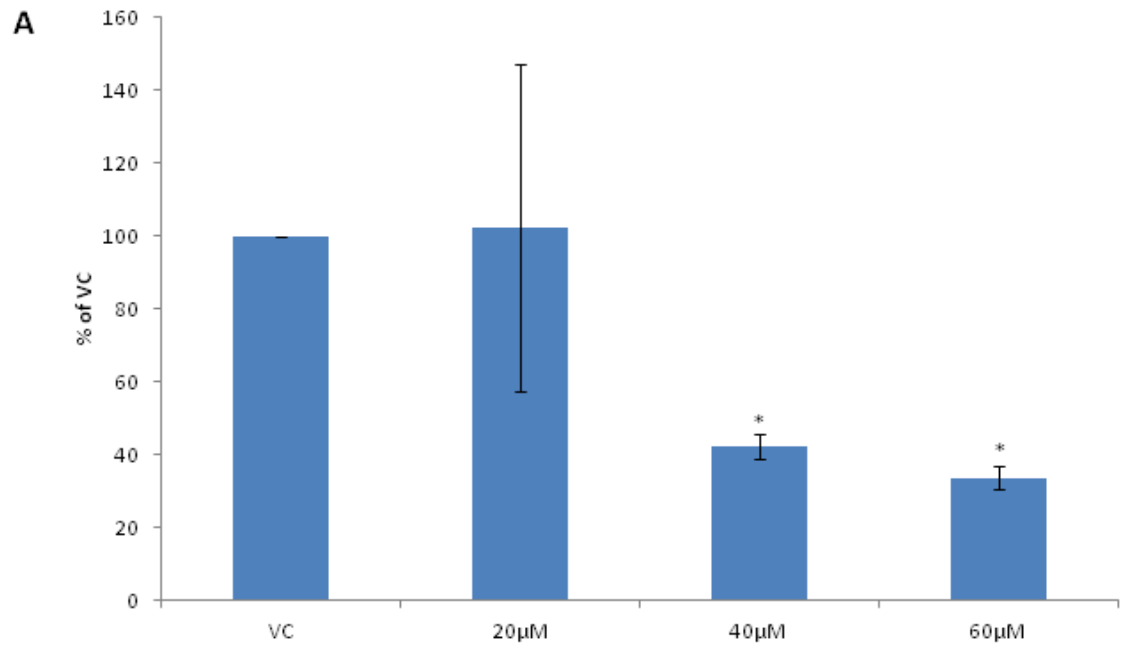
**Figure 5.5 ADO does not alter the rate of CD204 endocytosis or degradation.**

- A. Images were taken using the Leica TCS SP5 confocal microscope, and are representative of at least 2 independent experiments. Cells were pre-treated with DMSO or 100 $\mu$ M ADO for an hour, before incubation with anti-CD204 on ice. Cells were then replaced in 37 °C, allowed to internalise and fixed at various timepoints. The numbers at the top right-hand corner represent the Pearson's correlation for EEA-1 and CD204, and are averages of correlations taken from at least 7 images. Images are representative of at least 2 independent experiments. Scale bars are representative of 10  $\mu$ m. Arrows indicate co-localization of CD204 and EEA-1.
- B. CD204 endocytosis rates were quantified. Cells were pre-treated with DMSO or 50 $\mu$ M ADO for 3 h, before incubation with anti-CD204 on ice. Cells were then replaced in 37 °C and allowed to internalise, excess antibody on the surface was washed off with acid and fixed at various timepoints and endocytosed CD204 was analysed by flow cytometry.
- C. CD204 degradation rates are not affected upon ADO treatment. Cells were pretreated with DMSO or 50  $\mu$ M ADO for 2 h, before incubation with anti-CD204 on ice. Cells were then replaced in 37 °C and lysed at various timepoints and analysed by western blot. Western blots are representative of at least 2 independent experiments. VC, vehicle control; ADO, andrographolide.

Since both the endocytosis and degradation of CD204 was not affected by ADO, it appears that ADO effect on CD204 is different as compared to its effect on EGFR, and there could be a unique mechanism by which it decreases surface CD204. As CD204 containing endosomal structures were enlarged upon ADO treatment, we postulated that this phenomenon could result from ADO affecting secretion rates of CD204. CD204 is known to act as an adhesion molecule and is important in the formation of focal adhesion complexes (Post *et al.*, 2002). During our experiments, we have consistently observed the detachment of microglia cells from the tissue culture surfaces during treatment, indicating that CD204 secretion could be affected. In immunofluorescence studies, we also observed that CD204 could be secreted on the surface of the cover-slip, leaving a cellular “footprint”, and these “footprints” were reduced in the presence of ADO. These various lines of evidence led us to investigate if CD204 secretion was affected in the presence of ADO. Cells were treated with ADO for 8 hours, detached, and the amount of CD204 secreted was quantified. Levels of CD204 that were secreted dropped drastically up to 70% after 8 h of treatment (Figure 5.6A).

Since secretion of CD204 was affected, it was possible that this could have been due to ADO effect on cellular secretion mechanisms. The vesicle-associated membrane protein (VAMP)-8 is well-known to be responsible for controlling granular secretion in platelets (Polgar *et al.*, 2002), and it localises to secretory vesicles and controls degranulation (Jones *et al.*, 2012). Thus, we investigated if VAMP-8 co-localised to the enlarged CD204 endosomes. Cells were treated for 8 h, before they were fixed and stained for CD204 and VAMP-8 and visualized with the confocal microscope (Figure

5.6 B,C). As can be seen from the confocal images and the X-Z/Y-Z projections, CD204 and VAMP-8 do co-localise. Hence, it is possible that ADO could affect CD204 secretion via affecting VAMP-8 expression or function.





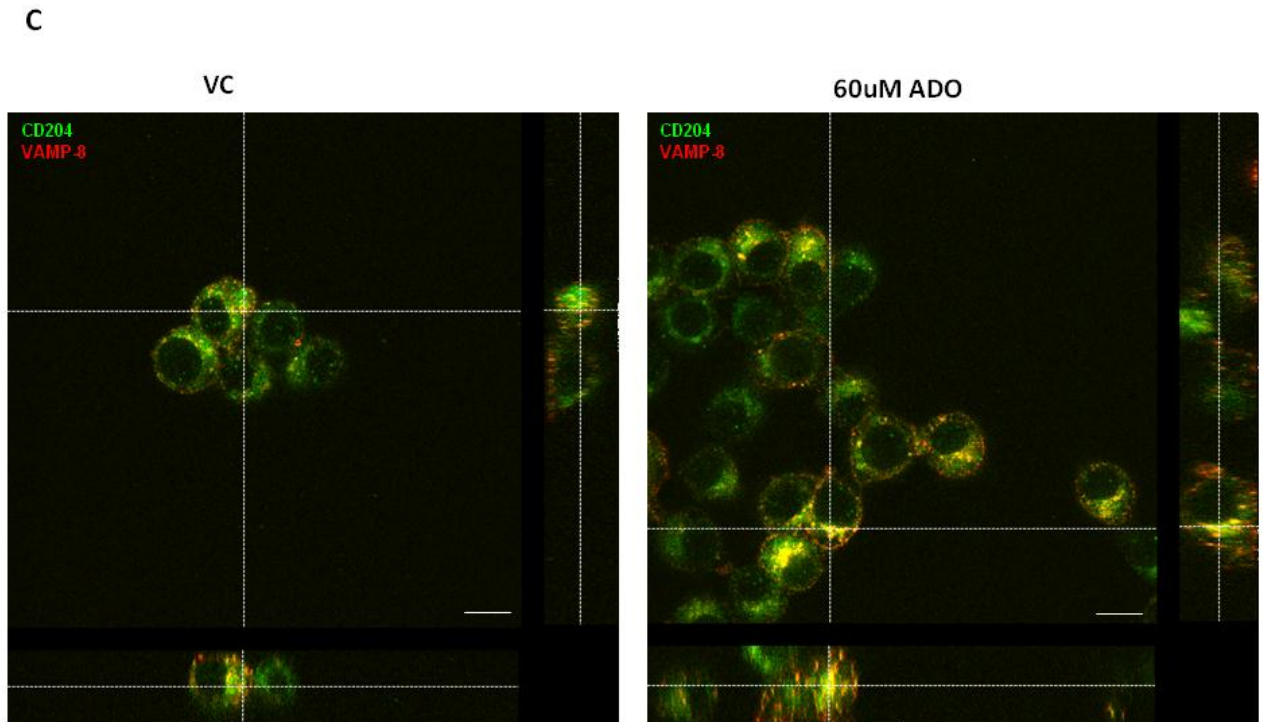


**Figure 5.6 Andrographolide affects the secretion of CD204**

- A. Secretion of CD204 was decreased upon ADO treatment. Cells were pre-treated with DMSO and varying concentrations of ADO for 8 h, before cells were detached and the secreted CD204 on the plate was fixed. Anti-CD204 antibody and the corresponding fluorescence conjugated secondary antibody was added and the levels of fluorescence detected by a fluorescent reader. Amount of CD204 secreted is expressed as a percentage of the vehicle control. Graph is representative of at least 2 independent experiments. \*,  $p < 0.05$ . VC, vehicle control.
- B. ADO-induced accumulated CD204 is trapped in VAMP-8 positive endosomal structures. Cells were pre-treated with DMSO and varying concentrations of ADO for 3 h, before cells were fixed and stained with anti-CD204 and anti-VAMP-8 antibody, followed by the fluorescence conjugated secondary antibody. Cells were visualized with the Leica TS5 confocal microscope. VC, vehicle control; ADO, andrographolide. Scale bars are representative of 10  $\mu\text{m}$ .
- C. X-Z/Y-Z projection of CD204 co-localization with VAMP-8. Images were taken using the Leica TS5 confocal microscope. X-Z/Y-Z projection was performed using the LAS AF Lite software. Scale bars are representative of 10  $\mu\text{m}$ .

#### 5.4. Discussion

Phagocytosis is the process by which antigen presenting cells (APCs) take up antigens present in the extracellular environment for processing before they are presented to the T cells. During phagocytosis, surface scavenger receptors such as CD204 bind to a bacterial ligand, which is then internalised by the APC to form phagosomes. The phagosome then undergoes maturation as different proteins are acquired and the phagosome becomes more acidic due to fusion with the lysosomes. This acidic environment activates the lysosomal cathepsins to degrade the antigens and peptides are produced, which are then complexed with MHC class II molecules. The antigen-bound MHC class II molecules would then be presented on the cell surface and serve as activators of T cells (Kinchen *et al.*, 2008). During ADO treatment, surface CD204 is decreased, leading to decreased bacteria binding and phagocytosis. Fewer peptides are hence present within lysosomes for loading onto MHC class II molecules. Subsequently, fewer antigen-bound MHC class II molecules are presented on the cell surface, resulting in a decreased activation of T cells, less immunostimulatory molecules like cytokines being released and reduced inflammation. ADO is known to be an immunosuppressive compound via suppressing activation of NF- $\kappa$ B (Xia *et al.*, 2004), as well as inhibiting T cell activation through decreasing antigen presentation (Iruetagoiena *et al.*, 2005). Thus, it has been shown to alleviate disease in many pre-clinical models of inflammation such as experimental autoimmune encephalomyelitis (EAE) (Figure 1.1). Here, we demonstrate a novel mechanism through which ADO may have immunosuppressive effects – through downregulating scavenger receptors to reduce phagocytosis, hence affecting antigen presentation.

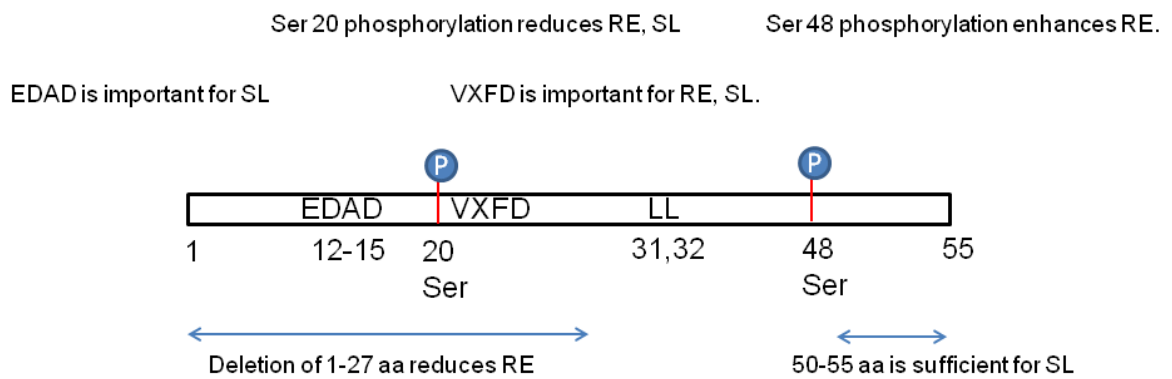
From our experiments, ADO does not affect surface expression of CD204 through the endocytic pathway or the degradation pathway, but by inhibiting its trafficking to the cell surface via the secretory pathway. ADO could possibly affect VAMP-8 function or expression, hence affecting the secretion of CD204 as it is co-localised with enlarged CD204 endosomal structures.

The ligand-independent endocytic pathway of CD204 is not fully characterised, although acetyl-low density lipoprotein (Ac-LDL) induced endocytosis has been investigated. Ac-LDL induced CD204 endocytosis is known to proceed via clathrin coated pits (Chen *et al.*, 2006), although a recent study found that fucoidan induced CD204 endocytosis via caveolae (Zhu *et al.*, 2011). SR-A is made up of three subtypes which form due to alternative splicing. SR-A I is the longest subtype, and exists as a trimer with six domains, of which the cytoplasmic domain has been shown to be important in regulating Ac-LDL endocytosis (Daugherty, 2000) (Figure 5.7). Phosphorylation of CD204 is important for controlling its endocytosis, as treatment with the protein kinase C inhibitor staurosporine inhibits Ac-LDL internalisation (Fong, 1996). However, phosphorylation can either enhance or inhibit internalisation, as inhibiting phosphorylation of the conserved residues serine 21 (serine 21 in the mouse, serine 20 in the human) increased internalisation, whereas inhibiting phosphorylated serine 49 (serine 49 in the mouse, serine 48 in the human) decreased internalisation (Fong & Le, 1999). Deletion studies which removed the first 49 amino acids (Kosswig *et al.*, 2003) as well as the first 27 amino acids (Chen *et al.*, 2006) of the cytoplasmic domain led to the reduced internalisation of Ac-LDL. The VXFD motif (residues 21-24 in human SR-A) as well as the di-leucine motif (which is

known to play a key role in the internalisation of other receptors) in the cytoplasmic domain were important for receptor internalisation (Morimoto *et al.*, 1999; Chen *et al.*, 2006), although the di-leucine motif was not responsible for binding to clathrin. Both deletion of the first 27 amino acids and mutation of the di-leucine motif to alanine also led to lowered Ac-LDL internalisation.

The motifs which control surface localization of SR-A are different although they also exist on the cytoplasmic domain. Six membrane proximal amino acids (after deletion of the first 49 amino acids) are sufficient for surface localization of SR-A. The cytoplasmic amino acid motif EDAD (residues 12 – 15) controls SR-A surface expression through interacting with the microtubule interacting protein Hook3 (Sano

### Cytoplasmic domain of human SR-A



RE: Receptor endocytosis  
 SL: Surface localization  
 AA: amino acid

**Figure 5.7 Sites regulating internalization and surface localization of SR-A.** Summary of the various amino acid motifs on the cytoplasmic domain shown to be important for regulating receptor endocytosis and surface localization.

*et al.*, 2007), and modification of the EDAD amino acids to amine derivatives resulted in the reduced surface localization of SR-A. In the presence of the PI3K inhibitor wortmannin, SR-A surface localization is lowered, but this reduction is not seen in the amine derivative, showing that this process is regulated by the phosphatidylinositol-3 kinase (PI3K) (Cholewa *et al.*, 2010). Thus, PI3K could either directly or indirectly affect SR-A interaction with Hook3, hence affecting its surface localization.

In our studies, we have observed that PI3 kinase inhibition by wortmannin also reduces the amount of SR-A on the cell surface, and that endocytosis of SR-A leads to enlarged SR-A positive endosomal structures. ADO was also capable of inhibiting phosphorylation of Akt at threonine 308 and serine 473, while it does not affect PDK-1 activation (Figure 5.8). Akt is well-known to be an indicator of PI3K activity, as PI3K phosphorylation causes phosphatidylinositol-4,5-diphosphate to be converted to phosphatidylinositol-3,4,5-triphosphate, and this causes Akt to be recruited to the plasma membrane through its pleckstrin homology (PH) domain. PDK1 is also recruited to the plasma membrane via its PH domain, and it phosphorylates Akt on threonine 308. It is still unclear which kinase is responsible for phosphorylating serine 473 (Cheng *et al.*, 2005). We speculate that another pathway through which ADO affects surface localization of CD204 is the inhibition of PI3K. However, further work is required to confirm that ADO inhibits PI3K, the endosomal pathway through which PI3K acts to inhibit SR-A surface localization, and the manner in which PI3K regulates SR-A binding to Hook3.

The effect of ADO on scavenger receptor surface expression does not only affect antigen presentation, it would also affect lipid uptake, as scavenger receptors are also involved in cholesterol uptake. The downregulation of surface scavenger receptors implies that ADO is likely to be efficacious in the treatment of atherosclerosis. During the initiation of atherosclerosis, low density lipoprotein is deposited in the subendothelial space, exposing them to modifications such as oxidation to form oxidized LDL (oxLDL). The presence of modified LDL leads to recruitment of monocytes into the arterial intima, where they differentiate into macrophages due to the presence of the colony stimulating factor (CSF). These macrophages express scavenger receptors, including CD204, CD36 and MARCO, which are known to be important receptors for binding and uptake of acetylated low density lipoproteins (acLDL), and oxidized LDL (oxLDL) to form foam cells. Foam cells are able to form atherosclerotic plaques and secrete pro-inflammatory factors, causing vascular remodeling and increasing the likelihood of thrombosis (Pluddemann *et al.*, 2007; Badimon *et al.*, 2011). ADO treatment would reduce surface scavenger receptor levels and hence lower overall uptake of oxLDL and formation of foam cells. This coupled with the inhibition of NF- $\kappa$ B activation in foam cells (Li & Li, 2011), decrease of the intercellular adhesion molecule 1 (ICAM-1), activation of NF- $\kappa$ B (Chao *et al.*, 2011) and induction of apoptosis in endothelial cells (Chen *et al.*, 2004) would lower the likelihood of atherosclerotic plaques forming.

Our results here demonstrate the inhibition of phagocytosis through downregulation of SR-A, which is a novel mechanism through which ADO may inhibit immune responses. SR-A downregulation is likely to be due to inhibition of its secretion by

ADO. Further work is needed to elucidate the mechanism of how CD204 trafficking can be controlled by downstream signalling pathways. More work is needed to define the manner in which phosphorylation controls internalisation of CD204, as phosphorylation of serine at different locations result in different effects. In addition, the action of ADO on VAMP-8 in affecting CD204 secretion also needs to be elucidated.

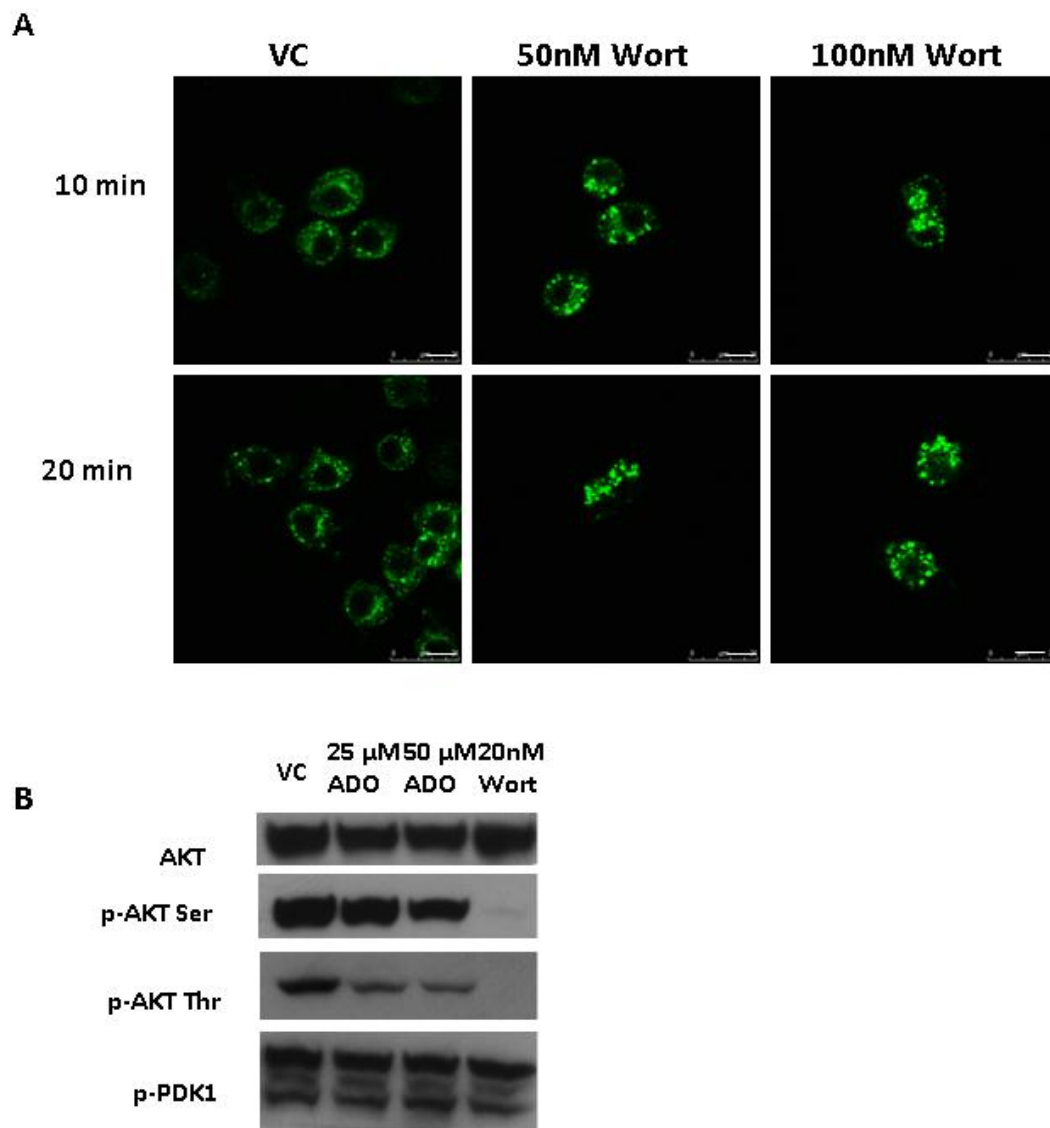


**Figure 5.8 Andrographolide acts as a PI3 kinase inhibitor.**

- A. Treatment of N9 microglia with wortmannin results in the formation of large CD204 positive endosomal structures. Cells were stained with anti-CD204 antibody for an hour, then allowed to endocytose at 37 °C for the timepoints indicated in the presence or absence of wortmannin. Scale bars are representative of 10  $\mu$ m.
- B. Treatment of N9 microglia with ADO or wortmannin results in inhibition of AKT phosphorylation. Cells were treated with the drug indicated for 3 h before they were collected, lysed and analysed by western blot.



# **Chapter 6**

## **Conclusions and Future Directions**

## 6. Conclusions and Future Directions

### 6.1. Conclusions

Our studies have shown that ADO is capable of downregulating surface receptors EGFR and scavenger receptors CD204 and CD36 in A-431 epidermoid carcinoma and N9 microglia respectively. This downregulation is mediated through receptor-specific mechanisms and not through general endocytosis pathways. p38 MAPK activation induces EGFR internalisation through phosphorylation at serine 1046/1047, whereas ADO affects CD204 surface expression by inhibiting its secretion. We have also shown how ADO regulation of signaling molecules can in turn perturb receptor trafficking. This is a novel finding, as previous studies on ADO induced signaling focused mainly on the downstream effects on gene expression.

### 6.2. Delving into additional drug mechanisms

One important point that our study demonstrates is the need to understand how drugs affect cellular mechanisms. Drugs are usually used to target specific proteins, such as to inhibit enzyme or transcription factor activity. However, each drug molecule is also capable of inducing multi-faceted effects on the cell, particularly when they affect signaling pathways, which are responsible for controlling various cellular processes such as gene expression. Hence, while the search is ongoing for drugs targeting specific proteins, it is also important to expand our understanding of how existing drugs may affect intracellular processes, as these could contribute to the side effects of the drug *in vivo*. Such studies can also reveal previously undiscovered mechanisms, and lead to the development of known drugs for novel therapies.

Cell surface receptors are the main conduits through which cells receive extracellular cues and initiate appropriate cellular responses. Thus, elucidating drug effect on receptor trafficking is critical to understanding the additional effects of a known drug. The most well-known mechanism of ADO is its ability to induce anti-inflammatory effects through inhibiting the NF- $\kappa$ B pathway. However, we have demonstrated here that it is also capable of inducing MAPK activation to affect EGFR trafficking. In a separate study on acetylsalicylic acid (ASA), which is a well-known pain reliever due to its inhibition of cyclooxygenase activity, EGFR and TfR was accumulated in the early sorting endosomes due to ASA enhancement on membrane recruitment of trafficking proteins sorting nexin 3 and 5 (Chiou *et al.*, 2011). These effects on downregulating surface EGFR and TfR could explain the anti-cancer effects of ADO and ASA, as EGFR is a receptor that is upregulated in different forms of cancer, and TfR is important for cell survival through maintaining iron uptake.

In order to study drug effect on receptor trafficking, it is important to have a good model which can allow for easy detection of minute changes. We have shown here that the A-431 cell line can be used as a model to detect drug-induced changes in receptor trafficking, and it can continue to be used in further studies of commonly used drugs to investigate previously undiscovered mechanisms (Tan *et al.*, 2010; Chiou *et al.*, 2011). A-431 offers a distinct advantage over other cell types as it expresses high levels of EGFR and TfR which can act as unique markers of the endocytic-degradation pathway and the endocytic-recycling pathway. Changes in

receptor trafficking are also easily captured as it is an epidermal cell line, and it is easily imaged.

### **6.3. Future Directions**

Many known drug with specific mechanisms have yet to be thoroughly investigated for its other effects on the cell. A recent trend in drug discovery is to relook at known pharmacophores for alternative uses in different diseases. One of the ways to achieve this is to gain a deeper understanding into the effects drugs may exert on the cell, specifically in the area of receptor trafficking. However, not all trafficking pathways of receptors have been fully characterised, unlike EGFR and TfR which have been very well-studied. Hence, it is necessary for us to expand our basic understanding of the various mechanisms which regulate specific receptor trafficking so that drugs targeting these mechanisms can be found. An example of this would be to further characterise mechanisms regulating CD204 surface localization, endocytosis and secretion, which is important, especially since CD204 mediates the uptake of many important molecules such as bacteria and lipoproteins.

# **Chapter 7**

# **Bibliography**

## 7. Bibliography

Adachi, S, Nagao, T, To, S, Joe, AK, Shimizu, M, Matsushima-Nishiwaki, R, Kozawa, O, Moriwaki, H, Maxfield, FR, Weinstein, IB (2008) (-)-Epigallocatechin gallate causes internalization of the epidermal growth factor receptor in human colon cancer cells. *Carcinogenesis* **29**(10): 1986-1993.

Adachi, S, Natsume, H, Yamauchi, J, Matsushima-Nishiwaki, R, Joe, AK, Moriwaki, H, Kozawa, O (2009a) p38 MAP kinase controls EGF receptor downregulation via phosphorylation at Ser1046/1047. *Cancer Lett* **277**(1): 108-113.

Adachi, S, Shimizu, M, Shirakami, Y, Yamauchi, J, Natsume, H, Matsushima-Nishiwaki, R, To, S, Weinstein, IB, Moriwaki, H, Kozawa, O (2009b) (-)-Epigallocatechin gallate downregulates EGF receptor via phosphorylation at Ser1046/1047 by p38 MAPK in colon cancer cells. *Carcinogenesis* **30**(9): 1544-1552.

Akouwah, GA, Zhari, I, Mariam, A, Yam, MF (2009) Absorption of andrographolides from *Andrographis paniculata* and its effect on CCl<sub>4</sub>-induced oxidative stress in rats. *Food Chem Toxicol* **47**(9): 2321-2326.

Amaryan, G, Astvatsatryan, V, Gabrielyan, E, Panossian, A, Panosyan, V, Wikman, G (2003) Double-blind, placebo-controlled, randomized, pilot clinical trial of ImmunoGuard--a standardized fixed combination of *Andrographis paniculata* Nees, with *Eleutherococcus senticosus* Maxim, *Schizandra chinensis* Bail. and *Glycyrrhiza glabra* L. extracts in patients with Familial Mediterranean Fever. *Phytomedicine* **10**(4): 271-285.

Amroyan, E, Gabrielian, E, Panossian, A, Wikman, G, Wagner, H (1999) Inhibitory effect of andrographolide from *Andrographis paniculata* on PAF-induced platelet aggregation. *Phytomedicine* **6**(1): 27-31.

Antonin, W, Holroyd, C, Tikkanen, R, Honing, S, Jahn, R (2000) The R-SNARE endobrevin/VAMP-8 mediates homotypic fusion of early endosomes and late endosomes. *Mol Biol Cell* **11**(10): 3289-3298.

Aromdee, C (2012) Modifications of andrographolide to increase some biological activities: a patent review (2006 - 2011). *Expert Opin Ther Pat* **22**(2): 169-180.

Aromdee, C, Suebsasana, S, Ekalaksananan, T, Pientong, C, Thongchai, S (2011) Stage of action of naturally occurring andrographolides and their semisynthetic analogues against herpes simplex virus type 1 in vitro. *Planta Med* **77**(9): 915-921.

Ashraf, MZ, Gupta, N (2011) Scavenger receptors: Implications in atherothrombotic disorders. *Int J Biochem Cell Biol* **43**(5): 697-700.

Badimon, L, Storey, RF, Vilahur, G (2011) Update on lipids, inflammation and atherothrombosis. *Thromb Haemost* **105 Suppl 1**: S34-42.

Bao, Z, Guan, S, Cheng, C, Wu, S, Wong, SH, Kemeny, DM, Leung, BP, Wong, WS (2009) A novel antiinflammatory role for andrographolide in asthma via inhibition of the nuclear factor-kappaB pathway. *Am J Respir Crit Care Med* **179**(8): 657-665.

Baranova, IN, Kurlander, R, Bocharov, AV, Vishnyakova, TG, Chen, Z, Remaley, AT, Csako, G, Patterson, AP, Eggerman, TL (2008) Role of human CD36 in bacterial recognition, phagocytosis, and pathogen-induced JNK-mediated signaling. *J Immunol* **181**(10): 7147-7156.

Bartok, B, Firestein, GS (2010) Fibroblast-like synoviocytes: key effector cells in rheumatoid arthritis. *Immunol Rev* **233**(1): 233-255.

Baud, V, Karin, M (2009) Is NF-kappaB a good target for cancer therapy? Hopes and pitfalls. *Nat Rev Drug Discov* **8**(1): 33-40.

Behrens, M, Brockhoff, A, Batram, C, Kuhn, C, Appendino, G, Meyerhof, W (2009) The human bitter taste receptor hTAS2R50 is activated by the two natural bitter terpenoids andrographolide and amarogentin. *J Agric Food Chem* **57**(21): 9860-9866.

Bothiraja, C, Shinde, MB, Rajalakshmi, S, Pawar, AP (2009) Evaluation of molecular pharmaceutical and in-vivo properties of spray-dried isolated andrographolide-PVP. *J Pharm Pharmacol* **61**(11): 1465-1472.

Brahmane, RI, Pathak, SS, Wanmali, VV, Salwe, KJ, Premendran, SJ, Shinde, BB (2011) Partial in vitro and in vivo red scorpion venom neutralization activity of *Andrographis paniculata*. *Pharmacognosy Res* **3**(1): 44-48.

Brasier, AR (2010) The nuclear factor-kappaB-interleukin-6 signalling pathway mediating vascular inflammation. *Cardiovasc Res* **86**(2): 211-218.

Burgos, RA, Caballero, EE, Sanchez, NS, Schroeder, RA, Wikman, GK, Hancke, JL (1997) Testicular toxicity assessment of *Andrographis paniculata* dried extract in rats. *J Ethnopharmacol* **58**(3): 219-224.

Burgos, RA, Hancke, JL, Bertoglio, JC, Aguirre, V, Arriagada, S, Calvo, M, Caceres, DD (2009) Efficacy of an *Andrographis paniculata* composition for the relief of rheumatoid arthritis symptoms: a prospective randomized placebo-controlled trial. *Clin Rheumatol* **28**(8): 931-946.

Caceres, DD, Hancke, JL, Burgos, RA, Sandberg, F, Wikman, GK (1999) Use of visual analogue scale measurements (VAS) to assess the effectiveness of standardized *Andrographis paniculata* extract SHA-10 in reducing the symptoms of common cold. A randomized double blind-placebo study. *Phytomedicine* **6**(4): 217-223.

Calabrese, C, Berman, SH, Babish, JG, Ma, X, Shinto, L, Dorr, M, Wells, K, Wenner, CA, Standish, LJ (2000) A phase I trial of andrographolide in HIV positive patients and normal volunteers. *Phytother Res* **14**(5): 333-338.

Calandra, T, Roger, T (2003) Macrophage migration inhibitory factor: a regulator of innate immunity. *Nat Rev Immunol* **3**(10): 791-800.

Capdevila, J, Elez, E, Macarulla, T, Ramos, FJ, Ruiz-Echarri, M, Taberner, J (2009) Anti-epidermal growth factor receptor monoclonal antibodies in cancer treatment. *Cancer Treat Rev* **35**(4): 354-363.

Carretta, MD, Alarcon, P, Jara, E, Solis, L, Hancke, JL, Concha, II, Hidalgo, MA, Burgos, RA (2009) Andrographolide reduces IL-2 production in T-cells by interfering with NFAT and MAPK activation. *Eur J Pharmacol* **602**(2-3): 413-421.

Cavalli, V, Vilbois, F, Corti, M, Marcote, MJ, Tamura, K, Karin, M, Arkinstall, S, Gruenberg, J (2001) The stress-induced MAP kinase p38 regulates endocytic trafficking via the GDI:Rab5 complex. *Mol Cell* **7**(2): 421-432.

Chan, SJ, Wong, WS, Wong, PT, Bian, JS (2010) Neuroprotective effects of andrographolide in a rat model of permanent cerebral ischaemia. *Br J Pharmacol* **161**(3): 668-679.

Chandrasekaran, CV, Thiyagarajan, P, Deepak, HB, Agarwal, A (2011) In vitro modulation of LPS/calcein induced inflammatory and allergic mediators by pure compounds of *Andrographis paniculata* (King of bitters) extract. *Int Immunopharmacol* **11**(1): 79-84.

Chandrasekaran, CV, Thiyagarajan, P, Sundarajan, K, Goudar, KS, Deepak, M, Murali, B, Allan, JJ, Agarwal, A (2009) Evaluation of the genotoxic potential and acute oral toxicity of standardized extract of *Andrographis paniculata* (KalmCold). *Food Chem Toxicol* **47**(8): 1892-1902.

Chao, CY, Lii, CK, Tsai, IT, Li, CC, Liu, KL, Tsai, CW, Chen, HW (2011) Andrographolide inhibits ICAM-1 expression and NF- $\kappa$ B activation in TNF- $\alpha$ -treated EA.hy926 cells. *J Agric Food Chem* **59**(10): 5263-5271.

Chao, HP, Kuo, CD, Chiu, JH, Fu, SL (2010a) Andrographolide exhibits anti-invasive activity against colon cancer cells via inhibition of MMP2 activity. *Planta Med* **76**(16): 1827-1833.



Chao, WW, Kuo, YH, Lin, BF (2010b) Anti-inflammatory activity of new compounds from *Andrographis paniculata* by NF-kappaB transactivation inhibition. *J Agric Food Chem* **58**(4): 2505-2512.

Chao, WW, Lin, BF (2010) Isolation and identification of bioactive compounds in *Andrographis paniculata* (Chuanxinlian). *Chin Med* **5**: 17.

Chellampillai, B, Pawar, AP (2011) Improved bioavailability of orally administered andrographolide from pH-sensitive nanoparticles. *Eur J Drug Metab Pharmacokinet* **35**(3-4): 123-129.

Chen, HW, Lin, AH, Chu, HC, Li, CC, Tsai, CW, Chao, CY, Wang, CJ, Lii, CK, Liu, KL (2011) Inhibition of TNF-alpha-Induced Inflammation by Andrographolide via Down-Regulation of the PI3K/Akt Signaling Pathway. *J Nat Prod*.

Chen, JH, Hsiao, G, Lee, AR, Wu, CC, Yen, MH (2004) Andrographolide suppresses endothelial cell apoptosis via activation of phosphatidyl inositol-3-kinase/Akt pathway. *Biochem Pharmacol* **67**(7): 1337-1345.

Chen, JX, Xue, HJ, Ye, WC, Fang, BH, Liu, YH, Yuan, SH, Yu, P, Wang, YQ (2009) Activity of andrographolide and its derivatives against influenza virus in vivo and in vitro. *Biol Pharm Bull* **32**(8): 1385-1391.

Chen, L, Yu, A, Zhuang, X, Zhang, K, Wang, X, Ding, L, Zhang, H (2007) Determination of andrographolide and dehydroandrographolide in rabbit plasma by on-line solid phase extraction of high-performance liquid chromatography. *Talanta* **74**(1): 146-152.

Chen, Y, Wang, X, Ben, J, Yue, S, Bai, H, Guan, X, Bai, X, Jiang, L, Ji, Y, Fan, L, Chen, Q (2006) The di-leucine motif contributes to class a scavenger receptor-mediated internalization of acetylated lipoproteins. *Arterioscler Thromb Vasc Biol* **26**(6): 1317-1322.

Cheng, JQ, Lindsley, CW, Cheng, GZ, Yang, H, Nicosia, SV (2005) The Akt/PKB pathway: molecular target for cancer drug discovery. *Oncogene* **24**(50): 7482-7492.

Cheung, HY, Cheung, SH, Li, J, Cheung, CS, Lai, WP, Fong, WF, Leung, FM (2005) Andrographolide isolated from *Andrographis paniculata* induces cell cycle arrest and mitochondrial-mediated apoptosis in human leukemic HL-60 cells. *Planta Med* **71**(12): 1106-1111.

Chinchore, Y, Mitra, A, Dolph, PJ (2009) Accumulation of rhodopsin in late endosomes triggers photoreceptor cell degeneration. *PLoS Genet* **5**(2): e1000377.

Chiou, WF, Chen, CF, Lin, JJ (2000) Mechanisms of suppression of inducible nitric oxide synthase (iNOS) expression in RAW 264.7 cells by andrographolide. *Br J Pharmacol* **129**(8): 1553-1560.

Chiou, WF, Lin, JJ, Chen, CF (1998) Andrographolide suppresses the expression of inducible nitric oxide synthase in macrophage and restores the vasoconstriction in rat aorta treated with lipopolysaccharide. *Br J Pharmacol* **125**(2): 327-334.

Chiuw, KH, Tan, Y, Chua, RY, Huang, D, Ng, ML, Torta, F, Wenk, MR, Wong, SH (2011) SNX3-dependent regulation of epidermal growth factor receptor (EGFR) trafficking and degradation by aspirin in epidermoid carcinoma (A-431) cells. *Cell Mol Life Sci*.

Cho, ML, Moon, YM, Heo, YJ, Woo, YJ, Ju, JH, Park, KS, Kim, SI, Park, SH, Kim, HY, Min, JK (2009) NF-kappaB inhibition leads to increased synthesis and secretion of MIF in human CD4+ T cells. *Immunol Lett* **123**(1): 21-30.

Cholewa, J, Nikolic, D, Post, SR (2010) Regulation of class A scavenger receptor-mediated cell adhesion and surface localization by PI3K: identification of a regulatory cytoplasmic motif. *J Leukoc Biol* **87**(3): 443-449.

Chow, CW, Dong, C, Flavell, RA, Davis, RJ (2000) c-Jun NH(2)-terminal kinase inhibits targeting of the protein phosphatase calcineurin to NFATc1. *Mol Cell Biol* **20**(14): 5227-5234.

Chun, JY, Tummala, R, Nadiminty, N, Lou, W, Liu, C, Yang, J, Evans, CP, Zhou, Q, Gao, AC (2010) Andrographolide, an herbal medicine, inhibits interleukin-6 expression and suppresses prostate cancer cell growth. *Genes Cancer* **1**(8): 868-876.

Clague, MJ, Urbe, S (2001) The interface of receptor trafficking and signalling. *J Cell Sci* **114**(Pt 17): 3075-3081.

Comhair, SA, Erzurum, SC (2010) Redox control of asthma: molecular mechanisms and therapeutic opportunities. *Antioxid Redox Signal* **12**(1): 93-124.

Coon, JT, Ernst, E (2004) *Andrographis paniculata* in the treatment of upper respiratory tract infections: a systematic review of safety and efficacy. *Planta Med* **70**(4): 293-298.

Daniels, TR, Delgado, T, Rodriguez, JA, Helguera, G, Penichet, ML (2006) The transferrin receptor part I: Biology and targeting with cytotoxic antibodies for the treatment of cancer. *Clin Immunol* **121**(2): 144-158.

Daugherty, A, D. L. Rateri, and S. C. Whitman. (2000) Class A scavenger receptors: recent advances in elucidation of structure-function relationships and their role in atherosclerosis. *Current Opinion in Cardiovascular, Pulmonary & Renal Investigational Drugs* **2**(3): 223-232.

Doi, T, Higashino, K, Kurihara, Y, Wada, Y, Miyazaki, T, Nakamura, H, Uesugi, S, Imanishi, T, Kawabe, Y, Itakura, H, et al. (1993) Charged collagen structure mediates the recognition of negatively charged macromolecules by macrophage scavenger receptors. *J Biol Chem* **268**(3): 2126-2133.

Dy, GK, Adjei, AA (2009) Emerging therapeutic targets in non-small cell lung cancer. *Proc Am Thorac Soc* **6**(2): 218-223.

Eskelinen, EL, Tanaka, Y, Saftig, P (2003) At the acidic edge: emerging functions for lysosomal membrane proteins. *Trends Cell Biol* **13**(3): 137-145.

Fong, LG (1996) Modulation of macrophage scavenger receptor transport by protein phosphorylation. *J Lipid Res* **37**(3): 574-587.

Fong, LG, Le, D (1999) The processing of ligands by the class A scavenger receptor is dependent on signal information located in the cytoplasmic domain. *J Biol Chem* **274**(51): 36808-36816.

Frey, MR, Dise, RS, Edelblum, KL, Polk, DB (2006) p38 kinase regulates epidermal growth factor receptor downregulation and cellular migration. *EMBO J* **25**(24): 5683-5692.

Fu, S, Sun, C, Tao, X, Ren, Y (2011) Anti-inflammatory effects of active constituents extracted from Chinese medicinal herbs against *Propionibacterium acnes*. *Nat Prod Res*.

Gabrielian, ES, Shukarian, AK, Goukasova, GI, Chandanian, GL, Panossian, AG, Wikman, G, Wagner, H (2002) A double blind, placebo-controlled study of *Andrographis paniculata* fixed combination Kan Jang in the treatment of acute upper respiratory tract infections including sinusitis. *Phytomedicine* **9**(7): 589-597.

Gerber, J, Nau, R (2010) Mechanisms of injury in bacterial meningitis. *Curr Opin Neurol* **23**(3): 312-318.

Ghosh, N, Ghosh, R, Mandal, V, Mandal, SC (2011) Recent advances in herbal medicine for treatment of liver diseases. *Pharm Biol* **49**(9): 970-988.

Goding, JW, Burns, GF (1981) Monoclonal antibody OKT-9 recognizes the receptor for transferrin on human acute lymphocytic leukemia cells. *J Immunol* **127**(3): 1256-1258.

Gold, KA, Lee, HY, Kim, ES (2009) Targeted therapies in squamous cell carcinoma of the head and neck. *Cancer* **115**(5): 922-935.

Grandal, MV, Grovdal, LM, Henriksen, L, Andersen, MH, Holst, MR, Madshus, IH, van Deurs, B (2011) Differential Roles of Grb2 and AP-2 in p38 MAPK- and EGF-Induced EGFR Internalization. *Traffic*.

Guay, J, Bateman, K, Gordon, R, Mancini, J, Riendeau, D (2004) Carrageenan-induced paw edema in rat elicits a predominant prostaglandin E2 (PGE2) response in the central nervous system associated with the induction of microsomal PGE2 synthase-1. *J Biol Chem* **279**(23): 24866-24872.

Gunn, EJ, Williams, JT, Huynh, DT, Iannotti, MJ, Han, C, Barrios, FJ, Kendall, S, Glackin, CA, Colby, DA, Kirshner, J (2011) The natural products parthenolide and andrographolide exhibit anti-cancer stem cell activity in multiple myeloma. *Leuk Lymphoma* **52**(6): 1085-1097.

Gupta, SC, Kim, JH, Prasad, S, Aggarwal, BB (2010) Regulation of survival, proliferation, invasion, angiogenesis, and metastasis of tumor cells through modulation of inflammatory pathways by nutraceuticals. *Cancer Metastasis Rev* **29**(3): 405-434.

Habashy, HO, Powe, DG, Staka, CM, Rakha, EA, Ball, G, Green, AR, Aleskandarany, M, Paish, EC, Douglas Macmillan, R, Nicholson, RI, Ellis, IO, Gee, JM (2009) Transferrin receptor (CD71) is a marker of poor prognosis in breast cancer and can predict response to tamoxifen. *Breast Cancer Res Treat*.

Han, Y, Bu, LM, Ji, X, Liu, CY, Wang, ZH (2005) Modulation of multidrug resistance by andrographolid in a HCT-8/5-FU multidrug-resistant colorectal cancer cell line. *Chin J Dig Dis* **6**(2): 82-86.

Hanahan, D, Weinberg, RA (2011) Hallmarks of cancer: the next generation. *Cell* **144**(5): 646-674.

Hawkes, M, Li, X, Crockett, M, Diassiti, A, Finney, C, Min-Oo, G, Liles, WC, Liu, J, Kain, KC (2010) CD36 deficiency attenuates experimental mycobacterial infection. *BMC Infect Dis* **10**: 299.

He, X, Li, J, Gao, H, Qiu, F, Hu, K, Cui, X, Yao, X (2003) Identification of a rare sulfonic acid metabolite of andrographolide in rats. *Drug Metab Dispos* **31**(8): 983-985.

Hidalgo, MA, Romero, A, Figueroa, J, Cortes, P, Concha, II, Hancke, JL, Burgos, RA (2005) Andrographolide interferes with binding of nuclear factor-kappaB to DNA in HL-60-derived neutrophilic cells. *Br J Pharmacol* **144**(5): 680-686.

Hong, W (2005) SNAREs and traffic. *Biochim Biophys Acta* **1744**(2): 120-144.

Hopkins, CR, Trowbridge, IS (1983) Internalization and processing of transferrin and the transferrin receptor in human carcinoma A431 cells. *J Cell Biol* **97**(2): 508-521.

Houston, MC (2010) The role of cellular micronutrient analysis, nutraceuticals, vitamins, antioxidants and minerals in the prevention and treatment of hypertension and cardiovascular disease. *Ther Adv Cardiovasc Dis* **4**(3): 165-183.

Hsieh, CY, Hsu, MJ, Hsiao, G, Wang, YH, Huang, CW, Chen, SW, Jayakumar, T, Chiu, PT, Chiu, YH, Sheu, JR (2010) Andrographolide enhances NF- $\kappa$ B subunit p65 Ser536 dephosphorylation through activation of protein phosphatase 2A (PP2A) in vascular smooth muscle cells. *J Biol Chem*.

Hung, SK, Hung, LC, Kuo, CD, Lee, KY, Lee, MS, Lin, HY, Chen, YJ, Fu, SL (2010) Andrographolide sensitizes Ras-transformed cells to radiation in vitro and in vivo. *Int J Radiat Oncol Biol Phys* **77**(4): 1232-1239.

Husemann, J, Loike, JD, Anankov, R, Febbraio, M, Silverstein, SC (2002) Scavenger receptors in neurobiology and neuropathology: their role on microglia and other cells of the nervous system. *Glia* **40**(2): 195-205.

Hyatt, DC, Ceresa, BP (2008) Cellular localization of the activated EGFR determines its effect on cell growth in MDA-MB-468 cells. *Exp Cell Res* **314**(18): 3415-3425.

Hynes, NE, Lane, HA (2005) ERBB receptors and cancer: the complexity of targeted inhibitors. *Nat Rev Cancer* **5**(5): 341-354.

Iruretagoyena, MI, Sepulveda, SE, Lezana, JP, Hermoso, M, Bronfman, M, Gutierrez, MA, Jacobelli, SH, Kalergis, AM (2006) Inhibition of nuclear factor-kappa B enhances the capacity of immature dendritic cells to induce antigen-specific tolerance in experimental autoimmune encephalomyelitis. *J Pharmacol Exp Ther* **318**(1): 59-67.

Iruretagoyena, MI, Tobar, JA, Gonzalez, PA, Sepulveda, SE, Figueroa, CA, Burgos, RA, Hancke, JL, Kalergis, AM (2005) Andrographolide interferes with T cell activation and reduces experimental autoimmune encephalomyelitis in the mouse. *J Pharmacol Exp Ther* **312**(1): 366-372.

Jada, SR, Hamzah, AS, Lajis, NH, Saad, MS, Stevens, MF, Stanslas, J (2006) Semisynthesis and cytotoxic activities of andrographolide analogues. *J Enzyme Inhib Med Chem* **21**(2): 145-155.

Jada, SR, Matthews, C, Saad, MS, Hamzah, AS, Lajis, NH, Stevens, MF, Stanslas, J (2008) Benzylidene derivatives of andrographolide inhibit growth of breast and colon cancer cells in vitro by inducing G(1) arrest and apoptosis. *Br J Pharmacol* **155**(5): 641-654.

Ji, L, Liu, T, Liu, J, Chen, Y, Wang, Z (2007) Andrographolide inhibits human hepatoma-derived Hep3B cell growth through the activation of c-Jun N-terminal kinase. *Planta Med* **73**(13): 1397-1401.

Ji, L, Shen, K, Jiang, P, Morahan, G, Wang, Z (2011) Critical roles of cellular glutathione homeostasis and jnk activation in andrographolide-mediated apoptotic cell death in human hepatoma cells. *Mol Carcinog* **50**(8): 580-591.

Jiang, CG, Li, JB, Liu, FR, Wu, T, Yu, M, Xu, HM (2007) Andrographolide inhibits the adhesion of gastric cancer cells to endothelial cells by blocking E-selectin expression. *Anticancer Res* **27**(4B): 2439-2447.

Jones, LC, Moussa, L, Fulcher, ML, Zhu, Y, Hudson, EJ, O'Neal, WK, Randell, SH, Lazarowski, ER, Boucher, RC, Kreda, SM (2012) VAMP8 is a vesicle SNARE that regulates mucin secretion in airway goblet cells. *J Physiol* **590**(Pt 3): 545-562.

Kang, CS, Pu, PY, Li, YH, Zhang, ZY, Qiu, MZ, Huang, Q, Wang, GX (2005) An in vitro study on the suppressive effect of glioma cell growth induced by plasmid-based small interference RNA (siRNA) targeting human epidermal growth factor receptor. *J Neurooncol* **74**(3): 267-273.

Kannappan, R, Gupta, SC, Kim, JH, Reuter, S, Aggarwal, BB (2011) Neuroprotection by spice-derived nutraceuticals: you are what you eat! *Mol Neurobiol* **44**(2): 142-159.

Kesari, S, Ramakrishna, N, Sauvageot, C, Stiles, CD, Wen, PY (2006) Targeted molecular therapy of malignant gliomas. *Curr Oncol Rep* **8**(1): 58-70.

Kim, KS (2003) Pathogenesis of bacterial meningitis: from bacteraemia to neuronal injury. *Nat Rev Neurosci* **4**(5): 376-385.

Kim, TG, Hwi, KK, Hung, CS (2005) Morphological and biochemical changes of andrographolide-induced cell death in human prostatic adenocarcinoma PC-3 cells. *In Vivo* **19**(3): 551-557.

Kinchen, JM, Doukoumetzidis, K, Almendinger, J, Stergiou, L, Tosello-Tramont, A, Sifri, CD, Hengartner, MO, Ravichandran, KS (2008) A pathway for phagosome maturation during engulfment of apoptotic cells. *Nat Cell Biol* **10**(5): 556-566.

Kirisits, A, Pils, D, Krainer, M (2007) Epidermal growth factor receptor degradation: an alternative view of oncogenic pathways. *Int J Biochem Cell Biol* **39**(12): 2173-2182.

Kligler, B, Ulbricht, C, Basch, E, Kirkwood, CD, Abrams, TR, Miranda, M, Singh Khalsa, KP, Giles, M, Boon, H, Woods, J (2006) *Andrographis paniculata* for the treatment of upper

respiratory infection: a systematic review by the natural standard research collaboration. *Explore (NY)* **2**(1): 25-29.

Kosswig, N, Rice, S, Daugherty, A, Post, SR (2003) Class A scavenger receptor-mediated adhesion and internalization require distinct cytoplasmic domains. *J Biol Chem* **278**(36): 34219-34225.

Kulichenko, LL, Kireyeva, LV, Malyshkina, EN, Wikman, G (2003) A randomized, controlled study of Kan Jang versus amantadine in the treatment of influenza in Volgograd. *J Herb Pharmacother* **3**(1): 77-93.

Kumar, RA, Sridevi, K, Kumar, NV, Nanduri, S, Rajagopal, S (2004) Anticancer and immunostimulatory compounds from *Andrographis paniculata*. *J Ethnopharmacol* **92**(2-3): 291-295.

Kumarappan, C, Jaswanth, A, Kumarasunderi, K (2011) Antihemolytic and snake venom neutralizing effect of some Indian medicinal plants. *Asian Pac J Trop Med* **4**(9): 743-747.

Lafky, JM, Wilken, JA, Baron, AT, Maihle, NJ (2008) Clinical implications of the ErbB/epidermal growth factor (EGF) receptor family and its ligands in ovarian cancer. *Biochim Biophys Acta* **1785**(2): 232-265.

Le Roy, C, Wrana, JL (2005) Clathrin- and non-clathrin-mediated endocytic regulation of cell signalling. *Nat Rev Mol Cell Biol* **6**(2): 112-126.

Lee, YC, Lin, HH, Hsu, CH, Wang, CJ, Chiang, TA, Chen, JH (2010) Inhibitory effects of andrographolide on migration and invasion in human non-small cell lung cancer A549 cells via down-regulation of PI3K/Akt signaling pathway. *Eur J Pharmacol* **632**(1-3): 23-32.

Lepelletier, Y, Camara-Clayette, V, Jin, H, Hermant, A, Coulon, S, Dussiot, M, Arcos-Fajardo, M, Baude, C, Canionni, D, Delarue, R, Brousse, N, Benaroch, P, Benhamou, M, Ribrag, V, Monteiro, RC, Moura, IC, Hermine, O (2007) Prevention of mantle lymphoma tumor establishment by routing transferrin receptor toward lysosomal compartments. *Cancer Res* **67**(3): 1145-1154.

Li, FX, Li, SS (2011) Effects of andrographolide on the activation of mitogen activated protein kinases and nuclear factor-kappa B in mouse peritoneal macrophage-derived foam cells. *Chin J Integr Med*.

Li, J, Cheung, HY, Zhang, Z, Chan, GK, Fong, WF (2007) Andrographolide induces cell cycle arrest at G2/M phase and cell death in HepG2 cells via alteration of reactive oxygen species. *Eur J Pharmacol* **568**(1-3): 31-44.

Li, YD, Ye, BQ, Zheng, SX, Wang, JT, Wang, JG, Chen, M, Liu, JG, Pei, XH, Wang, LJ, Lin, ZX, Gupta, K, Mackman, N, Slungaard, A, Key, NS, Geng, JG (2009) NF-kappaB transcription factor p50 critically regulates tissue factor in deep vein thrombosis. *J Biol Chem* **284**(7): 4473-4483.

Liang, FP, Lin, CH, Kuo, CD, Chao, HP, Fu, SL (2008) Suppression of v-Src transformation by andrographolide via degradation of the v-Src protein and attenuation of the Erk signaling pathway. *J Biol Chem* **283**(8): 5023-5033.

Lim, CW, Chan, TK, Ng, DS, Sagineedu, SR, Stanslas, J, Wong, WF (2011) Andrographolide and its analogues: versatile bioactive molecules for combating inflammation and cancer. *Clin Exp Pharmacol Physiol*.

Lin, HH, Tsai, CW, Chou, FP, Wang, CJ, Hsuan, SW, Wang, CK, Chen, JH (2011) Andrographolide down-regulates hypoxia-inducible factor-1alpha in human non-small cell lung cancer A549 cells. *Toxicol Appl Pharmacol* **250**(3): 336-345.

Liu, C, Nadiminty, N, Tummala, R, Chun, JY, Lou, W, Zhu, Y, Sun, M, Evans, CP, Zhou, Q, Gao, AC (2011) Andrographolide targets androgen receptor pathway in castration-resistant prostate cancer. *Genes Cancer* **2**(2): 151-159.

Lu, WJ, Lee, JJ, Chou, DS, Jayakumar, T, Fong, TH, Hsiao, G, Sheu, JR (2011) A novel role of andrographolide, an NF-kappa B inhibitor, on inhibition of platelet activation: the pivotal mechanisms of endothelial nitric oxide synthase/cyclic GMP. *J Mol Med (Berl)* **89**(12): 1261-1273.

Mace, G, Miaczynska, M, Zerial, M, Nebreda, AR (2005) Phosphorylation of EEA1 by p38 MAP kinase regulates mu opioid receptor endocytosis. *EMBO J* **24**(18): 3235-3246.

Madhus, IH, Stang, E (2009) Internalization and intracellular sorting of the EGF receptor: a model for understanding the mechanisms of receptor trafficking. *J Cell Sci* **122**(Pt 19): 3433-3439.

Maiti, K, Mukherjee, K, Murugan, V, Saha, BP, Mukherjee, PK (2010) Enhancing bioavailability and hepatoprotective activity of andrographolide from *Andrographis paniculata*, a well-known medicinal food, through its herbosome. *J Sci Food Agric* **90**(1): 43-51.

Manikam, SD, Stanslas, J (2009) Andrographolide inhibits growth of acute promyelocytic leukaemia cells by inducing retinoic acid receptor-independent cell differentiation and apoptosis. *J Pharm Pharmacol* **61**(1): 69-78.

Matsuzawa, A, Ichijo, H (2008) Redox control of cell fate by MAP kinase: physiological roles of ASK1-MAP kinase pathway in stress signaling. *Biochim Biophys Acta* **1780**(11): 1325-1336.



- Maxfield, FR, McGraw, TE (2004) Endocytic recycling. *Nat Rev Mol Cell Biol* **5**(2): 121-132.
- McCubrey, JA, Lahair, MM, Franklin, RA (2006) Reactive oxygen species-induced activation of the MAP kinase signaling pathways. *Antioxid Redox Signal* **8**(9-10): 1775-1789.
- Melchior, J, Spasov, AA, Ostrovskij, OV, Bulanov, AE, Wikman, G (2000) Double-blind, placebo-controlled pilot and phase III study of activity of standardized *Andrographis paniculata* Herba Nees extract fixed combination (Kan jang) in the treatment of uncomplicated upper-respiratory tract infection. *Phytomedicine* **7**(5): 341-350.
- Mese, H, Sasaki, A, Nakayama, S, Alcalde, RE, Matsumura, T (2000) The role of caspase family protease, caspase-3 on cisplatin-induced apoptosis in cisplatin-resistant A431 cell line. *Cancer Chemother Pharmacol* **46**(3): 241-245.
- Morimoto, K, Wada, Y, Hinagata, J, Imanishi, T, Kodama, T, Doi, T (1999) VXF1 in the cytoplasmic domain of macrophage scavenger receptors mediates their efficient internalization and cell-surface expression. *Biol Pharm Bull* **22**(10): 1022-1026.
- Mukhopadhyay, S, Chen, Y, Sankala, M, Peiser, L, Pikkarainen, T, Kraal, G, Tryggvason, K, Gordon, S (2006) MARCO, an innate activation marker of macrophages, is a class A scavenger receptor for *Neisseria meningitidis*. *Eur J Immunol* **36**(4): 940-949.
- Muzio, L, Martino, G, Furlan, R (2007) Multifaceted aspects of inflammation in multiple sclerosis: the role of microglia. *J Neuroimmunol* **191**(1-2): 39-44.
- Nakamura, K, Funakoshi, H, Miyamoto, K, Tokunaga, F, Nakamura, T (2001) Molecular cloning and functional characterization of a human scavenger receptor with C-type lectin (SRCL), a novel member of a scavenger receptor family. *Biochem Biophys Res Commun* **280**(4): 1028-1035.
- Nanduri, S, Nyavanandi, VK, Thunuguntla, SS, Kasu, S, Pallerla, MK, Ram, PS, Rajagopal, S, Kumar, RA, Ramanujam, R, Babu, JM, Vyas, K, Devi, AS, Reddy, GO, Akella, V (2004) Synthesis and structure-activity relationships of andrographolide analogues as novel cytotoxic agents. *Bioorg Med Chem Lett* **14**(18): 4711-4717.
- Nixon, RA, Yang, DS, Lee, JH (2008) Neurodegenerative lysosomal disorders: a continuum from development to late age. *Autophagy* **4**(5): 590-599.
- Ola, MS, Nawaz, M, Ahsan, H (2011) Role of Bcl-2 family proteins and caspases in the regulation of apoptosis. *Mol Cell Biochem* **351**(1-2): 41-58.

Orth, JD, Krueger, EW, Weller, SG, McNiven, MA (2006) A novel endocytic mechanism of epidermal growth factor receptor sequestration and internalization. *Cancer Res* **66**(7): 3603-3610.

Orth, JD, McNiven, MA (2006) Get off my back! Rapid receptor internalization through circular dorsal ruffles. *Cancer Res* **66**(23): 11094-11096.

Pannecouque, C, Daelemans, D, De Clercq, E (2008) Tetrazolium-based colorimetric assay for the detection of HIV replication inhibitors: revisited 20 years later. *Nat Protoc* **3**(3): 427-434.

Panossian, A, Davtyan, T, Gukassyan, N, Gukasova, G, Mamikonyan, G, Gabrielian, E, Wikman, G (2002) Effect of andrographolide and Kan Jang--fixed combination of extract SHA-10 and extract SHE-3--on proliferation of human lymphocytes, production of cytokines and immune activation markers in the whole blood cells culture. *Phytomedicine* **9**(7): 598-605.

Panossian, A, Hambartsumyan, M, Panosyan, L, Abrahamyan, H, Mamikonyan, G, Gabrielyan, E, Amaryan, G, Astvatsatryan, V, Wikman, G (2003) Plasma nitric oxide level in familial Mediterranean fever and its modulations by Immuno-Guard. *Nitric Oxide* **9**(2): 103-110.

Panossian, A, Hovhannisyan, A, Mamikonyan, G, Abrahamian, H, Hambardzumyan, E, Gabrielian, E, Gukasova, G, Wikman, G, Wagner, H (2000) Pharmacokinetic and oral bioavailability of andrographolide from *Andrographis paniculata* fixed combination Kan Jang in rats and human. *Phytomedicine* **7**(5): 351-364.

Parichatikanond, W, Suthisang, C, Dhepakson, P, Herunsalee, A (2010) Study of anti-inflammatory activities of the pure compounds from *Andrographis paniculata* (burm.f.) Nees and their effects on gene expression. *Int Immunopharmacol* **10**(11): 1361-1373.

Pike, LJ (2005) Growth factor receptors, lipid rafts and caveolae: an evolving story. *Biochim Biophys Acta* **1746**(3): 260-273.

Pimienta, G, Pascual, J (2007) Canonical and alternative MAPK signaling. *Cell Cycle* **6**(21): 2628-2632.

Pluddemann, A, Mukhopadhyay, S, Gordon, S (2006) The interaction of macrophage receptors with bacterial ligands. *Expert Rev Mol Med* **8**(28): 1-25.

Pluddemann, A, Mukhopadhyay, S, Sankala, M, Savino, S, Pizza, M, Rappuoli, R, Tryggvason, K, Gordon, S (2009) SR-A, MARCO and TLRs differentially recognise selected surface proteins from *Neisseria meningitidis*: an example of fine specificity in microbial ligand recognition by innate immune receptors. *J Innate Immun* **1**(2): 153-163.

Pluddemann, A, Neyen, C, Gordon, S (2007) Macrophage scavenger receptors and host-derived ligands. *Methods* **43**(3): 207-217.

Polgar, J, Chung, SH, Reed, GL (2002) Vesicle-associated membrane protein 3 (VAMP-3) and VAMP-8 are present in human platelets and are required for granule secretion. *Blood* **100**(3): 1081-1083.

Poolsup, N, Suthisisang, C, Prathanturarug, S, Asawamekin, A, Chanchareon, U (2004) *Andrographis paniculata* in the symptomatic treatment of uncomplicated upper respiratory tract infection: systematic review of randomized controlled trials. *J Clin Pharm Ther* **29**(1): 37-45.

Post, SR, Gass, C, Rice, S, Nikolic, D, Crump, H, Post, GR (2002) Class A scavenger receptors mediate cell adhesion via activation of G(i/o) and formation of focal adhesion complexes. *J Lipid Res* **43**(11): 1829-1836.

Premendran, SJ, Salwe, KJ, Pathak, S, Brahmane, R, Manimekalai, K (2011) Anti-cobra venom activity of plant *Andrographis paniculata* and its comparison with polyvalent anti-snake venom. *J Nat Sci Biol Med* **2**(2): 198-204.

Puri, A, Saxena, R, Saxena, RP, Saxena, KC, Srivastava, V, Tandon, JS (1993) Immunostimulant agents from *Andrographis paniculata*. *J Nat Prod* **56**(7): 995-999.

Qadura, M, Othman, M, Waters, B, Chegeni, R, Walker, K, Labelle, A, Ozelo, M, Hough, C, Lillcrap, D (2008) Reduction of the immune response to factor VIII mediated through tolerogenic factor VIII presentation by immature dendritic cells. *J Thromb Haemost* **6**(12): 2095-2104.

Qin, LH, Kong, L, Shi, GJ, Wang, ZT, Ge, BX (2006) Andrographolide inhibits the production of TNF-alpha and interleukin-12 in lipopolysaccharide-stimulated macrophages: role of mitogen-activated protein kinases. *Biol Pharm Bull* **29**(2): 220-224.

Quesnelle, KM, Boehm, AL, Grandis, JR (2007) STAT-mediated EGFR signaling in cancer. *J Cell Biochem* **102**(2): 311-319.

Rajagopal, S, Kumar, RA, Deevi, DS, Satyanarayana, C, Rajagopalan, R (2003) Andrographolide, a potential cancer therapeutic agent isolated from *Andrographis paniculata*. *J Exp Ther Oncol* **3**(3): 147-158.

Roy, P, Das, S, Bera, T, Mondol, S, Mukherjee, A (2010) Andrographolide nanoparticles in leishmaniasis: characterization and in vitro evaluations. *Int J Nanomedicine* **5**: 1113-1121.

Saez-Llorens, X, McCracken, GH, Jr. (2003) Bacterial meningitis in children. *Lancet* **361**(9375): 2139-2148.

Saitoh, M, Nishitoh, H, Fujii, M, Takeda, K, Tobiume, K, Sawada, Y, Kawabata, M, Miyazono, K, Ichijo, H (1998) Mammalian thioredoxin is a direct inhibitor of apoptosis signal-regulating kinase (ASK) 1. *EMBO J* **17**(9): 2596-2606.

Saksena, S, Emr, SD (2009) ESCRTs and human disease. *Biochem Soc Trans* **37**(Pt 1): 167-172.

Samy, RP, Thwin, MM, Gopalakrishnakone, P, Ignacimuthu, S (2008) Ethnobotanical survey of folk plants for the treatment of snakebites in Southern part of Tamilnadu, India. *J Ethnopharmacol* **115**(2): 302-312.

Sankala, M, Brannstrom, A, Schulthess, T, Bergmann, U, Morgunova, E, Engel, J, Tryggvason, K, Pikkarainen, T (2002) Characterization of recombinant soluble macrophage scavenger receptor MARCO. *J Biol Chem* **277**(36): 33378-33385.

Sano, H, Ishino, M, Kramer, H, Shimizu, T, Mitsuzawa, H, Nishitani, C, Kuroki, Y (2007) The microtubule-binding protein Hook3 interacts with a cytoplasmic domain of scavenger receptor A. *J Biol Chem* **282**(11): 7973-7981.

Satyanarayana, C, Deevi, DS, Rajagopalan, R, Srinivas, N, Rajagopal, S (2004) DRF 3188 a novel semi-synthetic analog of andrographolide: cellular response to MCF 7 breast cancer cells. *BMC Cancer* **4**: 26.

Sheeja, K, Kuttan, G (2007a) Activation of cytotoxic T lymphocyte responses and attenuation of tumor growth in vivo by *Andrographis paniculata* extract and andrographolide. *Immunopharmacol Immunotoxicol* **29**(1): 81-93.

Sheeja, K, Kuttan, G (2010) *Andrographis paniculata* downregulates proinflammatory cytokine production and augments cell mediated immune response in metastatic tumor-bearing mice. *Asian Pac J Cancer Prev* **11**(3): 723-729.

Sheeja, K, Kuttan, G (2008) Effect of *Andrographis paniculata* as an adjuvant in combined chemo-radio and whole body hyperthermia treatment - a preliminary study. *Immunopharmacol Immunotoxicol* **30**(1): 181-194.

Sheeja, K, Kuttan, G (2007b) Modulation of natural killer cell activity, antibody-dependent cellular cytotoxicity, and antibody-dependent complement-mediated cytotoxicity by andrographolide in normal and Ehrlich ascites carcinoma-bearing mice. *Integr Cancer Ther* **6**(1): 66-73.

Sheeja, K, Kuttan, G (2006) Protective effect of Andrographis paniculata and andrographolide on cyclophosphamide-induced urothelial toxicity. *Integr Cancer Ther* **5**(3): 244-251.

Sheeja, K, Shihab, PK, Kuttan, G (2006) Antioxidant and anti-inflammatory activities of the plant Andrographis paniculata Nees. *Immunopharmacol Immunotoxicol* **28**(1): 129-140.

Shen, YC, Chen, CF, Chiou, WF (2002) Andrographolide prevents oxygen radical production by human neutrophils: possible mechanism(s) involved in its anti-inflammatory effect. *Br J Pharmacol* **135**(2): 399-406.

Shi, MD, Lin, HH, Chiang, TA, Tsai, LY, Tsai, SM, Lee, YC, Chen, JH (2009) Andrographolide could inhibit human colorectal carcinoma Lovo cells migration and invasion via down-regulation of MMP-7 expression. *Chem Biol Interact* **180**(3): 344-352.

Shi, MD, Lin, HH, Lee, YC, Chao, JK, Lin, RA, Chen, JH (2008) Inhibition of cell-cycle progression in human colorectal carcinoma Lovo cells by andrographolide. *Chem Biol Interact* **174**(3): 201-210.

Shimizu, M, Shirakami, Y, Moriwaki, H (2008) Targeting Receptor Tyrosine Kinases for Chemoprevention by Green Tea Catechin, EGCG. *Int J Mol Sci* **9**(6): 1034-1049.

Sigismund, S, Argenzio, E, Tosoni, D, Cavallaro, E, Polo, S, Di Fiore, PP (2008) Clathrin-mediated internalization is essential for sustained EGFR signaling but dispensable for degradation. *Dev Cell* **15**(2): 209-219.

Sigismund, S, Woelk, T, Puri, C, Maspero, E, Tacchetti, C, Transidico, P, Di Fiore, PP, Polo, S (2005) Clathrin-independent endocytosis of ubiquitinated cargos. *Proc Natl Acad Sci U S A* **102**(8): 2760-2765.

Singha, PK, Roy, S, Dey, S (2007) Protective activity of andrographolide and arabinogalactan proteins from Andrographis paniculata Nees. against ethanol-induced toxicity in mice. *J Ethnopharmacol* **111**(1): 13-21.

Sinha, J, Mukhopadhyay, S, Das, N, Basu, MK (2000) Targeting of liposomal andrographolide to L. donovani-infected macrophages in vivo. *Drug Deliv* **7**(4): 209-213.

Sivagnanam, V, Zhu, X, Schlichter, LC (2010) Dominance of E. coli phagocytosis over LPS in the inflammatory response of microglia. *J Neuroimmunol* **227**(1-2): 111-119.

Sorkin, A, Goh, LK (2009) Endocytosis and intracellular trafficking of ErbBs. *Exp Cell Res* **315**(4): 683-696.

Sorkin, A, von Zastrow, M (2009) Endocytosis and signalling: intertwining molecular networks. *Nat Rev Mol Cell Biol* **10**(9): 609-622.

Spasov, AA, Ostrovskij, OV, Chernikov, MV, Wikman, G (2004) Comparative controlled study of *Andrographis paniculata* fixed combination, Kan Jang and an Echinacea preparation as adjuvant, in the treatment of uncomplicated respiratory disease in children. *Phytother Res* **18**(1): 47-53.

Stanslas, J, Liew, PS, Iftikhar, N, Lee, CP, Saad, S, Lajis, N, Robins, RA, Loadman, P, Bibby, MC (2001a) Potential of AG in the treatment of breast cancer. *European Journal of Cancer* **37**, Supplement 6(0): S169.

Stanslas, J, Liew, PS, Iftikhar, N, Lee, CP, Saad, S., Lajis, N, Robins, RA, Loadman, P, Bibby, MC (2001b) Potential of AG in the treatment of breast cancer. *European Journal of Cancer* **37**(Supplement 6): 169.

Stuart, LM, Deng, J, Silver, JM, Takahashi, K, Tseng, AA, Hennessy, EJ, Ezekowitz, RA, Moore, KJ (2005) Response to *Staphylococcus aureus* requires CD36-mediated phagocytosis triggered by the COOH-terminal cytoplasmic domain. *J Cell Biol* **170**(3): 477-485.

Suebsasana, S, Pongnaratorn, P, Sattayasai, J, Arkaravichien, T, Tiamkao, S, Aromdee, C (2009) Analgesic, antipyretic, anti-inflammatory and toxic effects of andrographolide derivatives in experimental animals. *Arch Pharm Res* **32**(9): 1191-1200.

Sukardiman, H, Widyawaruyanti, A, Sismindari, Zaini, NC (2007) Apoptosis inducing effect of andrographolide on TD-47 human breast cancer cell line. *Afr J Tradit Complement Altern Med* **4**(3): 345-351.

Sulaiman, MR, Zakaria, ZA, Abdul Rahman, A, Mohamad, AS, Desa, MN, Stanslas, J, Moin, S, Israf, DA (2010) Antinociceptive and antiedematogenic activities of andrographolide isolated from *Andrographis paniculata* in animal models. *Biol Res Nurs* **11**(3): 293-301.

Suo, XB, Zhang, H, Wang, YQ (2007) HPLC determination of andrographolide in rat whole blood: study on the pharmacokinetics of andrographolide incorporated in liposomes and tablets. *Biomed Chromatogr* **21**(7): 730-734.

Tan, Y, Chiow, KH, Huang, D, Wong, SH (2010) Andrographolide regulates epidermal growth factor receptor and transferrin receptor trafficking in epidermoid carcinoma (A-431) cells. *Br J Pharmacol* **159**(7): 1497-1510.

Thelen, T, Hao, Y, Medeiros, AI, Curtis, JL, Serezani, CH, Kobzik, L, Harris, LH, Aronoff, DM (2010) The class A scavenger receptor, macrophage receptor with collagenous structure, is

the major phagocytic receptor for *Clostridium sordellii* expressed by human decidual macrophages. *J Immunol* **185**(7): 4328-4335.

Thisoda, P, Rangkadilok, N, Pholphana, N, Worasuttayangkurn, L, Ruchirawat, S, Satayavivad, J (2006) Inhibitory effect of *Andrographis paniculata* extract and its active diterpenoids on platelet aggregation. *Eur J Pharmacol* **553**(1-3): 39-45.

Tsai, HR, Yang, LM, Tsai, WJ, Chiou, WF (2004) Andrographolide acts through inhibition of ERK1/2 and Akt phosphorylation to suppress chemotactic migration. *Eur J Pharmacol* **498**(1-3): 45-52.

Turjanski, AG, Vaque, JP, Gutkind, JS (2007) MAP kinases and the control of nuclear events. *Oncogene* **26**(22): 3240-3253.

Uawonggul, N, Chaveerach, A, Thammasirirak, S, Arkaravichien, T, Chuachan, C, Daduang, S (2006) Screening of plants acting against *Heterometrus laoticus* scorpion venom activity on fibroblast cell lysis. *J Ethnopharmacol* **103**(2): 201-207.

Vergarajauregui, S, San Miguel, A, Puertollano, R (2006) Activation of p38 mitogen-activated protein kinase promotes epidermal growth factor receptor internalization. *Traffic* **7**(6): 686-698.

Vermeulen, K, Van Bockstaele, DR, Berneman, ZN (2005) Apoptosis: mechanisms and relevance in cancer. *Ann Hematol* **84**(10): 627-639.

Wang, LJ, Zhou, X, Wang, W, Tang, F, Qi, CL, Yang, X, Wu, S, Lin, YQ, Wang, JT, Geng, JG (2011) Andrographolide inhibits oral squamous cell carcinogenesis through NF-kappaB inactivation. *J Dent Res* **90**(10): 1246-1252.

Wang, T, Liu, B, Zhang, W, Wilson, B, Hong, JS (2004) Andrographolide reduces inflammation-mediated dopaminergic neurodegeneration in mesencephalic neuron-glia cultures by inhibiting microglial activation. *J Pharmacol Exp Ther* **308**(3): 975-983.

Wang, W, Wang, J, Dong, SF, Liu, CH, Italiani, P, Sun, SH, Xu, J, Boraschi, D, Ma, SP, Qu, D (2010a) Immunomodulatory activity of andrographolide on macrophage activation and specific antibody response. *Acta Pharmacol Sin* **31**(2): 191-201.

Wang, YJ, Wang, JT, Fan, QX, Geng, JG (2007) Andrographolide inhibits NF-kappaBeta activation and attenuates neointimal hyperplasia in arterial restenosis. *Cell Res* **17**(11): 933-941.

- Wang, Z, Yu, P, Zhang, G, Xu, L, Wang, D, Wang, L, Zeng, X, Wang, Y (2010b) Design, synthesis and antibacterial activity of novel andrographolide derivatives. *Bioorg Med Chem* **18**(12): 4269-4274.
- Winograd-Katz, SE, Levitzki, A (2006) Cisplatin induces PKB/Akt activation and p38(MAPK) phosphorylation of the EGF receptor. *Oncogene* **25**(56): 7381-7390.
- Wong, SH, Xu, Y, Zhang, T, Griffiths, G, Lowe, SL, Subramaniam, VN, Seow, KT, Hong, W (1999) GS32, a novel Golgi SNARE of 32 kDa, interacts preferentially with syntaxin 6. *Mol Biol Cell* **10**(1): 119-134.
- Wong, SH, Zhang, T, Xu, Y, Subramaniam, VN, Griffiths, G, Hong, W (1998) Endobrevin, a novel synaptobrevin/VAMP-like protein preferentially associated with the early endosome. *Mol Biol Cell* **9**(6): 1549-1563.
- Wrann, MM, Fox, CF (1979) Identification of epidermal growth factor receptors in a hyperproducing human epidermoid carcinoma cell line. *J Biol Chem* **254**(17): 8083-8086.
- Wu, TT, Chen, TL, Chen, RM (2009) Lipopolysaccharide triggers macrophage activation of inflammatory cytokine expression, chemotaxis, phagocytosis, and oxidative ability via a toll-like receptor 4-dependent pathway: validated by RNA interference. *Toxicol Lett* **191**(2-3): 195-202.
- Xia, YF, Ye, BQ, Li, YD, Wang, JG, He, XJ, Lin, X, Yao, X, Ma, D, Slungaard, A, Hebbel, RP, Key, NS, Geng, JG (2004) Andrographolide attenuates inflammation by inhibition of NF-kappa B activation through covalent modification of reduced cysteine 62 of p50. *J Immunol* **173**(6): 4207-4217.
- Xu, L, Xiao, DW, Lou, S, Zou, JJ, Zhu, YB, Fan, HW, Wang, GJ (2009) A simple and sensitive HPLC-ESI-MS/MS method for the determination of andrographolide in human plasma. *J Chromatogr B Analyt Technol Biomed Life Sci* **877**(5-6): 502-506.
- Xu, Y, Chen, A, Fry, S, Barrow, RA, Marshall, RL, Mukkur, TK (2007) Modulation of immune response in mice immunised with an inactivated Salmonella vaccine and gavaged with *Andrographis paniculata* extract or andrographolide. *Int Immunopharmacol* **7**(4): 515-523.
- Yan, J, Chen, Y, He, C, Yang, ZZ, Lu, C, Chen, XS (2011) Andrographolide induces cell cycle arrest and apoptosis in human rheumatoid arthritis fibroblast-like synoviocytes. *Cell Biol Toxicol*.
- Yang, CS, Wang, X, Lu, G, Picinich, SC (2009a) Cancer prevention by tea: animal studies, molecular mechanisms and human relevance. *Nat Rev Cancer* **9**(6): 429-439.



Yang, L, Wu, D, Luo, K, Wu, S, Wu, P (2009b) Andrographolide enhances 5-fluorouracil-induced apoptosis via caspase-8-dependent mitochondrial pathway involving p53 participation in hepatocellular carcinoma (SMMC-7721) cells. *Cancer Lett* **276**(2): 180-188.

Yang, S, Evens, AM, Prachand, S, Singh, AT, Bhalla, S, David, K, Gordon, LI (2010) Mitochondrial-mediated apoptosis in lymphoma cells by the diterpenoid lactone andrographolide, the active component of *Andrographis paniculata*. *Clin Cancer Res* **16**(19): 4755-4768.

Yap, TA, Carden, CP, Kaye, SB (2009) Beyond chemotherapy: targeted therapies in ovarian cancer. *Nat Rev Cancer* **9**(3): 167-181.

Ye, L, Wang, T, Tang, L, Liu, W, Yang, Z, Zhou, J, Zheng, Z, Cai, Z, Hu, M, Liu, Z (2011) Poor oral bioavailability of a promising anticancer agent andrographolide is due to extensive metabolism and efflux by P-glycoprotein. *J Pharm Sci* **100**(11): 5007-5017.

Yoshioka, J, Schreiter, ER, Lee, RT (2006) Role of thioredoxin in cell growth through interactions with signaling molecules. *Antioxid Redox Signal* **8**(11-12): 2143-2151.

Yu, AL, Lu, CY, Wang, TS, Tsai, CW, Liu, KL, Cheng, YP, Chang, HC, Lii, CK, Chen, HW (2010) Induction of heme oxygenase 1 and inhibition of tumor necrosis factor alpha-induced intercellular adhesion molecule expression by andrographolide in EA.hy926 cells. *J Agric Food Chem* **58**(13): 7641-7648.

Zahorowska, B, Crowe, PJ, Yang, JL (2009) Combined therapies for cancer: a review of EGFR-targeted monotherapy and combination treatment with other drugs. *J Cancer Res Clin Oncol* **135**(9): 1137-1148.

Zhang, H, Berezov, A, Wang, Q, Zhang, G, Drebin, J, Murali, R, Greene, MI (2007) ErbB receptors: from oncogenes to targeted cancer therapies. *J Clin Invest* **117**(8): 2051-2058.

Zhao, F, He, EQ, Wang, L, Liu, K (2008) Anti-tumor activities of andrographolide, a diterpene from *Andrographis paniculata*, by inducing apoptosis and inhibiting VEGF level. *J Asian Nat Prod Res* **10**(5-6): 467-473.

Zhi-Tao, Z, Xue-Song, J, Bai-Chun, W, Wei-Xin, M, Hong-Yu, L, Ye, T (2011) Andrographolide Inhibits Intimal Hyperplasia in a Rat Model of Autogenous Vein Grafts. *Cell Biochem Biophys*.

Zhou, J, Lu, GD, Ong, CS, Ong, CN, Shen, HM (2008) Andrographolide sensitizes cancer cells to TRAIL-induced apoptosis via p53-mediated death receptor 4 up-regulation. *Mol Cancer Ther* **7**(7): 2170-2180.

Zhou, J, Ong, CN, Hur, GM, Shen, HM (2010) Inhibition of the JAK-STAT3 pathway by andrographolide enhances chemosensitivity of cancer cells to doxorubicin. *Biochem Pharmacol* **79**(9): 1242-1250.

Zhou, J, Zhang, S, Ong, CN, Shen, HM (2006) Critical role of pro-apoptotic Bcl-2 family members in andrographolide-induced apoptosis in human cancer cells. *Biochem Pharmacol* **72**(2): 132-144.

Zhu, XD, Zhuang, Y, Ben, JJ, Qian, LL, Huang, HP, Bai, H, Sha, JH, He, ZG, Chen, Q (2011) Caveolae-dependent endocytosis is required for class A macrophage scavenger receptor-mediated apoptosis in macrophages. *J Biol Chem* **286**(10): 8231-8239.

Zwang, Y, Yarden, Y (2006) p38 MAP kinase mediates stress-induced internalization of EGFR: implications for cancer chemotherapy. *EMBO J* **25**(18): 4195-4206.

# **Chapter 8**

# **Appendices**

## 8. Appendices

### 8.1. Appendix I – Tables from Literature Review

Maximum plasma levels of ADO	Dosage; formulation; route of administration	System	Method of measurement	Reference
1.273 µg/ml (20 mg/kg, oral, rats), 3.00 µg/ml (200 mg/kg, oral, rats)	20mg/kg (intravenous), 20 mg/kg, 200mg/kg (oral); <i>Andrographis paniculata</i> extract	Rats	High performance liquid chromatography (HPLC)/ UV detection, gas chromatography (GC)/ mass spectrometry (MS); capillary electrophoresis.	(Panossian <i>et al.</i> , 2000)
393 ng/ml	20mg; Kan Jang tablets, daily; oral	Humans		
2.28 µg/ml	35.2mg/kg; <i>Andrographis paniculata</i> aqueous extract; oral	Rabbits	(HPLC), solid phase extraction and ultraviolet detection.	(Chen <i>et al.</i> , 2007)
4.14 µg/ml	10mg/kg; liposomal ADO; intravenous	Rats	HPLC, UV detection.	(Suo <i>et al.</i> , 2007)
1.62 µg/ml	10mg/kg; powder tablet ADO; oral			
58.62ng/ml	200mg; tablet ADO; oral	Humans	HPLC, electrospray ionization tandem mass spectrometry	(Xu <i>et al.</i> , 2009)
1.42 µg/ml	1g/kg; <i>Andrographis paniculata</i> aqueous extract; oral	Rats	HPLC, UV detection.	(Akowuah <i>et al.</i> , 2009)
6.79 µg/ml	25mg/kg; ADO; oral	Rats	HPLC, UV detection	(Maiti <i>et al.</i> , 2010)
9.64 µg/ml	25mg/kg; phospholipid-ADO complex (herbasome); oral			
0.83 µg/ml	10mg/kg; ADO; oral	Rats	HPLC, UV detection.	(Chellampillai & Pawar, 2011)
2.67 µg/ml	10mg/kg; ADO-Eudragit® EPO complex; oral			

**Table 8.1 Maximal plasma concentrations ( $C_{max}$ ) levels of differing treatments of ADO**

General effect of ADO	Cellular System	Specific effect	Reference
Reduction of production of pro-inflammatory molecules	LPS stimulated RAW264.7 macrophages	iNOS upregulation suppressed	(Chiou <i>et al.</i> , 1998; Chiou <i>et al.</i> , 2000)
	HL-60 derived neutrophils	Inhibition of COX-2 expression	(Hidalgo <i>et al.</i> , 2005)
	LPS stimulated mouse peritoneal macrophages	Reduction of TNF- $\alpha$ and IL-12 via possible suppression of ERK phosphorylation	(Qin <i>et al.</i> , 2006)
	Human keratinocyte HaCaT cells induced with dead <i>Propionibacterium acne</i>	Inhibition of IL-8 and TNF- $\alpha$ secretion.	(Fu <i>et al.</i> , 2011)
	Human whole blood	Reduction of pro-inflammatory cytokines TNF- $\alpha$ , IL-6, IL-1 $\beta$ and anti-inflammatory cytokine IL-10 due to downregulation of mRNA expression (except for IL-1 $\beta$ )	(Parichatikanond <i>et al.</i> , 2010)
	PMA/ Ionomycin stimulated Jurkat T cells	Reduction of IL-2 production via NFAT inhibition	(Carretta <i>et al.</i> , 2009)
	LPS, TNF- $\alpha$ , PMA induced HUVECS, macrophages, pulmonary vascular endothelial cells (PVECS)	Reduction in tissue factor (TF) mRNA and protein expression levels and TF activity through inhibition of p50 binding to TF promoter.	(Li <i>et al.</i> , 2009)
	LPS stimulated J774A.1 macrophages;	Reduction of NO, PGE <sub>2</sub> , IL-1 $\beta$ , IL-6 production	(Chandrasekaran <i>et al.</i> , 2011)
	A23187 differentiated HL-60 promyelocytic leukaemia cells	Reduction of TXB <sub>2</sub> production	(Chandrasekaran <i>et al.</i> , 2011)
Reduced monocyte adhesion and migration	fMLP stimulated peripheral human neutrophils	Reduced neutrophil adhesion and transmigration	(Shen <i>et al.</i> , 2002)
	C5a, MIP1- $\alpha$ stimulated RAW264.7 macrophages,	Reduction of chemotactic migration via inhibition of PI3K and suppression of MEK1/2.	(Tsai <i>et al.</i> , 2004)
	HL-60 binding to TNF- $\alpha$ induced human endothelial cell lines EA.hy926; HUVEC	Inhibition of TNF- $\alpha$ induced expression of ICAM-1 on endothelial cells leading to decreased monocyte adhesion	(Habtemariam 1997, Yu <i>et al.</i> , 2010; Chen <i>et al.</i> , 2011)

General effect of ADO	Cellular System	Specific effect	Reference
Reduced activation of immune cells	LPS, IL-4 activated macrophages	Reduction of macrophage activation by both LPS and IL-4, decrease in cell surface MHC class I, CD40, CD80, CD86, CD206;	(Wang <i>et al.</i> , 2010a)
	PAF induced HL-60 derived neutrophils; LPS stimulated mouse MLE-12 cells; TNF stimulated 293T embryonic kidney cells;	Inhibition of NF- $\kappa$ B activation	(Xia <i>et al.</i> , 2004; Hidalgo <i>et al.</i> , 2005; Iruretagoyena <i>et al.</i> , 2006)
	Human platelet cell suspension; human whole blood	Inhibition of COX-1 and COX-2 activities	(Parichatikanond <i>et al.</i> , 2010)
	Mixed lymphocyte reaction from lymph node cell suspensions	Reduction of T cell activation through inhibition of antigen processing and DC maturation	(Iruretagoyena <i>et al.</i> , 2005; Iruretagoyena <i>et al.</i> , 2006)
	LPS induced ventral mesencephalic microglia culture; BV-2 microglia	Protection against LPS induced neurotoxicity and activation leading to reduced levels of superoxide, TNF- $\alpha$ , nitric oxide, PGE <sub>2</sub> ; mRNA expression of COX-2 & TNF- $\alpha$ reduced, with reduction in COX-2 protein stability.	(Wang <i>et al.</i> , 2004)
	CD4 <sup>+</sup> T cells isolated from haemophilic mice co-cultured with dendritic cells pulsed with canine FVIII	Increase in T cell secretion of immunosuppressive cytokines IL-10, TGF- $\beta$ .	(Qadura <i>et al.</i> , 2008)
	LPS & IFN- $\gamma$ stimulated rat primary vascular smooth muscle cells	Suppression of iNOS and MMP-9 expression, reduced NF- $\kappa$ B transcription activity, inhibition of phosphorylation on p65 serine <sup>536</sup> .	(Hsieh <i>et al.</i> , 2010)

General effect of ADO	Cellular System	Specific effect	Reference
Induction of apoptosis	Human primary rheumatoid arthritis fibroblast-like synoviocytes	Induction of cell cycle arrest at G0/G1 phase, induction of apoptosis due to increase in expression of pro-apoptotic molecule Bax, release of cytochrome c and the corresponding increase of cleaved caspase 3.	(Yan <i>et al.</i> , 2011)
Inhibition of platelet aggregation	PAF induced human blood platelets	Inhibition of platelet aggregation	(Amroyan <i>et al.</i> , 1999)
	Thrombin induced rat platelets	Inhibition of platelet aggregation through downregulation of ERK2 phosphorylation	(Thisoda <i>et al.</i> , 2006)
	Arachidonic acid, collagen or thrombin induced human platelets	Inhibition of collagen induced platelet aggregation through activation of eNOS-cyclic GMP pathway and inhibition of the PI3K-Akt-p38 MAPK, PLC- $\gamma$ 2-DAG-PKC pathway.	(Lu <i>et al.</i> , 2011)

**Table 8.2 Anti-inflammatory effects of ADO *in vitro*.**

<b>System</b>	<b>Effect of ADO</b>	<b>Reference</b>
Mouse model of acute peritonitis induced by TNF- $\alpha$ , IL1- $\beta$ , LPS	Reduced peritoneal leukocyte infiltration due to reduction in E-selectin expression on stimulated endothelial cells	(Xia <i>et al.</i> , 2004)
Mouse model of septic shock induced by LPS	Increased mouse survival	(Xia <i>et al.</i> , 2004)
Asthma mouse model induced by OVA sensitization.	Inhibition of ovalbumin induced asthma via inhibiting IKK $\beta$	(Xia <i>et al.</i> , 2004; Bao <i>et al.</i> , 2009)
Mouse model of EAE induced by injection of myelin oligodendrocyte glycoprotein derived peptide	Reduction of EAE severity due to diminished antimyelin T cell and antibody response, as well as upregulation of myelin specific Fox3p regulatory T cells	(Iruretagoyena <i>et al.</i> , 2005; Iruretagoyena <i>et al.</i> , 2006)
Mice induced with OVA and Freund's adjuvant	Decreased level of delayed type hypersensitivity reaction	(Iruretagoyena <i>et al.</i> , 2005)
Carageenan induced paw oedema	Antiedematogenic activities, reduced paw swelling.	(Sheeja <i>et al.</i> , 2006; Suebsasana <i>et al.</i> , 2009; Sulaiman <i>et al.</i> , 2010)
Mouse models of pain: acetic acid induced writhing; hot plate test.	Antinociceptive activities: reduced nociception through a non-opoid mechanism.	(Sulaiman <i>et al.</i> , 2010)
Hemophilic mice infused with immature dendritic cells pulsed with canine FVIII (cFVIII) treated with or without ADO	Decrease in FVIII inhibitors, no change in CD4+Foxp3+ regulatory T cells.	(Qadura <i>et al.</i> , 2008)
Rat model of permanent cerebral ischaemia	Reduced infarct volume, decrease in OX-42 activated microglia, pro-inflammatory cytokines IL-1 $\beta$ , TNF- $\alpha$ & PGE <sub>2</sub> , reduced NF- $\kappa$ B nuclear translocation.	(Chan <i>et al.</i> , 2010)
Mouse model of arterial ligation; rat model of autografting veins	Reduction in neointima hyperplasia and reduction in neointima to media ratio; reduction in E-selectin, NF- $\kappa$ B p65, MMP-9, VCAM-1, tissue factor mRNA and protein expression.	(Wang <i>et al.</i> , 2007; Zhi-Tao <i>et al.</i> , 2011)
Mice primed with Hepatitis B antigen	Reduction in antibody production	(Wang <i>et al.</i> , 2010a)
Mouse model of deep vein thrombosis	Reduction of venous thrombosis through reducing tissue factor expression	(Li <i>et al.</i> , 2009)
Mouse model of sodium induced microthrombi	Longer time of vessel occlusion, lowered mortality rates	(Lu <i>et al.</i> , 2011)

**Table 8.3 Anti-inflammatory effects of ADO *in vivo*.**



Type of drug; dosage	Effect of drug	Reference
Immunoguard® ( <i>Andrographis paniculata</i> ; <i>Eleutherococcus senticosus</i> ; <i>Schizandra chinensis</i> ; <i>Glycyrrhiza glabra</i> ); 48mg ADO/day	<ul style="list-style-type: none"> <li>• Decrease in duration, frequency and severity of attacks in familial mediterranean fever (FMF)</li> <li>• Increases nitric oxide levels and decreases IL-6 in FMF patients</li> </ul>	(Amaryan <i>et al.</i> , 2003; Panossian <i>et al.</i> , 2003)
Kan Jang ( <i>Andrographis paniculata</i> , <i>Eleutherococcus senticosus</i> ) or <i>Andrographis paniculata</i> dried extract (Caceres <i>et al.</i> ); 60mg ADO/day or 1200 mg /day of extract; target group: adults	<ul style="list-style-type: none"> <li>• Symptoms in upper respiratory tract infections were markedly improved – sore throat, dryness in throat; headache; nasal symptoms, malaise.</li> <li>• Similar symptoms in sinusitis groups and common cold were relieved by Kan Jang.</li> <li>• Recovery at a faster, rate, reduction in number of days of sick leave.</li> </ul>	(Caceres <i>et al.</i> , 1999; Melchior <i>et al.</i> , 2000; Gabrielian <i>et al.</i> , 2002; Kulichenko <i>et al.</i> , 2003)
Kan Jang ( <i>Andrographis paniculata</i> , <i>Eleutherococcus senticosus</i> ); 30mg ADO/day; target group: children	<ul style="list-style-type: none"> <li>• Recovery from uncomplicated common cold at a faster rate</li> <li>• Reduction in nasal secretion and nasal congestion.</li> </ul>	(Spasov <i>et al.</i> , 2004)
Paractin ® ( <i>Andrographis paniculata</i> ) 30mg ADO 3 times/day )	<ul style="list-style-type: none"> <li>• Reduction of grade and number of swollen and tender joints in rheumatoid arthritis patients.</li> <li>• Reduction of rheumatoid factor, IgA, IgM levels in blood.</li> </ul>	(Burgos <i>et al.</i> , 2009)

**Table 8.4 Anti-inflammatory effects of ADO or *Andrographis paniculata* in humans**

Type of drug; dosage; route	System	Effect of drug	Reference
ADO and ethanol extract of <i>A. paniculata</i> (APE); APE: 25mg/kg, oral; ADO: 1 mg/kg, oral or 4mg/kg, intra-peritoneal.	Balb/c mice immunized with red blood cells (RBC)	Increase in RBC specific antibody titres, increase in haemolytic plaque forming cells, increase in delayed type hypersensitivity	(Puri <i>et al.</i> , 1993)
ADO (PN355); 5mg/kg for 3 weeks and 10mg/ kg for 3 weeks; oral	HIV positive patients	Increase in number of CD4+ lymphocytes in HIV positive patients.	(Calabrese <i>et al.</i> , 2000)
ADO and Kan Jang ( <i>Andrographis paniculata</i> , <i>Eleutherococcus senticosus</i> ); 2µM to 10 µM; <i>in vitro</i>	Human peripheral blood lymphocytes	<p>Proliferation of PHA induced leukocytes:  ADO: 5% increase; Kan Jang: 16.4% decrease;</p> <p>Cytokine and immune activation markers (without PHA):  ADO: IFN- <math>\gamma</math> increase 23.3%, Neopterin increase 22.2%, <math>\beta</math>2MG increase 270%.  Kan Jang: IFN- <math>\gamma</math> increase 20.9%; Neopterin increase 16.7%; <math>\beta</math>2MG increase 310%.</p> <p>Cytokine and immune activation markers (with PHA):  ADO: TNF-<math>\alpha</math> increase 22.6%, <math>\beta</math>2MG increase 82.4%.  Kan Jang: TNF-<math>\alpha</math> increase 1091%, <math>\beta</math>2MG increase 138%.</p>	(Panossian <i>et al.</i> , 2002)
ADO, 14-deoxy-11,12-didehydroandrographolide, 14-deoxy-andrographolide; 0 – 100 µM for 48 h, <i>in vitro</i> .	Human blood peripheral lymphocytes	Increase in lymphocyte proliferation and IL-2 secretion.	(Kumar <i>et al.</i> , 2004)

Type of drug; dosage; route	System	Effect of drug	Reference
ADO and ethanol extract of <i>A. paniculata</i> (APE); 1mg/kg or 4mg/kg ADO; 25mg/kg or 50mg/kg (APE) fed for 14 or 28 days; oral gavage	Balb/c mice intra peritoneally immunised with inactivated <i>Salmonella typhimurium aroA</i> strain SL3261	Serum IgG levels for ADO and APE treatment: increase approximately 400%;  IFN- $\gamma$ secretion by splenocytes: increase 700 % (APE); increase 800 % (ADO)	(Xu <i>et al.</i> , 2007)
Andrographolide; 15-30 $\mu$ M for 24 h; <i>in vitro</i> .	Human CD4 <sup>+</sup> T cells	Increased MIF synthesis and secretion through induction of reactive oxygen species	(Cho <i>et al.</i> , 2009)

**Table 8.5 Immunostimulatory effects of ADO or *Andrographis paniculata***

Mechanism	Type of drug; dosage; route	System	Effect of Drug	References
Inhibition of proliferation	ADO, methanol, petroleum ether, dichloromethane, aqueous extract of <i>A. paniculata</i> ; various concentrations for 48 h; <i>in vitro</i> .	Colon, breast, CNS, lung, melanoma, prostate, ovarian and renal cancer cell lines.	ADO: inhibits all types of cancer cell lines; Methanol, petroleum ether, dichloromethane extracts of <i>A. paniculata</i> : inhibits HT-29 human colon cancer	(Kumar <i>et al.</i> , 2004)
	ADO and 25 analogues;	Colon, breast, CNS, lung, prostate, ovarian and renal cancer cell lines.	ADO: inhibits all types of cancer cell lines.	(Nanduri <i>et al.</i> , 2004)
Induction of cell cycle arrest	ADO	MCF-7 (hormone dependent) and MDA-MB-231 (hormone independent) breast cancer cells, <i>in vivo</i> MCF-7 tumour xenograft.	Induction of cell cycle arrest at G1 phase, inhibition of <i>in vivo</i> tumour growth.	(Stanslas <i>et al.</i> , 2001a)

	ADO	Various cancer cell lines	Induction of cell cycle arrest at G0/G1 phase	(Rajagopal <i>et al.</i> , 2003)
	ADO, DRF3188; 5 – 25 $\mu$ M for 24 or 48 h; <i>in vitro</i>	MCF-7 breast cancer cells	Induction of cell cycle arrest at G0/G1 due to upregulation of p27, and decrease in Cdk4 (ADO, DRF3188), decrease in Cdk 1 (ADO)	(Satyanarayana <i>et al.</i> , 2004)
	ADO, DRF3188; 0 – 100 mg/kg (ADO), 0 – 50 mg/kg (DRF3188); intra-peritoneal.	MCF-7-hollow fibre assay implanted in peritoneum (IP) and subcutaneous (SC) sites of Swiss Albino mice	Decrease in proliferation (IP and SC); upregulation of p27 and decrease in Cdk4 (IP) (ADO, DRF3188).	
	ADO, ethanol extract of <i>A. paniculata</i> (APE), deoxyandrographolide, neoandrographolide	HL-60 human promyelocytic leukaemia cells, KB epidermoid carcinoma cells, H4-II-E hepatoma cells, CNE3 human nasopharynx cells.	ADO and APE inhibit all types of cancer cell growth; induction of G0/G1 phase arrest and mitochondria-dependent pathway of apoptosis.	(Cheung <i>et al.</i> , 2005)
	ADO; 0 – 30 $\mu$ M; <i>in vitro</i>	Human colorectal carcinoma Lovo cells	Inhibition of cell growth, G1 arrest, decrease in cyclin A/Cdk 2 & cyclin D/Cdk 4 complex, upregulation of p21 & p16; phosphorylation of p53, increase in Rb/E2F complex.	(Shi <i>et al.</i> , 2008)
	ADO and ADO benzylidene derivatives SRJ09, SRJ10, SRJ23.	MCF-7 breast cancer cells, HCT-116 colon cancer cells, National Cancer Institute cancer cell line screen	Inhibition of growth, induction of G1 arrest, and apoptosis. SRJ9 downregulated CDK4 but not CDK1.	(Jada <i>et al.</i> , 2008)
Induction of apoptosis	ADO, 0 – 150 $\mu$ M for 24 – 72 h, <i>in vitro</i> .	HepG2 human hepatoma cells	Decrease in cell viability with $IC_{50}$ 40.2 $\mu$ M for 48 h, G2/M cell cycle arrest, induction of apoptosis with caspase-3 activation and loss of	(Li <i>et al.</i> , 2007)

			mitochondria membrane potential. Increase in Bax, phosphorylated cdc2, p53 expression. Increase in amount of H <sub>2</sub> O <sub>2</sub> , decrease in superoxide radicals, decrease in GSH, increase in SOD activity	
ADO, 35 µg/ml for 1-12 h, <i>in vitro</i> .	Human prostatic adenocarcinoma PC-3 cells		Induction of apoptosis: change in morphological characteristics, activation of caspase-3 and caspase-8.	(Kim <i>et al.</i> , 2005)
ADO, 0 – 100 µM, 24 h, <i>in vitro</i> .	HepG2 human hepatoma cells, Hela human cervical cancer cell line, MDA-MB-231 human breast cancer cell line		Induction of apoptosis: caspase-8 and -9, cleavage of Bid, conformational change in Bax and increase in Bax mitochondrial translocation leading to cytochrome c release.	(Zhou <i>et al.</i> , 2006)
ADO, 0 – 1.4mM, 24 – 72 h, <i>in vitro</i> .	TD47 human breast cancer cells		Reduction of cell viability, induction of apoptosis: increase in Bax and p53, reduction in Bcl-2 expression.	(Sukardiman <i>et al.</i> , 2007)
ADO, 0 – 90 µM, 2 – 24 h, <i>in vitro</i> .	HepG2 and Hep3B human liver cancer cells, Hela human cervical cancer cells, HCT116 human colorectal cancer cells treated with or without TRAIL		Reduction of cell viability, induction of apoptosis: PARP cleavage, induction of caspase-8 apoptosis pathway, increased expression of DR4, increased p53 due to increased stabilization, increased p21 expression, JNK activation.	(Zhou <i>et al.</i> , 2008)
ADO, 0 – 100 µM for up to 96 h, <i>in vitro</i> .	Promyelocytic leukaemia cell lines HL-60, NB-4 and all-trans retinoic acid resistant NB4-R2		Growth inhibition of leukaemia cell lines, induction of differentiation to mature granulocytes, induction of apoptosis – membrane blebbing, nuclear condensation and fragmentation.	(Manikam & Stanslas, 2009)
ADO, 0 – 200 µg/ml for 24 – 48 h, <i>in vitro</i> .	SMMC-7721 human hepatocellular carcinoma treated with or without 5-fluorouracil		Inhibition of cellular proliferation, induction of apoptosis: change in Bax conformation, induction of caspase-8 apoptosis pathway, upregulation of p53 expression.	(Yang <i>et al.</i> , 2009b)

	ADO, 0 – 200 $\mu$ M for 48 h, <i>in vitro</i> .	PC-3 prostate cancer cells	IC <sub>50</sub> : 23.3 $\mu$ M; induction of apoptosis: upregulation of Bax and downregulation of Bcl-2, activation of caspase-3 and decrease in VEGF production.	(Zhao <i>et al.</i> , 2008)
	ADO, 0 – 100 $\mu$ M for 24h or 48 h, <i>in vitro</i> .	Ramos p53-mutated Burkitt lymphoma; SUDHL4 diffuse large B cell lymphoma (DLBCL); HF-1 follicular lymphoma (FL), Granta mantle cell lymphoma (MCL); patient samples for DLBCL, FL, MCL.	Decrease in cell viability, increase in ROS, induction of apoptosis: activation of caspase 3, 8 and 9, cleavage of Bid and PARP, conformational change in Bax and Bax mitochondrial translocation.	(Yang <i>et al.</i> , 2010)
	ADO, 0 – 100 $\mu$ M for 48 h, <i>in vitro</i>	Multiple myeloma cancer stem cell in 2-D cell culture or with human bone marrow stromal in 3-D cell culture	Decrease in cell viability, induction of apoptosis: Annexin V positive, activation of caspase 3/7, 8 and 9.	(Gunn <i>et al.</i> , 2011)
	ADO, 0 – 50 $\mu$ M for 0 – 48 h, <i>in vitro</i> .	Hep3B, HepG2 human hepatoma cells.	Decrease in cell viability, reduction in colony forming units, induction of apoptosis: DNA fragmentation; reduction in cellular glutathione, activation of JNK and p38 and activation of JNK signalling cascade in presence of BSO.	(Ji <i>et al.</i> , 2011)
	ADO, 10mg/kg once daily for 16 days, intra-peritoneal.	Hep3B cells xenografted onto nude mice	Decrease in tumour volume and approximately 50% decrease in tumour weight.	
Inhibition of tumour promoting signalling	ADO, 0 – 15 $\mu$ M for up to 18h, <i>in vitro</i> .	HepG2 human hepatoma cells, HCT116 human colorectal cancer cells, Hela human cervical cancer cell line, MDA-MB-231 human breast cancer cell line treated with or without doxorubicin	Suppression of constitutive and IL-6 induced STAT3 activation, IL-6 induced nuclear translocation, suppression of JAK1/2 activation, sensitization to doxorubicin induced cytotoxicity.	(Zhou <i>et al.</i> , 2010)
	ADO, 0 – 20 $\mu$ M for 24 – 48 h, <i>in vitro</i> .	LNCaP, DU145, PC-3 prostate cancer cells	Inhibition of IL-6 expression, IL-6 induced signalling, inhibition of cell viability and	(Chun <i>et al.</i> ,

			induction of apoptosis.	2010)
	ADO, 4mg/kg every 2 days for 8 weeks, intra-peritoneal	DU145 xenografted nude mice prostate cancer model	Suppression of tumour growth	
	ADO, 0 – 30 $\mu$ M, 0 – 96 h, <i>in vitro</i> .	H-ras transformed rat kidney epithelial cell line with or without radiation, SW480 human colon cancer cells	Sensitization of Ras-transformed cells to radiation, decrease of Akt activation, inhibition of radiation-induced NF- $\kappa$ B activity.	(Hung <i>et al.</i> , 2010)
	ADO, 300 mg/kg, subcutaneous and peritumour injection	Male nude mice subcutaneously injected with Ras-transformed cells	Increase in tumour growth delay	
	ADO, 0 – 40 $\mu$ M for 6 – 24 h, <i>in vitro</i> .	C4-2, CWR22Rv1 and LNCaP, prostate cancer cells.	Inhibition of AR synthesis and expression, inhibits downstream transcription of PSA, nuclear translocation of AR leading to apoptosis and inhibition of cell growth; inhibition of AR binding to Hsp90.	(Liu <i>et al.</i> , 2011)
	ADO, 6.2 $\mu$ g/ml twice/ week for 5 weeks, intra-peritoneal.	Hamster buccal pouch model of squamous cell carcinogenesis	Decreased tumour volume, cell proliferation and tumour vascularisation, increased apoptosis, inhibition of NF- $\kappa$ B activation.	(Wang <i>et al.</i> , 2011)
	ADO, 0 – 200 $\mu$ M for 24 to 72 h, <i>in vitro</i> .	Tb human tongue carcinoma cells	Reduction of cell viability, induction of apoptosis and G2/M arrest through decrease in NF- $\kappa$ B activation and drop in p65, c-Myc and cyclin D1 expression.	
Inhibition of migration	ADO, 0 – 50 $\mu$ M for 6 h, <i>in vitro</i> .	HUVECs	Lowered cancer cell adhesion to endothelial cells through inhibition of TNF- $\alpha$ induced E-selectin expression on endothelial cells and decrease of sle <sup>x</sup> expression on gastric cancer cells.	(Jiang <i>et al.</i> , 2007)
	ADO, 0 – 5 $\mu$ M for 24 h, <i>in vitro</i> .	Temperature sensitive v-Src transformed RK3E rat kidney	Inhibited v-Src induced morphological transformation, downregulation of E-Cadherin,	(Liang <i>et al.</i> ,

		epithelial cells	actin filament disorganization and ERK1/2 phosphorylation. This is due to cellular decrease in tyrosine phosphorylation, because of downregulation of v-src expression due to increased degradation from increased ubiquitination.	(2008)
	ADO, 0 – 5 $\mu$ M for 24 h, <i>in vitro</i> .	Lovo human colorectal carcinoma cells	Inhibition of motility and invasion, through decrease in MMP-7 activity, expression and synthesis, AP-1 DNA binding reduced.	(Shi <i>et al.</i> , 2009)
	ADO, 1 – 10 $\mu$ M for 24 h, <i>in vitro</i> .	CT26, HT29 human colon cancer cells	Decrease in invasion ability, inhibition of MMP-2 activity but not expression, attenuation of ERK1/2 signalling.	(Chao <i>et al.</i> , 2010a)
	ADO, 0 – 5 $\mu$ M for 24 h, <i>in vitro</i> .	A549 non small cell lung cancer cells	Decreased motility and invasion, decrease in MMP-7 activity and synthesis due to inhibition of PI3K signalling leading to decreased AP-1 DNA binding.	(Lee <i>et al.</i> , 2010)
Induction of anti-tumour response	Ethanol extract of <i>A. paniculata</i> , 10mg/dose/animal, for 10 days ; ADO, 500 $\mu$ g/dose/animal; for 10 days.	EL4 thymoma cells inoculated into Balb/c mice with alloimmunization	Increase in mice survival time, increase in IL-2 and IFN- $\gamma$ production	(Sheeja & Kuttan, 2007a)
	Ethanol extract of <i>A. paniculata</i> (APE), 10mg/dose/animal, for 5 days; ADO, 500 $\mu$ g/dose/animal; for 5 days.	Balb/c mice injected peritoneally with Ehrlich ascites carcinoma (EAC).	Increase in natural killer cell activity, antibody dependent cell cytotoxicity, antibody dependent complement mediated cytotoxicity, proliferation in the presence of mitogens – splenocytes, thymocytes and bone marrow derived cells for both APE and ADO, increase in IL-2 and IFN- $\gamma$ levels.	(Sheeja & Kuttan, 2007b)
	Ethanol extract of <i>A. paniculata</i> (APE),	DLA Dalton's lymphoma ascites cells injected into right hind limb of	Increase in total white blood cell count, decrease in tumour volume, increase in IL-2, GM-CSF,	(Sheeja & Kuttan, 2008)



	10mg/dose/animal for 10 days; used with or without chemotherapy (cyclophosphamide, 25mg/kg intraperitoneal), hyperthermia (43°C for 30 minutes), or radiation (4Gy/animal).	Swiss albino mice	TNF- $\alpha$ levels, decrease in myeloperoxidase activity.	
Other factors	ADO, 0 – 2.4 mg/ml for 1 to 5 days, <i>in vitro</i> .	Multidrug resistant HCT-8 colorectal cancer cells treated with 5-FU, ADM and DDP	Increased cell growth inhibition and increase in apoptosis, possibly due to lower expression of efflux glycoprotein P-170.	(Han <i>et al.</i> , 2005)
	ADO (0 – 5 $\mu$ M) for up to 1 h.	A549, H1355, H1299, CL1-0, CL1-5 non small cell lung cancer cell lines	Inhibition of TGF- $\beta$ signalling resulting in increased PHD2, causing increased proteolytic degradation of HIF-1 $\alpha$ , leading to decrease in VEGF signalling.	(Lin <i>et al.</i> , 2011)

**Table 8.6 Anti-cancer effects of ADO or *Andrographis paniculata***

**8.2. Appendix II – Buffer Preparation****Cell culture media (500ml)**

450 or 425 ml	High glucose Dulbecco's modified eagle medium (DMEM)
50 ml or 25 ml	Fetal bovine serum (FBS) [for 10% or 5% complete medium]
5ml	100X Antibiotics-antimycotics
5ml	10mM MEM Non-essential amino acids
5ml	200mM L-glutamine
2.5ml	1M 4-(2-hydroxyethyl)-1-piperazineethanesulfonic acid (HEPES) buffer

For serum-free media, the components are similar, with the exception that no FBS is added, and 500ml of DMEM is used.

**Immunofluorescence buffers****Permeabilization buffer (100 ml)**

0.1 g	Saponin powder
100 ml	PBS

**Western Blot Gel composition**

<b>Resolving gel (10 mL):</b>			
	<b>8%</b>	<b>10%</b>	<b>12%</b>
H <sub>2</sub> O	5.3 mL	4.8 mL	4.3 mL
Acrylamide/bisacrylamide (40%, ratio 19:1)	2 mL	2.5 mL	3 mL
1.5 M Tris-HCl pH8.8	2.5mL		
10% SDS (w/v)	100 µL		
10% APS (w/v)	100 µL		
TEMED	8 µL		

**5 % Stacking gel (1ml)**

730 µL	H <sub>2</sub> O
125 µL	Acrylamide/bisacrylamide (40%, ratio 19:1)
125 µL	1 M Tris-HCl pH 6.8
10 µL	10% SDS (w/v)
10 µL	10% APS (w/v)
1 µL	TEMED

**Western Blot Buffers****5x SDS Loading Buffer**

12.5 mL of 1 M stock	Tris-HCl pH 6.8
5 g	SDS
0.25 g	Bromophenol blue
29 mL of 87 % stock	Glycerol
5 % (v/v)	β-mercaptoethanol

Top up to 50 mL with distilled water

**10x Tris Glycine Buffer (5 L)**

30.2g Tris Base

188g Glycine

Top up to 1 L with distilled water

**SDS-PAGE Running Buffer (2 L)**

200 ml 10x Tris glycine buffer

20 ml 10% SDS

Top up to 2 L with distilled water

**Transfer Buffer (2 L)**

200 ml 10x Tris glycine buffer

400 ml Methanol

Top up to 2 L with distilled water

**Blocking Buffer (100 ml)**

100 ml 0.1% PBS-Tween 20 (PBST)

5 g Skim milk powder

**Western Blot Lysis Buffer (1 ml)**900  $\mu$ l 1 X autoclaved PBS100  $\mu$ l 10 % Triton X-10020  $\mu$ l 100mM PMSF20  $\mu$ l 2X Roche complete protease inhibitor EDTA-free